# A Genetic and Biochemical Approach to Identify Function of Novel Proteins in *Francisella tularensis*

Cheryl N. Miller

A dissertation submitted to the faculty of the University of North Carolina at Chapel Hill in partial fulfillment of the requirements for the degree of Doctor of Philosophy in the Department of Microbiology and Immunology.

Chapel Hill
2013

Approved by,

Tom Kawula

Miriam Braunstein

Anthony Richardson

Virginia Miller

Peggy Cotter

Corbin Jones

ABSTRACT

CHERYL N. MILLER: A Genetic and Biochemical Approach to Identify Function of Novel Proteins in *Francisella tularensis*
(Under the direction of Tom Kawula)

*Francisella tularensis* is a Gram-negative bacterial pathogen that can infect a broad range of hosts and is the etiologic agent of the human disease tularemia. Members of the family Francisellaceae have few close relatives, and about 30% of the *F. tularensis* genome encodes hypothetical proteins, or proteins with unknown function. We used biochemical techniques and developed genetic tools to identify and characterize two proteins of unknown function in *F. tularensis*. First we identified a conserved cytoplasmic membrane protein with unknown function, which we termed RipA. In *F. tularensis,* RipA is required for intracellular growth and virulence in the mouse model of tularemia. As a means to determine RipA function, we isolated and mapped independent extragenic suppressor mutants of a Δ*ripA* strain that restored growth in host cells. Each suppressor mutation mapped to one of two essential genes, *lpxA* or *glmU*, which are involved in lipid A synthesis. We found that the ratio of C:18 to C:16 fatty acids in lipid A was greater in the presence of RipA. Furthermore, LpxA was more abundant in the presence of RipA. Induced expression of *lpxA* in the Δ*ripA* strain stopped bacterial division. Together these data suggest RipA modulates the activity and abundance of LpxA in *F. tularensis* during adaptation to the host cell environment. Furthermore, we characterized the function, and named a second conserved protein in *F. tularensis,* PanG,

which was required for pantothenate (vitamin $B_5$) synthesis. PanG is a novel ketopantoate reductase (KPR) that can convert 2-dehydropantoate to pantoate. Both the homologous gene from *Enterococcus faecalis* (EF1861) and the analogous gene, *panE,* from *Escherichia coli* functionally complemented the *Francisella novicida* KPR mutant. Using genetic and chemical complementation we confirmed the *in silico* predicted genes involved in pantothenate synthesis in *Francisella novicida* and *tularensis* and identified a novel KPR, PanG. Together this work provided functional characterization of two *F. tularensis* proteins that were previously unknown. However, there remain over 500 genes in *F. tularensis* that are either annotated as hypothetical or unknown, which need to be characterized.

## ACKNOWLEDGMENTS

To complete a project of this magnitude requires a network of support, and I am indebted to many people.

I would first like to thank my advisor Tom Kawula, who has been an exceptional mentor throughout my entire graduate career. His passion for science and involvement in graduate education has been inspiring. I will be his 11th PhD student, following 10 outstanding scientists that Tom has mentored though graduate school. Tom has been generous in providing me with opportunities to attend both national and international meetings. I have to give him credit for my postdoctoral offer to work with Jean Celli because he gave me the opportunity to network and participate in five conferences. I appreciate how dedicated he is to his students. His door is always open and he is always interested in discussing and analyzing data. He also has taught me important life lessons, how to balance life, and academia. I am grateful to have had such a fantastic mentor. Tom is an exceptional individual whom I will always look up to.

Both past and present Kawula lab members have made work such a friendly environment. Sharon, Todd, Brittany, Eric, Jason, Shaun, and Lydia have helped make my graduate experience engaging, enlightening, and entertaining. I will really miss the chocolates that Shaun would make for the lab and the cinnamon rolls Tom and Sharon would always bring in.

I would like to thank Corey Quackenbush for being supportive through the whole process and helping me through the toughest moments. I would like to thank Corey especially for his technical computer talents—he helped improve the quality of many figures, taught me how to use Photoshop, and fixed all my computer issues. Corey taught me many formatting techniques that saved me a lot of time, and always was willing to help with computer technology. I would also like to thank Corey for all his patience with me.

I am grateful to my parents, Warner and Cathy Miller for their guidance, encouragement, and interest in my project. I would like to thank my two little sisters Anna and Megan for always believing in me. I enjoyed the times when they came and visited me in North Carolina especially when the whole family was here for Thanksgiving. The time my mom came to run the DNA Day 5K and the time my dad came to bike the 65 mile Cup-n-Cone ride were very special to me. I would also like to thank my parents for supporting and encouraging me to pursue my two passions: science and athletics.

I could write an entire book on the wonderful collaborations that were developed during my graduate career. Ronald Jenkins and Garry Dotson and the University of Michigan helped develop the fluorescence enzyme assay that was instrumental in characterizing my suppressor mutants. Sorab Habibi was a fantastic collaborator that taught me how to use the MALDI mass spectrometer at the Department of Chemistry (UNC Chapel Hill). I would like to thank Corbin Jones and Artur Romanchuk for their help sequencing and aligning the entire genome of *F. tularensis*. I would also like to thank Edward Collins for his tremendous help and feedback on my project with RipA.

I could always count on my committee to have great ideas. I would like to thank Mariam Braunstein, Tony Richardson, Virginia Miller, Peggy Cotter and Corbin Jones for always having engaging conversations with me about my research, and teaching me how to be a better scientist.

I would also like to thank all my close friends that would play hard with me when I got a chance to step away from lab. I will miss the Thursday bike rides, the races, and the trips to the beach, mountains, and lakes. I would like to thank Martha Clark for making me a serious biker, Jennifer Parks and Thomas Revelle for encouraging me to do my first half iron man, and Curtis Taylor for helping me become a stronger biker with all the Wednesday morning rides.

I would like to thank Dixie, Theresa and Lisa for being such an outstanding administrative staff.

I would also like to thank the entire BBSP staff for their endless support and friendship. I enjoyed organizing the first annual DNA Day 5K with Jeff Steinbach, Corey Quackenbush, the committee, and all of our wonderful sponsors.

## DEDICATION

I wish to dedicate my dissertation to my Grandfather who has always been my role model and whom I miss dearly.

# TABLE OF CONTENTS

**LIST OF TABLES** ..... **xv**

**LIST OF FIGURES** ..... **xvi**

**Chapter 1** ..... **1**

***Francisella tularensis* Introduction: History, Epidemiology, Medical Relevance, Taxonomy, Microbiology and Pathogenesis** ..... **1**

History ..... 1

Epidemiology ..... 3

Medical Relevance ..... 3

Taxonomy ..... 5

Microbiology ..... 7

Function of Two Novel Proteins in *Francisella tularensis* ..... 14

Figures ..... 16

Tables ..... 20

References ..... 23

**Chapter 2** ..... **33**

**Effects of the putative transcriptional regulator IclR on *Francisella tularensis* pathogenesis** ..... **33**

Overview ..... 33

Introduction ..... 34

Materials And Methods ..... 36

Bacterial strains ..... 36

Cell Culture ..... 36

Molecular techniques and allelic exchange ..... 37

Gentamicin protection assays ..... 38

Mouse infections ..... 38

IL-1β ELISAs and cytotoxicity assays ..... 39

Microarrays ..... 39

Quantitative RT-PCR ..... 40

Antibiotic sensitivity assays ..... 41

Microarray data accession numbers ..... 41

Results ..... 42

Comparison of iclR alleles among *F. tularensis* subspecies and construction of *iclR* deletion mutants ..... 42

LVS and SchuS4 *iclR* deletion mutants are competent for intracellular replication ..... 44

LVSΔ*iclR* is not attenuated following intranasal or intradermal inoculation of mice ..... 44

SchuS4Δ*iclR* is not attenuated following intranasal inoculation of mice ..... 45

*F. novicida* U112 *iclR* transposon mutant is attenuated following intranasal inoculation of mice ..... 46

Deletion of *iclR* does not affect IL-1β expression or cytotoxicity of infected cells ..... 46

The effects of IclR on gene expression ..... 47

Comparison of IclR-regulated genes between LVS, SchuS4 and U112 ..... 48

The effects of IclR on antibiotic resistance ..... 50

Discussion ..... 51

Figures ..... 55

Tables ..... 63

References ..... 64

**Chapter 3 ..... 69**

**TetR-based Gene Regulation Systems for *Francisella tularensis* ..... 69**

Overview ..... 69

Introduction ..... 70

Materials And Methods ..... 71

Bacterial strains, transformation and cell culture ..... 71

*secA* mutagenesis and allelic exchange ..... 72

Plasmid construction ..... 73

Broth culture luminescence assay and SecA depletion assay ..... 73

Intracellular induction and *ripA* growth rescue ..... 73

Results ..... 74

Discussion ..... 79

Figures ..... 80

Tables ..... 87

References ..... 88

**Chapter 4 ..... 92**

**RipA modulates the acyl chain specificity and stability of LpxA in *Francisella tularensis* ..... 92**

Overview ..... 92

Introduction ..... 93

Materials And Methods ..... 95

Bacterial Strains ..... 95

Whole Genome Sequencing and PCR Verification ..... 96

Gentamicin Protection Assay ..... 96

Extragenic Suppressor Repair Using Allelic Exchange ..... 97

Co-immunoprecipitation of LpxA and RipA ..... 97

Membrane Fractionation ..... 98

Membrane Purification and Thin Layer Chromatography ..... 98

Western Blots ..... 99

Lipid A Purification ..... 100

Positive Ion Mode Mass Spectrometry on Lipid A ..... 101

Negative Ion Mode Mass Spectrometry on Purified Membrane Samples ..... 101

Quantitative RT-PCR ..... 101

Anhydrotetracycline Inducible Gene Expression System for *lpxA* and *ripA* ..... 102

Circular Dichroism ..... 102

LpxA-$His_6$ Purification for Enzyme Assay ..... 103

Fluorescent Enzyme Assay for LpxA-$His_6$ ..... 103

Results ..... 104

Extragenic Suppressor Mutation Enrichment in the Δ*ripA* Background ..... 104

LpxA T36N Rescued Growth of Δ*ripA* in Eukaryotic Cells ..... 106

LpxA and RipA Co-immunoprecipitate ..... 107

Mass Spectrometry Lipid A Profiles for Wild Type *F. tularensis*, Δ*ripA*, and Δ*ripA* Suppressor S102 are Similar ..... 109

LpxA Protein Levels are Significantly Lower in the Δ*ripA* Strain Compared to Wild Type ..... 110

Inducing Expression of *lpxA* Negatively Affects the Δ*ripA* Strain ..... 111

LpxA T36N is Less Stable than Wild Type LpxA and has Reduced Enzyme Activity ..... 112

Discussion ..... 114

Figures ..... 118

Tables ..... 130

**References ..... 135**

**Chapter 5 ..... 139**

**PanG, A New Ketopantoate Reductase Involved in Pantothenate Synthesis ..... 139**

Overview ..... 139

Introduction ..... 140

Materials And Methods ..... 143

Bacterial strains and cell culture ..... 143

Growth Assays ..... 143

Construction of the E.coli double mutant *ilvC:*::flp/*panE*::kan using FLP/FRT recombination and λ-Red recombineering ..... 144

*F. novicida* Coenzyme A levels ..... 145

Replacing LVS *panD* (*panD*$_{LVS}$) with *F. novicida panD* (*panD*$_{U112}$) ..... 146

Deletion of FTT1388 (*panG*) in Schu S4 ..... 146

Mouse infection ..... 146

Results ..... 147

Organization of the *Francisella* pantothenate biosynthesis pathway ..... 147

The *Francisella panBCD* genes are required for growth in the absence of pantothenate ..... 148

A new class of ketopantoate reductase found in a number or pathogenic organisms ..... 150

*Francisella novicida* Coenzyme A Levels ..... 152

*Francisella tularensis* LVS is a β-alanine auxotroph ..... 152

*Francisella tularensis* Schu S4 Δ*panG* is a pantothenate auxotroph ..... 153

Discussion ..... 154

Figures ..... 158

Tables ..... 170

References ..... 172

**Chapter 6 ..... 177**

**Discussion, Conclusions, And Future Directions ..... 177**

References ..... 185

# LIST OF TABLES

TABLE 1.1. *FRANCISELLA TULARENSIS* COMMON AND HISTORICAL NAMES ..... 20

TABLE 1.2. WHOLE GENOME SEQUENCING OF FRANCISELLACEAE ..... 21

TABLE 1.3. GENOME COMPARISON OF LABORATORY STRAINS ..... 22

TABLE 2.1. MICROARRAY GENE EXPRESSION IN LVSΔ*ICLR* ..... 63

TABLE 3.1. BACTERIAL STRAINS AND PLASMIDS ..... 87

TABLE 4.1. WHOLE GENOME SEQUENCING RESULTS FOR SUPPRESSOR S102 ..... 130

TABLE 4.2. INITIAL RATE OF LPXA-CATALYZED ACYL GROUP TRANSFER ..... 130

TABLE 4.3. BACTERIAL STRAINS, PLASMIDS, AND PRIMERS ..... 131

TABLE 4.4 ZERO COVERAGE REGIONS DETECTED BY WHOLE GENOME SEQUENCING ..... 133

TABLE 5.1. BACTERIAL STRAINS AND PLASMIDS ..... 170

# LIST OF FIGURES


FIGURE 1.1. SCANNING ELECTRON MICROSCOPY OF *F. TULARENSIS* SUBSPECIES *TULARENSIS* ..... 16

FIGURE 1.2. PHYLOGENY OF FRANCISELLACEAE ..... 17

FIGURE 1.3. GEOGRAPHICAL DISTRIBUTION OF FRANCISELLACEAE ..... 18

FIGURE 1.4. FLUORESCENCE MICROSCOPY IMAGE FROM INFECTED CELL ..... 19

FIGURE 2.1. COMPARISON OF ICLR IN THREE FRANCISELLA STRAINS ..... 55

FIGURE 2.2. INTRACELLULAR REPLICATION OF LVSΔ*ICLR* AND SCHUS4Δ*ICLR* ..... 56

FIGURE 2.3. RECOVERY OF LVSΔ*ICLR* MUTANT IN MICE FOLLOWING I.N. OR I.D. INOCULATION ..... 57

FIGURE 2.4. RECOVERY OF SCHUS4Δ*ICLR* MUTANT IN MICE FOLLOWING I.N. INOCULATION ..... 58

FIGURE 2.5. RECOVERY OF U112 ICLR TRANSPOSON MUTANT IN MICE FOLLOWING I.N. INOCULATION ..... 59

FIGURE 2.6. IL-1B RELEASE AND CYTOTOXICITY IN MACROPHAGES INFECTION WITH LVSΔ*ICLR* ..... 60

FIGURE 2.7. DIFFERENCES IN TRANSCRIPT LEVELS OF GENES IN LVS VERSUS LVSΔ*ICLR* ..... 61

FIGURE 2.8. ANTIBIOTIC SENSITIVITY OF LVSΔ*ICLR* ..... 62

FIGURE 3.1. FRANCISELLA TETRACYCLINE REGULATED PROMOTER ..... 80

FIGURE 3.2. MAPS OF THE *FTRP-LUXCDABE* VECTORS ..... 81

FIGURE 3.3. THE TETR SYSTEM ..... 82

FIGURE 3.4. THE TETR SYSTEM RESCUES LVSΔ*RIPA* INTRACELLULAR GROWTH IN J774A.1 MACROPHAGES ..... 84

FIGURE 3.5. THE REVTETR SYSTEM ..... 85

FIGURE 3.6. SECA IS ESSENTIAL ..... 86

FIGURE 4.1. EXTRAGENIC SUPPRESSOR ENRICHMENT IN J774A.1 MACROPHAGE LIKE CELLS ..... 118

FIGURE 4.2. EXTRAGENIC SUPPRESSOR MUTATIONS MAP TO *LPXA* AND *GLMU* ..... 119

FIGURE 4.3. THE BIOSYNTHETIC PATHWAY OF LPXA AND GLMU ..... 120

FIGURE 4.4. THE S102 EXTRAGENIC SUPPRESSOR MUTANT PHENOTYPE AND REPAIR IN J774A.1 AND TC-1 CELLS ..... 121

FIGURE 4.5. LPXA AND RIPA CO-IMMUNOPRECIPITATE ..... 122

FIGURE 4.6. LPXA LOCALIZES TO THE INNER MEMBRANE ..... 123

FIGURE 4.7. MEMBRANE AND LPS COMPOSITION OF SUPPRESSOR S102 ..... 124

FIGURE 4.8. MASS SPECTROMETRY ON LIPID A AND MEMBRANE FRACTIONS ..... 125

FIGURE 4.9. RIPA IS NECESSARY FOR STABILITY OF LPXA ..... 127

FIGURE 4.10. INDUCED EXPRESSION OF *LPXA* STOPS Δ*RIPA* GROWTH ..... 128

FIGURE 4.11. CIRCULAR DICHROISM SPECTRA AND ENZYME ASSAY WITH LPXA AND LPXA T36N ..... 129

FIGURE 5.1. THE BIOSYNTHETIC PATHWAY IN *FRANCISELLA* SPECIES AND THE PUTATIVE PANTOTHENATE OPERON. ..... 158

FIGURE 5.2. FUNCTIONAL COMPLEMENTATION OF *PANB*::TN, *PANC*:TN, *PAND*::TN, *ILVC*::TN, AND *PANG*::TN. ..... 160

FIGURE 5.3. PHYLOGENETIC TREE OF KNOWN KETOPANTOATE REDUCTASE PROTEINS AND PANG. ..... 161

FIGURE 5.4. GENETIC COMPLEMENTATION OF THE *F. NOVICIDA,* AND *E. COLI* KPR DOUBLE MUTANT WITH *PANG*. ..... 163

FIGURE 5.5. *F. NOVICIDA* COENZYME A LEVELS. ..... 165

FIGURE 5.6. *F. TULARENSIS* SCHU S4, *F. TULARENSIS* LVS, *F. NOVICIDA* GROWTH IN PANTOTHENATE DROP OUT MEDIA. ..... 166

FIGURE 5.7. REPAIR OF *F. TULARENSIS* LVS B-ALANINE AUXOTROPHY. ..... 167

FIGURE 5.8. *F. TULARENSIS* SUBSPECIES *TULARENSIS* SCHU S4 Δ*PANG* GROWTH AND VIRULENCE PHENOTYPE. ..... 168

## LIST OF SYMBOLS AND ABBREVIATIONS

| | |
|---|---|
| Δ | Gene deletion |
| [θ] | Molar ellipticity |
| ATc | Anhydrotetracycline |
| BHI | Brain heart infusion |
| BMDM | Bone marrow-derived macrophages |
| BSL | Biological safety level |
| CDC | Centers for Disease Control and Prevention |
| CDM | Chamberlain's defined medium |
| CDS | Coding sequence for proteins |
| CFU | Colony forming units |
| CoA | Coenzyme A |
| DHB | Dihydrozybenzoic acid |
| DNA | Deoxyribonucleic acid |
| ELISA | Enzyme-linked immunosorbent assay |
| FPI | *Francisella* pathogenicity island |
| FTMS | Fourier transform mass spectrometer |
| HPLC | High performance liquid chromatography |
| i.d. | Intradermal |
| i.n. | Intranasal |

| | |
|---|---|
| IPTG | Isopropyl β-D-1-thiogalactopyranoside |
| Kdo | 3-deoxy-D-manno-octulosonic acid |
| KPR | Ketopantoate reductase |
| $LD_{50}$ | Median lethal dose |
| LPS | Lipopolysaccharide |
| LVS | Live vaccine strain |
| MALDI | Matrix assisted laser desorption ionization |
| MCS | Multiple cloning site |
| MOI | Multiplicity of infection |
| NADPH | Nicotinamide adenine dinucleotide phosphate |
| ORF | Open reading frame |
| PAGE | Polyacrylamide gel electrophoresis |
| PAMP | Pathogen associated molecular patterns |
| PCR | Polymerase chain reaction |
| PBS | Phosphate buffered saline |
| PFA | Paraformaldehyde |
| PI | Post inoculation |
| RNA | Ribonucleic acid |
| RT-PCR | Reverse transcriptase polymerase chain reaction |
| RFU | Relative fluorescence units |
| SDS | Sodium dodecyl sulfate |
| SQ | Starting quantity |
| TLC | Thin layer chromatography |
| TLR | Toll-like receptor |
| TOF | Time of flight |

| | |
|---|---|
| U112 | Utah 112 |
| UDP | Uridine diphosphate |
| UDP-GlcNAc | Uridine diphosphate *N*-acetylglucosamine |
| Vitamin $B_5$ | Pantothenate |
| WGS | Whole genome sequencing |

# Chapter 1

## *Francisella tularensis* Introduction:

## History, Epidemiology, Medical Relevance, Taxonomy, Microbiology and Pathogenesis

*Francisella tularensis* is an extremely small (0.2-0.7 μm), non-mobile, Gram-negative bacterial pathogen that infects a broad range of organisms, and grows efficiently in the cytoplasm of many different cell types (37, 81). In humans, inhaling as few as 10 *F. tularensis* organisms can cause the lethal disease tularemia (73). *F. tularensis* is found predominantly throughout the Northern Hemisphere, but recently tularemia infections have also been reported in areas as far south as Australia (42, 95). According to the CDC about 100 cases of tularemia are reported each year in the United States, which has declined significantly since its discovery in the early twentieth century (1).

## History

*F. tularensis* was first identified by George McCoy in 1911 in Tulare County California during an outbreak in ground squirrels that was mistakenly thought to be plague (56). McCoy determined the outbreak was not due to *Yersinia pestis* the causative agent of plague, but was an unknown organism with plague like characteristics. McCoy isolated and grew *F. tularensis* and developed both the agglutination test and the complement fixation test used to diagnose tularemia (44). Shortly following the

identification of *F. tularensis* many human infections were identified. The first diagnosed tularemia case was in 1913 when a butcher in Cincinnati developed an eye infection with severe conjunctivitis and yellow necrotic ulcers (76, 97).

Dr. Edward Francis recorded over 14,000 cases of tularemia and determined the distribution of tularemia in the early part of the twentieth century (27). Edward Francis was one of the many scientists to contract the disease during his research. Laboratory acquired tularemia was common and frequently recurrent in the early twentieth century before containment facilities were built and safety protocols were developed.

The bacterium *Francisella tularensis* and the disease it causes, tularemia, were derived from the word Tulare based upon the location of the initial outbreaks in Tulare County, California. *Francisella* was derived from Francis in recognition of Dr. Francis' contributions to our understanding of tularemia epidemiology. Other common names of the disease are listed in Table 1.

While McCoy and Francis were researching tularemia, Dr. Hachiro Ohara, a scientist in Japan, was also studying the same disease in Tokyo. He observed that human cases of the disease were associated with rabbit hunting and dressing (44). Dr. Ohara used his wife, Mme Ohara, as a volunteer to demonstrate that the disease (tularemia) is transmittable by infected rabbits (44).

*F. tularensis* is now considered a Category A Select Agent based on probability of use, distribution, availability, and risk assessment. In particular, the CDC specified 6 agents that have the highest risk: anthrax, plague, tularemia, botulinum toxin, smallpox, and viral hemorrhagic fever. During WWII the US, Japan, and the former USSR developed weapons to aerosolize *F. tularensis* (61). The US military stockpiled the

weapon in the 1960s and destroyed the stockpile in 1973 (61). The Soviet Union continued their weapon production of *F. tularensis* into the early 1990s.

## Epidemiology

*Francisella* species can survive for weeks in Brackish-water (10), soil (11), moist straw (64), and animal carcasses (3). The natural reservoir for *F. tularensis* is currently debated and under investigation, but is thought to be present in protozoa, and in arthropod vectors (38, 83). The broad range of species *F. tularensis* can infect is numerous and diverse. In particular, *F. tularensis* commonly infects and kills many small mammals, such as rabbits, aquatic rodents, rats, muskrats, squirrels, lemmings, and mice within days of infection (58). Over 250 other species have been identified, including marsupials, birds, amphibians, and fish (58). Transmission of tularemia to humans can occur by several routes including inhalation, entry through skin abrasions, insect bites, ingestion of contaminated food or water, and contact of infected material with mucus membranes (16). No human-to-human transmission has been reported. Vectors that are known to transmit the disease are ticks, mosquitoes, mites, fleas, and deer flies (25).

## Medical Relevance

In an attempt to develop a vaccine for tularemia, Dr. Samuel Saslaw, conducted experiments on inmates of the Ohio State Penitentiary during the 1960s (73, 74). The prisoners were intranasally and intracutaneously infected with *F. tularensis* and were rigorously monitored during the course of the experiments; daily temperatures, symptoms, lesion size, blood cultures, complete blood counts, urinalysis, chest x-rays,

and agglutination experiments were performed and recorded. These experiments on inmates, though an ethically contentious practice, have provided a substantial amount of data on human tularemia infections and prognosis.

The incubation period for tularemia is about 1-14 days depending on route and dose (35). Signs and symptoms generally start to develop between 3-5 days. Symptoms consist of fever, headache, chills, rigors, sore throat, and can also include loss of energy, appetite and weight (73, 74).

The disease manifestations depend on the route of infection, and there are seven clinical types of tularemia. Ulceroglandular tularemia is the most common form of the disease (84) and is often caused by arthropod bites, or by contact with an infected animal. In this case an ulcer develops at the site of infection, and the draining lymph node becomes inflamed. Glandular tularemia is similar to ulceroglandular, but the primary lesion is not evident while the regional or superficial lymph nodes are involved. Ingestion of contaminated food or water can lead to either oropharyngeal or typhoidal tularemia, where the ulcer is located in the throat, or gastrointestinal tract, respectively. Finally, pneumonic tularemia is caused by inhalation of aerosolized *F. tularensis* and is the most fatal form of the disease (24). *F. tularensis* can quickly become septic if left untreated and can spread to the lung, liver, and spleen (35).

Before antibiotics were developed, a case of pneumonic tularemia had a 30 to 60% mortality rate depending on the strain and dose (63, 77). With antibiotic therapy the potential of tularemia fatalities has dropped, however due to the rare prevalence of outbreaks, delayed diagnosis can lead to incorrect antibiotic treatments and potential death (39). Antibiotics used to treat tularemia are Streptomycin and aminoglycoside

gentamicin, tetracycline and chloramphenicol quinolones (ciprofloxacin) doxycycline (70).

In the United States, the most recent outbreak of tularemia occurred in Martha's Vineyard in 2000 (11). Fifteen landscapers from Martha's Vineyard contracted pneumonic tularemia, with one fatality. The individuals infected were mowing and brush cutting, identifying new risk factors for contracting tularemia (24). Most cases occur in rural environments where hunting is common. The number of reported cases of tularemia has declined recently and this is due to both the development of effective antibiotics and a decrease in hunting and trapping.

Although there is no requirement to report tularemia cases in the United States, other countries are recording the number of sera positive individuals (65). In 2009, 2.3% of 2,416 people screened positive for antibodies against *F tularensis* in a Southern German urban population located in Leutkirch (78). Although tularemia remains relatively rare, it is important to immediately diagnose and treat the disease with such a low infectious dose and a high mortality rate.

## Taxonomy

To date, *Francisella* is the only genus belonging to the family Francisellaceae of the class gammaproteobacteria. Francisellaceae have few close relatives, and is only distantly related to two human pathogens, *Coxiella burnetii*, and *Legionella pneumophila* (83). One of the closest relatives to Francisellaceae is a fish pathogen *Piscirickettsia salmonis* with 84% sequence identity. Currently, the genus *Francisella* contains five groups *F. novicida*, *F. noatunensis*, *F. philomiragia*, *F. piscicida* and *F. tularensis,* which differ in virulence in humans and animals. There has been considerable debate about the

classification of *F. novicida* (46), and throughout this dissertation it will be considered its own species distinct from *F. tularensis*. The human tularemia cases are caused predominantly by *F. tularensis* (61). There are three subspecies of *Francisella tularensis*, each having distinct geographical distribution and disease severity (17).

The most widespread subspecies, *F. tularensis* subsp. *holarctica* (type B), is found in Europe, Asia, North America, and Australia and is responsible for the mild cases of human tularemia. *F. tularensis* subsp. *tularensis* (type A) has been found almost exclusively in North America, although cases have also been reported in Europe and is responsible for the majority of human fatalities. *F. tularensis* subsp. *mediasiatica* has been identified in limited portions of Central Asia and has not been associated with human disease (95).

The whole genome of the most virulent strain *Francisella tularensis* subspecies *tularensis* was sequenced in 2005, and consists of a 1,892,819 bp circular chromosome with G+C content of 32.9% (52). Now with the available affordable sequencing technology there are 18 complete genomes sequenced within Francisellaceae, and 18 whole genome sequencing reads available online (32). Table 1.2 lists the available genome sequences on the Pathosystems Resource Integration Center (PATRIC) (32). In this dissertation, the focus of research is on *F. tularensis*, but the other species can be helpful tools for understanding the evolutionary differences between highly virulent and less virulent species. Our laboratory conducts research using two subspecies of *F. tularensis* and one species of *F. novicida*. *F. tularensis* subspecies *tularensis* Schu S4 is the most virulent subspecies we work with, which was isolated from a human infection in 1941 from Ohio, USA and is a strictly regulated BSL-3 select agent (69). *F. tularensis* subspecies *holarctica* live vaccine strain (LVS) is an attenuated strain of holarctica that

was developed in Russia in the 1930s as a vaccine and is a BSL-2 agent (22). The source of the attenuation of the LVS strain is in part due to the loss of *pilA*, encoding a putative type IV pilin, and FTT0918, encoding an outer membrane protein required for iron acquisition (71). *F. novicida* is a BSL-2 organism that is rarely associated with human infections and was isolated from water in Utah, USA in the 1950s (69).

## Microbiology

The expansive host range and geographic distribution of *F. tularensis* is indicative of its evolutionary success. There have been a number of animal models developed for studying *Francisella* pathogenesis, including non-human primates, mice, rabbits, guinea pigs, rats, zebrafish, amoebae, and *Drosophila melanogaster* (2, 8, 87, 88, 96, 98). In addition to the diverse host range, *Francisella tularensis* can infect an array of host cell types: including macrophages, dendritic cells, polymorphonuclear neutrophils, hepatocytes, endothelial cells, type II alveolar lung epithelial cells, and even red blood cells (16, 21, 37, 41). The success of *Francisella* as a pathogen is intimately associated with its ability to enter host cells and replicate in the cytosol (Figure 1.4). A number of receptors have been identified to be important for *Francisella* uptake, and the receptor and uptake mechanism profoundly impacts the outcome of infection. Normally, phagocytic cells and the complement complex bind an invading pathogen and either engulf the pathogen or mark it for destruction. *F. tularensis* can avoid complement lysis by cleaving C3 to prevent the formation of the membrane attack complex (9). The exact mechanism of this process is not fully understood, and the bacterial factors likely involved in this process are O-antigen and capsule, which are discussed in more detail below (47). The mannose receptor (MR) plays an important role in nonopsonic uptake of

*F. tularensis* into macrophage cells (31). However, during opsonizing conditions *F. tularensis* has markedly enhanced uptake by looping phagocytosis through interaction with actin microfilaments and the complement receptor 3 (CR3) (20). The Fcγ receptors, surfactant protein A, class A scavenger receptors and nucleolin have all been identified as important for *Francisella* uptake (6, 31). It is likely that more receptors have yet to be identified that are important for infection considering the vast array of cell types that can be infected with *F. tularensis.*

Following uptake, *Francisella tularensis* resides in a phagosome that sequentially acquires markers of early and late endosomes. *F. tularensis* can escape the phagosome before lysosome fusion, which is a hallmark of the *Francisella* intracellular life cycle (16). The key aspect of *Francisella* pathogenesis is the ability to survive and replicate efficiently in the cytoplasm of the host cell (93). To date only a few *Francisella* factors have been identified to be required for cytosolic replication including, the purine biosynthesis genes (62) and several genes of unknown function, FTT0369 (*dipA*) (19), FTT0989 (13), and FTT0181 (*ripA*) (28). *F. tularensis* has been shown to grow extracellularly in mice as well, demonstrating the versatility of this organism (26).

***F. tularensis* Virulence Factors**

Considering the versatility of *F. tularensis* pathogenesis, there is much left to understand about the unique mechanisms employed by *F. tularensis* to cause disease. Interestingly, *F. tularensis* does not express virulence factors commonly associated with Gram-negative bacterial pathogens, including Type III, IV, and V secretion systems, flagella, or secreted toxins (52). Furthermore, genetic tools have only recently been created to develop transposon mutant libraries to screen for genes required for intracellular survival and virulence (7, 14, 30, 49, 53, 55). Several genome-wide screens

have identified *F. tularensis* virulence factors including the capsule, Type IV pilus, several proteases, iron acquisition systems, and the most interesting *Francisella* Pathogenicity Island (FPI) (63, 66, 75, 79, 94). Depending on the subspecies, the comprehensive collection of transposon mutant screens have revealed that 4% to 16% of the genome encodes proteins involved in *Francisella* virulence and 20% to 49% of these genes are either annotated as hypothetical or encode proteins with unknown function that remain uncharacterized (63).

***F. tularensis* Pathogenicity Island**

The Francisella Pathogenicity Island (FPI) is a conserved 30kb genetic element that contains about 17 open reading frames that are required for *F. tularensis* pathogenesis and are highly expressed during infection, but the function of these genes are still under investigation (59, 93). The FPI has a low G+C content (27.5%) compared to the rest of the genome, and it is flanked by a rRNA operon and an insertion element (ISFtu1), suggestive of being acquired by horizontal transfer. The FPI is duplicated in the most virulent strains: *F. tularensis* subsp. *tularensis* and *F. tularensis* subsp. *holarctica*, while *F. novicida* contains only one copy. Although, *F. tularensis* subsp. *mediasiatica* has not been associated with any human infections it also contains two copies of the FPI. A lot of the initial studies conducted on the FPI were in *F. novicida* because of the difficulties generating double deletions in the more clinically relevant strains. One putative operon within the FPI contains genes encoding the intracellular growth locus (*iglABCD*), and mutations within these genes attenuated growth of *Francisella* in macrophages, and mice (33, 34, 48). A number of the proteins encoded in the FPI share distant homology to type six secretion proteins in *Vibrio cholerae*, and *Pseudomonas aeruginosa*. The most highly induced gene during *F. tularensis* internalization is *iglC*,

and it is essential for growth in macrophages and virulence in mice; however the specific function encoded by *iglC* is unknown (33).

**Genome Decay**

Acquiring virulence factors by horizontal transfer is one mechanism emerging pathogenic bacteria use to exploit novel intracellular niches. As mentioned above, an example of this was demonstrated with the pathogenicity island in *Francisella tularensis*. Gene loss can be just as critical to microbial survival as gene acquisition (12). More than 10% of the CDSs in the Schu S4 genome are pseudogenes or gene fragments (52). The *F. tularensis* genome is in an advanced state of decay and is likely a result from adapting to a more specific niche inside host cells. The loss of *pepO* is one of many examples of gene loss in *Francisella tularensis* that has enhanced pathogenesis. The inactivation of *pepO* in *F. tularensis* prevents host vasoconstriction and permits the spread of the bacteria to systemic sites (36). In addition, numerous restriction / modification systems have been lost in the evolution of the human pathogenic subspecies, which may allow for increase horizontal gene transfer (29).

One mechanism that has contributed to accelerated loss of genes in *Francisella* species is the activity of insertion sequence elements (IS elements), which encode transposable elements that move within a genome (81). Five IS elements have been identified in the genome of *Francisella* species and the number of each IS element varies greatly between species (TABLE 1.3) (52, 69).

The most common IS elements in *F. tularensis* are ISFtu1 that belongs to the IS630 Tc-1 mariner family and ISFtu2, an IS5 family element. When performing genomic comparisons between different subspecies of *F. tularensis*, IS elements appear to play a prominent role in rearrangement events in *F. tularensis* because 82% of

breakpoints found between *F. tularensis* subsp. *tularensis* and subsp. *holarctica* are bordered by IS elements (69). The ubiquitous polyamines spermine and spermidine are environmental signals that activate transcription of IS elements in addition to nearby genes, which is a novel gene regulation mechanism that has been shown to be important during infection to prevent proinflammatory cytokine production (15).

**Cell Envelope: Lipid A, LPS, and Capsule**

The defining characteristic of Gram-negative bacteria is their cell envelope, which is composed of two membranes—the inner and outer membranes separated by the periplasm that contains a thin peptidoglycan layer. Both the inner and outer membranes are lipid bilayers but have dramatic differences in their structure and composition. The lipid composition in *F. tularensis* is high relative to other Gram-negative bacteria consisting of 21% lipid relative to total dry weight (4). *F. tularensis* phospholipids consist mainly of long chain phophadidylethanolamine, phosphatidylglycerol, phosphatidylcholine, and free lipid A (92), while cardiolipin and phosphatidylserine are not present (4).

The outer membrane separates the bacterium from the external environment and is a selective barrier that is critical for bacterial survival inside host cells. *F. tularensis* is unique in all aspects of its cell envelope. Modifications to the *F. tularensis* membrane components, such as lipid A, the O-antigen, and the capsule are essential for the successful establishment of infection.

LPS is the major glycolipid molecule present on the outer membrane of most Gram-negative bacteria that is in direct contact with the external environment. LPS is made up of three domains, the first domain is lipid A (endotoxin) the hydrophobic domain that anchors LPS to the outer membrane. The second domain is a non-repeating

core oligosaccharide (KDO), and the third domain is a distal polysaccharide (O-antigen) that varies greatly even between subspecies of *F. tularensis* (86). Lipid A is referred to as endotoxin in most Gram-negative bacteria because it typically induces a massive cytokine response when recognized by host cell TLR4/MD2 receptors (67). However *F. tularensis* Lipid A does not induce a cytokine response and is not recognized by TLR4/MD2, because lipid A is modified to avoid host detection. The 4' phosphate and the 3' hydroxyacyl are removed to make a tetra-acylated disaccharide of glucosamine with a 1' phosphate (90, 91). NaxD is a deacetylase that removes the 1' galactosamine on lipid A in *F. tularensis* and is critical for growth inside cells (54). Another unique property of *F. tularensis* lipid A is the majority of lipid A is free of the O-antigen sugars (60, 80, 92). What role free lipid A plays in the pathogenesis of *F. tularensis* is not fully understood, but could change the host receptors used for adherence and uptake, dictating the fate of the infection (43). In addition to immune evasion, LPS also plays an important positive role in the assembly of many outer membrane proteins and free lipid A may influence the composition of proteins on the surface of the bacteria (51).

The O-antigen sugars help bacteria resist antibiotics, the complement pathway, and other environmental stresses (68). The *wbt* gene cluster of *F. tularensis* is involved in O-antigen biosynthesis and contains 15 ORFs (82). In contrast, the gene cluster in *F. novicida* contained only 12 ORFs. The LPS O-antigens of *F. novicida* and *F. tularensis* have been shown to be structurally and immunologically distinct due in part to the differences in the *wbt* genes. The core two carbohydrate residues are the same in both species consisting of two α-D-GalNacAN sugars, but the anchor and distal residues differ and are composed of α-D-GalNAcAN and β-DQui2NAc4NAc in *F. novicida* and β-D-Qui4NFn and β-D-QuiNAc in *F. tularensis* (85, 86, 89). *F. novicida* LPS has greater

immunobiological activity in mice when compared to *F. tularensis*, which can be explained by the difference in the O-antigen sugars composition (50).

In addition to the LPS sugars, the capsule is another barrier that protects many pathogenic bacteria from host detection and destruction. A *F. tularensis* capsule was identified to be an important virulence factor (40). Mutants lacking the capsule structure have increased sensitivity to serum and are attenuated in mouse models of tularemia (40, 72). The composition and expression of the capsule can change depending on the growth conditions (18). The *F. tularensis capBCD* locus has partial homology to the locus in *B. anthracis* that encode proteins needed to synthesize poly-D-glutamic acid capsules, however no poly-D-glutamic acid capsule has been identified in *F. tularensis* (57). The *F. tularensis capBCD* locus is required for intracellular growth and in a mouse model of tularemia (45). Recent composition analysis and mass spectrometry determined that the capsule is at least in part composed of O-antigen sugars similar the composition of LPS (5). Although the O-antigen sugars have been characterized as part of the composition of the capsule, it will be interesting to identify what molecule the *cap* locus synthesizes in *F. tularensis* that are required for virulence.

I have highlighted only a few of the key pathogenic mechanisms used by *F. tularensis* to cause disease, and recently a substantial amount of progress has been made on identifying factors important for *F. tularensis* virulence (63). What is now critical for future progress is defining function to the proteins used by *Francisella tularensis* to survival and replication within host cells, which will be the key for developing effective drug targets to prevent tularemia.

## Function of Two Novel Proteins in *Francisella tularensis*

With the continued advancement and availability of whole genome sequencing, the list of hypothetical proteins keeps growing. It is important to characterize the function of hypothetical proteins so we can identify better drug targets and develop new strategies to fight disease at the same time we can develop new tools to advance future research in microbiology.

Francisellaceae is only distantly related to all other known gammaproteobacteria (Figure 1). About thirty percent of the *F. tularensis* genome encodes hypothetical proteins or proteins with unknown function, and many of the unique virulence mechanisms used by *F. tularensis* to cause disease remain unknown (61). We therefore have focused on identifying and characterizing proteins with unknown function in order to better understand *F. tularensis* pathogenesis. We characterized the function of two proteins that were initially annotated as hypothetical. We recently elucidated the function of a hypothetical protein, FTL_1914, which we named RipA (28). Through the use of extragenic suppressor mutations we discovered that RipA modulates LpxA stability and activity in *F. tularensis* (Chapter 4). We also identified the function of a second protein, FTL_1351, which we named PanG (Chapter 5). PanG is novel ketopantoate reductase required for vitamin $B_5$ synthesis in *F. tularensis* and homologs of *panG* are found in other bacterial pathogens: *Clostridium difficile*, *Coxiella burnetii*, and *Enterococcus faecalis* (Chapter 5). Both RipA and PanG are conserved in all sequenced species of *F. tularensis* and are highly expressed during intracellular growth (93). We also developed the first anhydrotetracycline inducible and repressible system for *F. tularensis* to control gene expression, and using this tool we determined the induced expression of *lpxA* was detrimental for growth of *F. tularensis* lacking the *ripA* locus, while the wild type strain

containing *ripA* was unaffected by the production of *lpxA*. We therefore have focused on identifying and characterizing proteins with unknown function in *F. tularensis*. We identified a novel modulator of lipid A synthesis, and a new ketopantoate reductase involved in vitamin $B_5$ synthesis.

## Figures

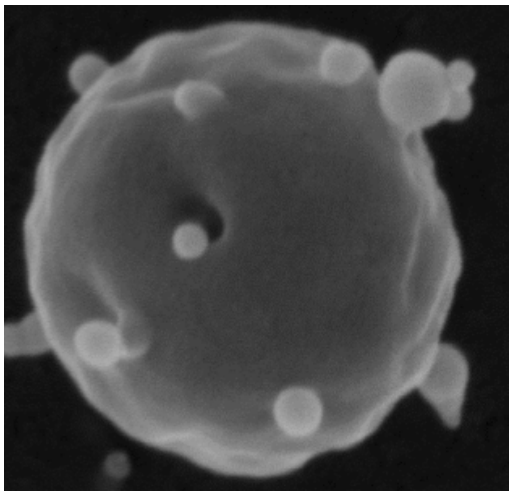

**Figure 1.1. Scanning Electron Microscopy of *F. tularensis* subspecies *tularensis***

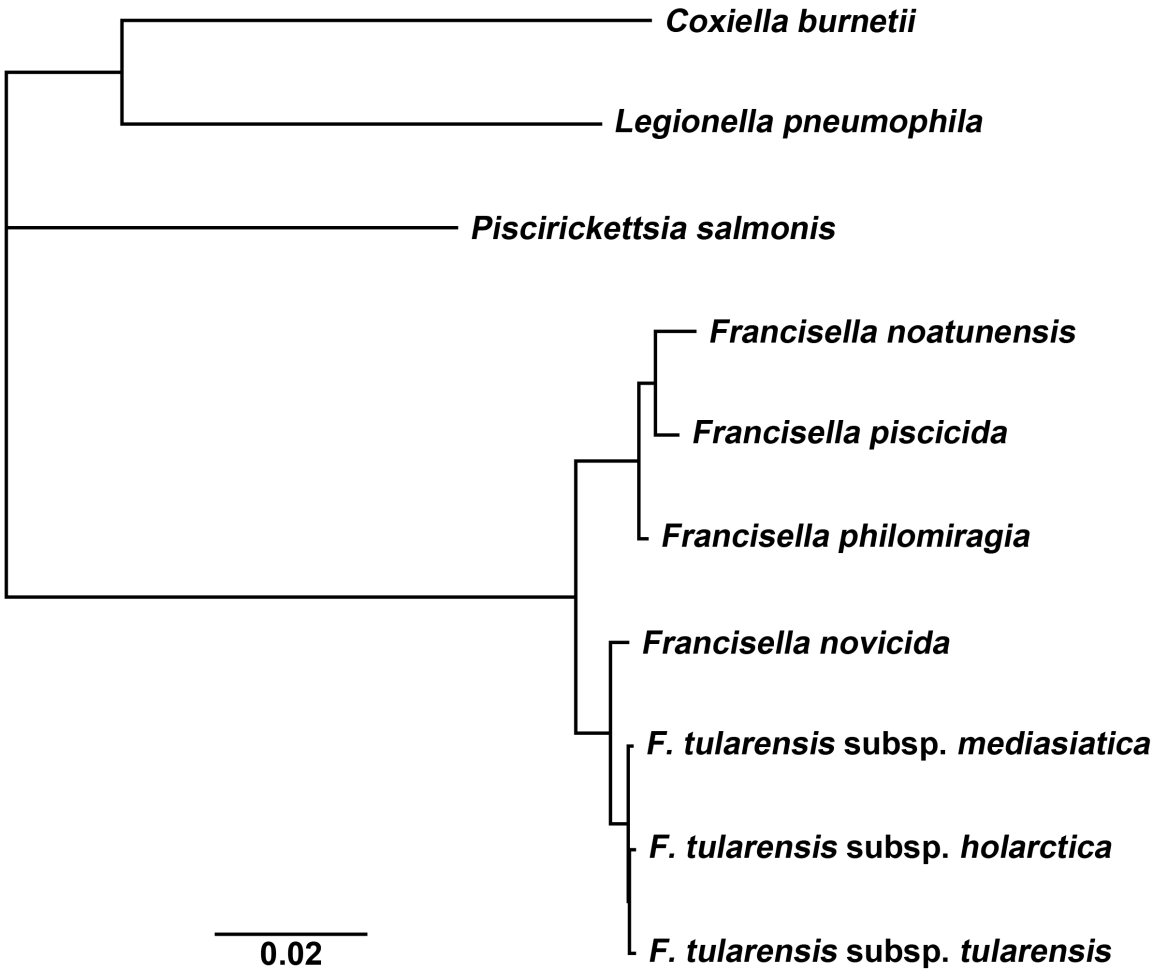


**Figure 1.2. Phylogeny of Francisellaceae**

Phylogenetic tree of Francisellaceae by analysis of ribosomal RNA SNP variations. The evolutionary history of Francisellaceae was inferred from analysis of SNP sequences located within the ribosomal RNA gene locus. The tree is drawn to scale with branch lengths calculated using the standard methods in Geneious Pro 5.5.6 (23).

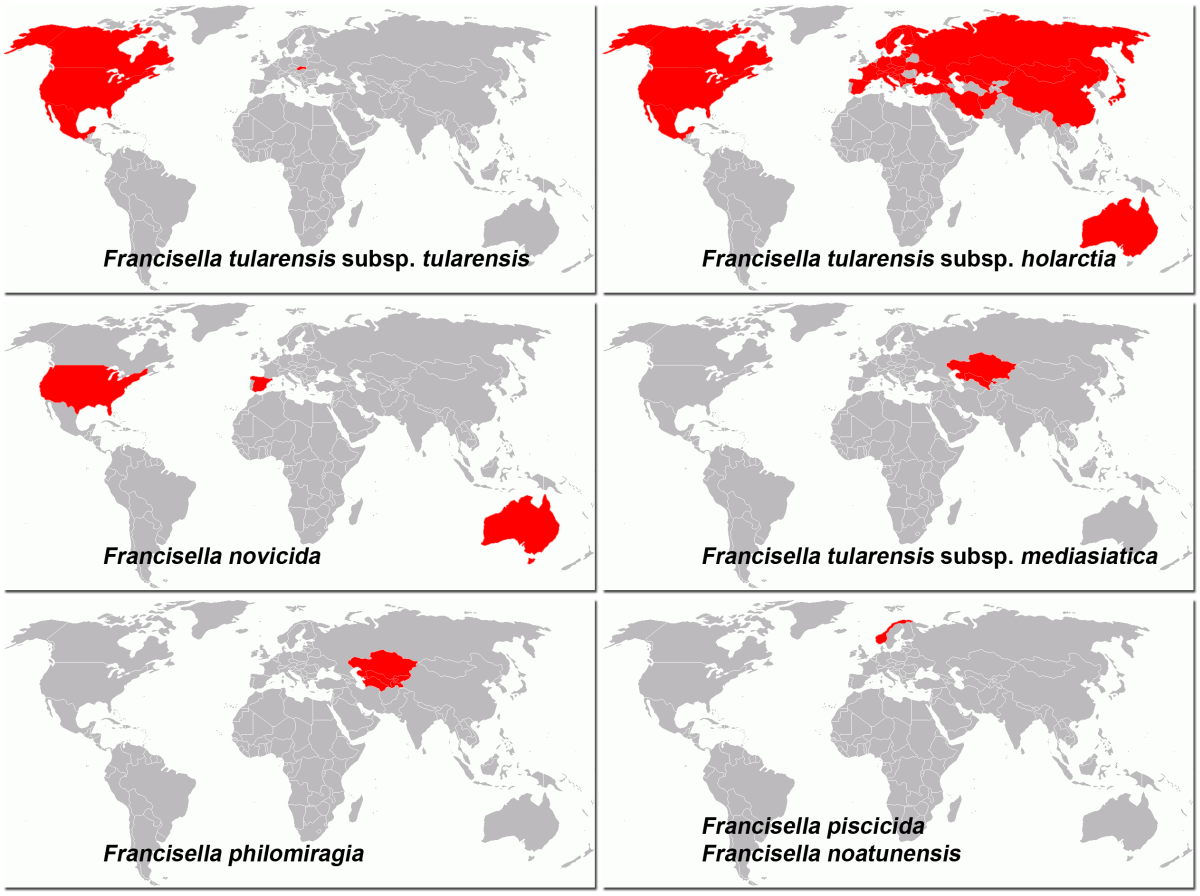


**Figure 1.3. Geographical distribution of Francisellaceae**

Geographical distribution of *F. novicida*, *F. noatunensis*, *F. piscicida*, *F. philomiragia*, and the three *F. tularensis* subspecies. The regions where the strains of *Francisella* and subspecies of *F. tularensis* have been isolated are shown in red.

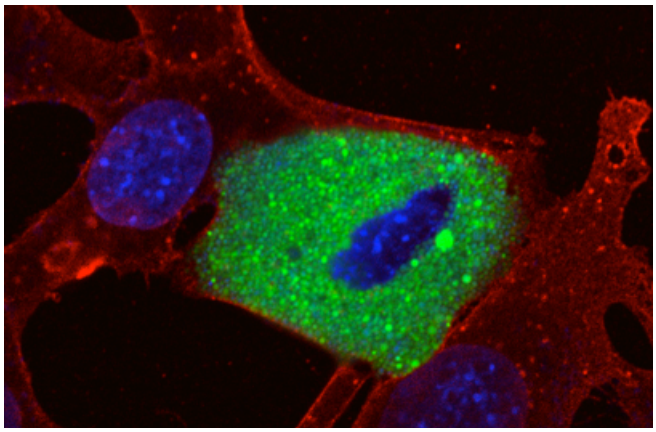

**Figure 1.4. Fluorescence microscopy image from infected cell**

Mouse embryonic fibroblast 24 hours post infection with wild type *F. tularensis*. GFP *F. tularensis* bacteria are depicted in green, DAPI in blue, and wheat germ agglutinin in red.

## Tables

### Table 1.1. *Francisella tularensis* common and historical names

| Name | Location or Dates |
|---|---|
| Deer-fly fever | Utah |
| Rabbit fever | Central States |
| Glandular tick fever | Idaho and Montana |
| Lemming fever | Norway |
| Market men's disease | Washington D.C. |
| Hunter's disease | Central States |
| Ohara's disease | Japan |
| *Bacterium tularense* | 1950s and earlier |
| *Pasteurella tularense* | 1966 and earlier |

## Table 1.2. Whole genome sequencing of Francisellaceae

| Genome Name | NCBI Taxon Id | Genome Status | Completion Date |
|---|---|---|---|
| Francisella cf. novicida 3523 | 676032 | Complete | 2011-04-08 |
| Francisella cf. novicida Fx1 | 984129 | Complete | 2011-04-08 |
| Francisella noatunensis subsp. orientalis str. Toba 04 | 1163389 | Complete | 2012-05-10 |
| Francisella novicida FTE | 545422 | WGS | 2008-07-18 |
| Francisella novicida FTG | 563990 | WGS | 2008-10-06 |
| Francisella novicida GA99-3548 | 442346 | WGS | 2007-05-31 |
| Francisella novicida GA99-3549 | 430558 | WGS | 2007-05-14 |
| Francisella novicida U112 | 401614 | Complete | 2006-11-28 |
| Francisella philomiragia subsp. philomiragia ATCC 25015 | 539329 | WGS | 2008-12-22 |
| Francisella philomiragia subsp. philomiragia ATCC 25017 | 484022 | Complete | 2008-02-11 |
| Francisella sp. TX077308 | 573569 | Complete | 2011-06-20 |
| Francisella tularensis subsp. holarctica | 119857 | Complete | 2006-03-02 |
| Francisella tularensis subsp. holarctica 257 | 412422 | WGS | 2006-12-18 |
| Francisella tularensis subsp. holarctica F92 | 1232394 | Complete | 2012-11-19 |
| Francisella tularensis subsp. holarctica FSC022 | 430556 | WGS | 2007-05-14 |
| Francisella tularensis subsp. holarctica FSC200 | 351581 | WGS | 2006-11-21 |
| Francisella tularensis subsp. holarctica FTNF002-00 | 458234 | Complete | 2007-08-23 |
| Francisella tularensis subsp. holarctica OSU18 | 393011 | Complete | 2006-09-20 |
| Francisella tularensis subsp. holarctica OSU18 (Prj:32025) | 393011 | Complete | |
| Francisella tularensis subsp. holarctica URFT1 | 445226 | WGS | 2009-09-03 |
| Francisella tularensis subsp. mediasiatica FSC147 | 441952 | Complete | 2008-05-07 |
| Francisella tularensis subsp. tularensis 3571 | 1292388 | WGS | 2013-03-14 |
| Francisella tularensis subsp. tularensis 70001275 | 1208319 | WGS | 2012-11-15 |
| Francisella tularensis subsp. tularensis 70102010 | 1210518 | WGS | 2012-10-16 |
| Francisella tularensis subsp. tularensis 80700075 | 1210520 | WGS | 2012-10-16 |
| Francisella tularensis subsp. tularensis 80700103 | 1210519 | WGS | 2012-10-16 |
| Francisella tularensis subsp. tularensis 831 | 1210521 | WGS | 2012-10-16 |
| Francisella tularensis subsp. tularensis AS_713 | 1210522 | WGS | 2012-10-16 |
| Francisella tularensis subsp. tularensis FSC033 | 430557 | WGS | 2007-05-14 |
| Francisella tularensis subsp. tularensis FSC198 | 393115 | Complete | 2006-07-12 |
| Francisella tularensis subsp. tularensis MA00-2987 | 543737 | WGS | 2008-08-26 |
| Francisella tularensis subsp. tularensis NE061598 | 510831 | Complete | 2009-12-28 |
| Francisella tularensis subsp. tularensis SCHU S4 | 177416 | Complete | 2004-12-17 |
| Francisella tularensis subsp. tularensis TI0902 | 1001534 | Complete | 2012-02-23 |
| Francisella tularensis subsp. tularensis TIGB03 | 1001542 | Complete | 2012-02-23 |
| Francisella tularensis subsp. tularensis WY96-3418 | 418136 | Complete | 2007-03-24 |

**Table 1.3. Genome comparison of laboratory strains**

| Property | Strain (subspecies) | | |
|---|---|---|---|
| | U112 (novicida) | LVS (holarctica) | Schu S4 (tularensis) |
| Genome size (bp) | 1,910,031 | 1,895,998 | 1,892,819 |
| Pseudogenes | 14 | 303 | 254 |
| ISFtu1 | 1 | 59 | 53 |
| ISFtu2 | 18 | 43 | 18 |
| Other IS elements | 7 | 7 | 8 |

## References


1. **(CDC), C. f. D. C. a. P.** September 29, 2011 2011, posting date. Reported tularemia cases by year, United States, 1950 - 2010. Centers for Disease Control and Prevention, National Center for Emerging and Zoonotic Infectious Diseases (NCEZID), Division of Vector-Borne Diseases (DVBD). [Online.]

2. **Abd, H., T. Johansson, I. Golovliov, G. Sandstrom, and M. Forsman.** 2003. Survival and growth of *Francisella tularensis* in *Acanthamoeba castellanii*. Applied and environmental microbiology **69:**600-606.

3. **Airapetian, V. G., A. B. Khachatrian, and A. A. Pogosian.** 1957. [Prolonged survival of *Pasteurella tularensis* in frozen carcass]. Zh Mikrobiol Epidemiol Immunobiol **28:**21-25.

4. **Anderson, R., and A. R. Bhatti.** 1986. Fatty acid distribution in the phospholipids of F*rancisella tularensis*. Lipids **21:**669-671.

5. **Apicella, M. A., D. M. Post, A. C. Fowler, B. D. Jones, J. A. Rasmussen, J. R. Hunt, S. Imagawa, B. Choudhury, T. J. Inzana, T. M. Maier, D. W. Frank, T. C. Zahrt, K. Chaloner, M. P. Jennings, M. K. McLendon, and B. W. Gibson.** 2010. Identification, characterization and immunogenicity of an O-antigen capsular polysaccharide of *Francisella tularensis*. PLoS One **5:**e11060.

6. **Balagopal, A., A. S. MacFarlane, N. Mohapatra, S. Soni, J. S. Gunn, and L. S. Schlesinger.** 2006. Characterization of the receptor-ligand pathways important for entry and survival of *Francisella tularensis* in human macrophages. Infect Immun **74:**5114-5125.

7. **Baron, G. S., and F. E. Nano.** 1999. An erythromycin resistance cassette and mini-transposon for constructing transcriptional fusions to cat. Gene **229:**59-65.

8. **Bell, J. F., C. R. Owen, and C. L. Larson.** 1955. Virulence of Bacterium tularense. I. A study of the virulence of *Bacterium tularense* in mice, guinea pigs, and rabbits. J Infect Dis **97:**162-166.

9. **Ben Nasr, A., J. Haithcoat, J. E. Masterson, J. S. Gunn, T. Eaves-Pyles, and G. R. Klimpel.** 2006. Critical role for serum opsonins and complement receptors CR3 (CD11b/CD18) and CR4 (CD11c/CD18) in phagocytosis of *Francisella tularensis* by human dendritic cells (DC): uptake of *Francisella* leads to activation of immature DC and intracellular survival of the bacteria. J Leukoc Biol **80:**774-786.

10. **Berrada, Z. L., and S. R. Telford Iii.** 2011. Survival of *Francisella tularensis* Type A in brackish-water. Archives of microbiology **193:**223-226.

11. **Berrada, Z. L., and S. R. Telford, 3rd.** 2010. Diversity of *Francisella* species in environmental samples from Martha's Vineyard, Massachusetts. Microb Ecol **59:**277-283.

12. **Bliven, K. A., and A. T. Maurelli.** 2012. Antivirulence genes: insights into pathogen evolution through gene loss. Infect Immun **80:**4061-4070.

13. **Brotcke, A., D. S. Weiss, C. C. Kim, P. Chain, S. Malfatti, E. Garcia, and D. M. Monack.** 2006. Identification of MglA-regulated genes reveals novel virulence factors in *Francisella tularensis*. Infect Immun **74:**6642-6655.

14. **Buchan, B. W., M. K. McLendon, and B. D. Jones.** 2008. Identification of differentially regulated *Francisella tularensis* genes by use of a newly developed Tn5-based transposon delivery system. Applied and environmental microbiology **74:**2637-2645.

15. **Carlson, P. E., Jr., J. Horzempa, D. M. O'Dee, C. M. Robinson, P. Neophytou, A. Labrinidis, and G. J. Nau.** 2009. Global transcriptional response to spermine, a component of the intramacrophage environment, reveals regulation of *Francisella* gene expression through insertion sequence elements. Journal of bacteriology **191:**6855-6864.

16. **Celli, J., and T. C. Zahrt.** 2013. Mechanisms of Francisella tularensis intracellular pathogenesis. Cold Spring Harb Perspect Med **3:**a010314.

17. **Champion, M. D., Q. Zeng, E. B. Nix, F. E. Nano, P. Keim, C. D. Kodira, M. Borowsky, S. Young, M. Koehrsen, R. Engels, M. Pearson, C. Howarth, L. Larson, J. White, L. Alvarado, M. Forsman, S. W. Bearden, A. Sjostedt, R. Titball, S. L. Michell, B. Birren, and J. Galagan.** 2009. Comparative genomic characterization of *Francisella tularensis* strains belonging to low and high virulence subspecies. PLoS Pathog **5:**e1000459.

18. **Cherwonogrodzky, J. W., M. H. Knodel, and M. R. Spence.** 1994. Increased encapsulation and virulence of *Francisella tularensis* live vaccine strain (LVS) by subculturing on synthetic medium. Vaccine **12:**773-775.

19. **Chong, A., T. D. Wehrly, R. Child, B. Hansen, S. Hwang, H. W. Virgin, and J. Celli.** 2012. Cytosolic clearance of replication-deficient mutants reveals *Francisella tularensis* interactions with the autophagic pathway. Autophagy **8:**1342-1356.

20. **Clemens, D. L., B. Y. Lee, and M. A. Horwitz.** 2004. Virulent and avirulent strains of *Francisella tularensis* prevent acidification and maturation of their phagosomes and escape into the cytoplasm in human macrophages. Infect Immun **72:**3204-3217.

21. **Craven, R. R., J. D. Hall, J. R. Fuller, S. Taft-Benz, and T. H. Kawula.** 2008. *Francisella tularensis* invasion of lung epithelial cells. Infect Immun **76:**2833-2842.

22. **Dennis, D. T., T. V. Inglesby, D. A. Henderson, J. G. Bartlett, M. S. Ascher, E. Eitzen, A. D. Fine, A. M. Friedlander, J. Hauer, M. Layton, S. R. Lillibridge, J. E. McDade, M. T. Osterholm, T. O'Toole, G. Parker, T. M. Perl, P. K. Russell, and K. Tonat.** 2001. Tularemia as a biological weapon: medical and public health management. Jama **285:**2763-2773.

23. **Drummond AJ, A. B., Buxton S, Cheung M, Cooper A, Duran C, Field M, Heled J, Kearse M, Markowitz S, Moir R, Stones-Havas S, Sturrock S, Thierer T, Wilson A.** 2011. Geneious *v5.5*. http://www.geneious.com.

24. **Feldman, K. A., R. E. Enscore, S. L. Lathrop, B. T. Matyas, M. McGuill, M. E. Schriefer, D. Stiles-Enos, D. T. Dennis, L. R. Petersen, and E. B. Hayes.** 2001. An outbreak of primary pneumonic tularemia on Martha's Vineyard. N Engl J Med **345:**1601-1606.

25. **Foley, J. E., and N. C. Nieto.** 2010. Tularemia. Vet Microbiol **140:**332-338.

26. **Forestal, C. A., M. Malik, S. V. Catlett, A. G. Savitt, J. L. Benach, T. J. Sellati, and M. B. Furie.** 2007. *Francisella tularensis* has a significant extracellular phase in infected mice. J Infect Dis **196:**134-137.

27. **Francis, E.** 1922. Tularemia francis 1921 - A new disease of man. J Amer Med Assoc **78:**1015-1018.

28. **Fuller, J. R., R. R. Craven, J. D. Hall, T. M. Kijek, S. Taft-Benz, and T. H. Kawula.** 2008. RipA, a cytoplasmic membrane protein conserved among *Francisella* species, is required for intracellular survival. Infect Immun **76:**4934-4943.

29. **Gallagher, L. A., M. McKevitt, E. R. Ramage, and C. Manoil.** 2008. Genetic dissection of the *Francisella novicida* restriction barrier. Journal of bacteriology **190:**7830-7837.

30. **Gallagher, L. A., E. Ramage, M. A. Jacobs, R. Kaul, M. Brittnacher, and C. Manoil.** 2007. A comprehensive transposon mutant library of *Francisella novicida*, a bioweapon surrogate. Proceedings of the National Academy of Sciences of the United States of America **104:**1009-1014.

31. **Geier, H., and J. Celli.** 2011. Phagocytic receptors dictate phagosomal escape and intracellular proliferation of *Francisella tularensis*. Infect Immun **79:**2204-2214.

32. **Gillespie, J. J., A. R. Wattam, S. A. Cammer, J. L. Gabbard, M. P. Shukla, O. Dalay, T. Driscoll, D. Hix, S. P. Mane, C. Mao, E. K. Nordberg, M. Scott,**

**J. R. Schulman, E. E. Snyder, D. E. Sullivan, C. Wang, A. Warren, K. P. Williams, T. Xue, H. S. Yoo, C. Zhang, Y. Zhang, R. Will, R. W. Kenyon, and B. W. Sobral.** 2011. PATRIC: the comprehensive bacterial bioinformatics resource with a focus on human pathogenic species. Infect Immun **79:**4286-4298.

33. **Golovliov, I., V. Baranov, Z. Krocova, H. Kovarova, and A. Sjostedt.** 2003. An attenuated strain of the facultative intracellular bacterium *Francisella tularensis* can escape the phagosome of monocytic cells. Infect Immun **71:**5940-5950.

34. **Gray, C. G., S. C. Cowley, K. K. Cheung, and F. E. Nano.** 2002. The identification of five genetic loci of *Francisella novicida* associated with intracellular growth. FEMS microbiology letters **215:**53-56.

35. **Guthrie, A. L., K. L. Gailbreath, E. A. Cienava, D. S. Bradway, and J. F. Munoz Gutierrez.** 2012. Septic tularemia in 2 cottontop tamarins(Sanguinus oedipus). Comp Med **62:**225-228.

36. **Hager, A. J., D. L. Bolton, M. R. Pelletier, M. J. Brittnacher, L. A. Gallagher, R. Kaul, S. J. Skerrett, S. I. Miller, and T. Guina.** 2006. Type IV pili-mediated secretion modulates *Francisella* virulence. Molecular microbiology **62:**227-237.

37. **Hall, J. D., M. D. Woolard, B. M. Gunn, R. R. Craven, S. Taft-Benz, J. A. Frelinger, and T. H. Kawula.** 2008. Infected-host-cell repertoire and cellular response in the lung following inhalation of *Francisella tularensis* Schu S4, LVS, or U112. Infect Immun **76:**5843-5852.

38. **Hansen, C. M., A. J. Vogler, P. Keim, D. M. Wagner, and K. Hueffer.** 2011. Tularemia in Alaska, 1938 - 2010. Acta Vet Scand **53:**61.

39. **Hatipoglu, C. A., U. Bayiz, S. K. Firat, F. S. Erdinc, N. Tulek, and S. Gedikoglu.** 2005. [Case report: a case of tularemia with delayed diagnosis]. Mikrobiyol Bul **39:**89-94.

40. **Hood, A. M.** 1977. Virulence factors of *Francisella tularensis*. J Hyg (Lond) **79:**47-60.

41. **Horzempa, J., D. M. O'Dee, D. B. Stolz, J. M. Franks, D. Clay, and G. J. Nau.** 2011. Invasion of erythrocytes by *Francisella tularensis*. J Infect Dis **204:**51-59.

42. **Jackson, J., A. McGregor, L. Cooley, J. Ng, M. Brown, C. W. Ong, C. Darcy, and V. Sintchenko.** 2012. *Francisella tularensis* subspecies *holarctica*, Tasmania, Australia, 2011. Emerg Infect Dis **18:**1484-1486.

43. **Jacques, M.** 1996. Role of lipo-oligosaccharides and lipopolysaccharides in bacterial adherence. Trends Microbiol **4:**408-409.

44. **Jellison, W. L.** 1974. Tularemia in North America, 1930-1974. University of Montana, University of Montana Foundation, Missoula.

45. **Jia, Q., B. Y. Lee, R. Bowen, B. J. Dillon, S. M. Som, and M. A. Horwitz.** 2010. A *Francisella tularensis* live vaccine strain (LVS) mutant with a deletion in capB, encoding a putative capsular biosynthesis protein, is significantly more attenuated than LVS yet induces potent protective immunity in mice against *F. tularensis* challenge. Infect Immun **78:**4341-4355.

46. **Johansson, A., J. Celli, W. Conlan, K. L. Elkins, M. Forsman, P. S. Keim, P. Larsson, C. Manoil, F. E. Nano, J. M. Petersen, and A. Sjostedt.** 2010. Objections to the transfer of *Francisella novicida* to the subspecies rank of *Francisella tularensis*. Int J Syst Evol Microbiol **60:**1717-1718; author reply 1718-1720.

47. **Jones, C. L., B. A. Napier, T. R. Sampson, A. C. Llewellyn, M. R. Schroeder, and D. S. Weiss.** 2012. Subversion of host recognition and defense systems by *Francisella* spp. Microbiol Mol Biol Rev **76:**383-404.

48. **Kadzhaev, K., C. Zingmark, I. Golovliov, M. Bolanowski, H. Shen, W. Conlan, and A. Sjostedt.** 2009. Identification of genes contributing to the virulence of *Francisella tularensis* SCHU S4 in a mouse intradermal infection model. PLoS One **4:**e5463.

49. **Kawula, T. H., J. D. Hall, J. R. Fuller, and R. R. Craven.** 2004. Use of transposon-transposase complexes to create stable insertion mutant strains of *Francisella tularensis* LVS. Applied and environmental microbiology **70:**6901-6904.

50. **Kieffer, T. L., S. Cowley, F. E. Nano, and K. L. Elkins.** 2003. *Francisella novicida* LPS has greater immunobiological activity in mice than *F. tularensis* LPS, and contributes to *F. novicida* murine pathogenesis. Microbes Infect **5:**397-403.

51. **Kloser, A. W., M. W. Laird, and R. Misra.** 1996. *asmB*, a suppressor locus for assembly-defective OmpF mutants of *Escherichia coli*, is allelic to *envA* (*lpxC*). J Bacteriol **178:**5138-5143.

52. **Larsson, P., P. C. Oyston, P. Chain, M. C. Chu, M. Duffield, H. H. Fuxelius, E. Garcia, G. Halltorp, D. Johansson, K. E. Isherwood, P. D. Karp, E. Larsson, Y. Liu, S. Michell, J. Prior, R. Prior, S. Malfatti, A. Sjostedt, K. Svensson, N. Thompson, L. Vergez, J. K. Wagg, B. W. Wren, L. E. Lindler, S. G. Andersson, M. Forsman, and R. W. Titball.** 2005. The complete genome sequence of *Francisella tularensis*, the causative agent of tularemia. Nat Genet **37:**153-159.

53. **Liu, J., X. Zogaj, J. R. Barker, and K. E. Klose.** 2007. Construction of targeted insertion mutations in *Francisella tularensis* subsp. *novicida*. Biotechniques **43:**487-490, 492.

54. **Llewellyn, A. C., J. Zhao, F. Song, J. Parvathareddy, Q. Xu, B. A. Napier, H. Laroui, D. Merlin, J. E. Bina, P. A. Cotter, M. A. Miller, C. R. Raetz, and D. S. Weiss.** 2012. NaxD is a deacetylase required for lipid A modification and *Francisella* pathogenesis. Molecular microbiology **86:**611-627.

55. **Maier, T. M., R. Pechous, M. Casey, T. C. Zahrt, and D. W. Frank.** 2006. In vivo Himar1-based transposon mutagenesis of *Francisella tularensis*. Applied and environmental microbiology **72:**1878-1885.

56. **McCoy, G. W.** 1911. Studies upon plague in ground squirrels. A plaguelike disease of rodents. Public Health Bulletin **43:**53-71.

57. **Michell, S. L., R. E. Dean, J. E. Eyles, M. G. Hartley, E. Waters, J. L. Prior, R. W. Titball, and P. C. Oyston.** 2010. Deletion of the *Bacillus anthracis capB* homologue in *Francisella tularensis* subspecies *tularensis* generates an attenuated strain that protects mice against virulent tularaemia. J Med Microbiol **59:**1275-1284.

58. **Morner, T.** 1992. The ecology of tularaemia. Rev Sci Tech **11:**1123-1130.

59. **Nano, F. E., and C. Schmerk.** 2007. The *Francisella* pathogenicity island. Ann N Y Acad Sci **1105:**122-137.

60. **Okan, N. A., S. Chalabaev, T. H. Kim, A. Fink, R. A. Ross, and D. L. Kasper.** 2013. Kdo hydrolase is required for *Francisella tularensis* virulence and evasion of TLR2-mediated innate immunity. mBio **4:**e00638-00612.

61. **Oyston, P. C., A. Sjostedt, and R. W. Titball.** 2004. Tularaemia: bioterrorism defence renews interest in *Francisella tularensis*. Nat Rev Microbiol **2:**967-978.

62. **Pechous, R., J. Celli, R. Penoske, S. F. Hayes, D. W. Frank, and T. C. Zahrt.** 2006. Construction and characterization of an attenuated purine auxotroph in a *Francisella tularensis* live vaccine strain. Infect Immun **74:**4452-4461.

63. **Pechous, R. D., T. R. McCarthy, and T. C. Zahrt.** 2009. Working toward the future: insights into *Francisella tularensis* pathogenesis and vaccine development. Microbiol Mol Biol Rev **73:**684-711.

64. **Pomanskaia, L. A.** 1957. [Length of preservation of tularemia bacilli on grain and straw]. Zh Mikrobiol Epidemiol Immunobiol **28:**133-139.

65. **Porsch-Ozcurumez, M., N. Kischel, H. Priebe, W. Splettstosser, E. J. Finke, and R. Grunow.** 2004. Comparison of enzyme-linked immunosorbent assay,

Western blotting, microagglutination, indirect immunofluorescence assay, and flow cytometry for serological diagnosis of tularemia. Clin Diagn Lab Immunol **11:**1008-1015.

66. **Qin, A., and B. J. Mann.** 2006. Identification of transposon insertion mutants of *Francisella tularensis tularensis* strain Schu S4 deficient in intracellular replication in the hepatic cell line HepG2. BMC microbiology **6:**69.

67. **Raetz, C. R., Z. Guan, B. O. Ingram, D. A. Six, F. Song, X. Wang, and J. Zhao.** 2009. Discovery of new biosynthetic pathways: the lipid A story. J Lipid Res **50 Suppl:**S103-108.

68. **Raetz, C. R., and C. Whitfield.** 2002. Lipopolysaccharide endotoxins. Annu Rev Biochem **71:**635-700.

69. **Rohmer, L., C. Fong, S. Abmayr, M. Wasnick, T. J. Larson Freeman, M. Radey, T. Guina, K. Svensson, H. S. Hayden, M. Jacobs, L. A. Gallagher, C. Manoil, R. K. Ernst, B. Drees, D. Buckley, E. Haugen, D. Bovee, Y. Zhou, J. Chang, R. Levy, R. Lim, W. Gillett, D. Guenthener, A. Kang, S. A. Shaffer, G. Taylor, J. Chen, B. Gallis, D. A. D'Argenio, M. Forsman, M. V. Olson, D. R. Goodlett, R. Kaul, S. I. Miller, and M. J. Brittnacher.** 2007. Comparison of *Francisella tularensis* genomes reveals evolutionary events associated with the emergence of human pathogenic strains. Genome Biol **8:**R102.

70. **Russell, P., S. M. Eley, M. J. Fulop, D. L. Bell, and R. W. Titball.** 1998. The efficacy of ciprofloxacin and doxycycline against experimental tularaemia. J Antimicrob Chemother **41:**461-465.

71. **Salomonsson, E., K. Kuoppa, A. L. Forslund, C. Zingmark, I. Golovliov, A. Sjostedt, L. Noppa, and A. Forsberg.** 2009. Reintroduction of two deleted virulence loci restores full virulence to the live vaccine strain of *Francisella tularensis*. Infect Immun **77:**3424-3431.

72. **Sandstrom, G., S. Lofgren, and A. Tarnvik.** 1988. A capsule-deficient mutant of *Francisella tularensis* LVS exhibits enhanced sensitivity to killing by serum but diminished sensitivity to killing by polymorphonuclear leukocytes. Infect Immun **56:**1194-1202.

73. **Saslaw, S., H. T. Eigelsbach, J. A. Prior, H. E. Wilson, and S. Carhart.** 1961. Tularemia vaccine study. II. Respiratory challenge. Arch Intern Med **107:**702-714.

74. **Saslaw, S., H. T. Eigelsbach, H. E. Wilson, J. A. Prior, and S. Carhart.** 1961. Tularemia vaccine study. I. Intracutaneous challenge. Arch Intern Med **107:**689-701.

75. **Schulert, G. S., R. L. McCaffrey, B. W. Buchan, S. R. Lindemann, C. Hollenback, B. D. Jones, and L. A. Allen.** 2009. *Francisella tularensis* genes required for inhibition of the neutrophil respiratory burst and intramacrophage growth identified by random transposon mutagenesis of strain LVS. Infect Immun **77:**1324-1336.

76. **Simpson, W. M.** 1929. Tularemia; history, pathology, diagnosis and treatment. Hoeber, New York.

77. **Sjostedt, A.** 2006. Intracellular survival mechanisms of *Francisella tularensis*, a stealth pathogen. Microbes Infect **8:**561-567.

78. **Splettstoesser, W. D., I. Piechotowski, A. Buckendahl, D. Frangoulidis, P. Kaysser, W. Kratzer, P. Kimmig, E. Seibold, and S. O. Brockmann.** 2009. Tularemia in Germany: the tip of the iceberg? Epidemiol Infect **137:**736-743.

79. **Su, J., J. Yang, D. Zhao, T. H. Kawula, J. A. Banas, and J. R. Zhang.** 2007. Genome-wide identification of *Francisella tularensis* virulence determinants. Infect Immun **75:**3089-3101.

80. **Telepnev, M., I. Golovliov, T. Grundstrom, A. Tarnvik, and A. Sjostedt.** 2003. *Francisella tularensis* inhibits Toll-like receptor-mediated activation of intracellular signalling and secretion of TNF-alpha and IL-1 from murine macrophages. Cell Microbiol **5:**41-51.

81. **Thomas, R., A. Johansson, B. Neeson, K. Isherwood, A. Sjostedt, J. Ellis, and R. W. Titball.** 2003. Discrimination of human pathogenic subspecies of *Francisella tularensis* by using restriction fragment length polymorphism. J Clin Microbiol **41:**50-57.

82. **Thomas, R. M., R. W. Titball, P. C. Oyston, K. Griffin, E. Waters, P. G. Hitchen, S. L. Michell, I. D. Grice, J. C. Wilson, and J. L. Prior.** 2007. The immunologically distinct O antigens from *Francisella tularensis* subspecies *tularensis* and *Francisella novicida* are both virulence determinants and protective antigens. Infect Immun **75:**371-378.

83. **Titball, R. W., A. Johansson, and M. Forsman.** 2003. Will the enigma of *Francisella tularensis* virulence soon be solved? Trends Microbiol **11:**118-123.

84. **Treat, J. R., S. D. Hess, K. L. McGowan, A. C. Yan, and C. L. Kovarik.** 2011. Ulceroglandular tularemia. Pediatr Dermatol **28:**318-320.

85. **Vinogradov, E., W. J. Conlan, J. S. Gunn, and M. B. Perry.** 2004. Characterization of the lipopolysaccharide O-antigen of *Francisella novicida* (U112). Carbohydr Res **339:**649-654.

86. **Vinogradov, E. V., A. S. Shashkov, Y. A. Knirel, N. K. Kochetkov, N. V. Tochtamysheva, S. F. Averin, O. V. Goncharova, and V. S. Khlebnikov.**

1991. Structure of the O-antigen of *Francisella tularensis* strain 15. Carbohydr Res **214:**289-297.

87. **Vojtech, L. N., G. E. Sanders, C. Conway, V. Ostland, and J. D. Hansen.** 2009. Host immune response and acute disease in a zebrafish model of *Francisella pathogenesis*. Infect Immun **77:**914-925.

88. **Vonkavaara, M., M. V. Telepnev, P. Ryden, A. Sjostedt, and S. Stoven.** 2008. *Drosophila melanogaster* as a model for elucidating the pathogenicity of *Francisella tularensis*. Cell Microbiol **10:**1327-1338.

89. **Wang, Q., X. Shi, N. Leymarie, G. Madico, J. Sharon, C. E. Costello, and J. Zaia.** 2011. A typical preparation of *Francisella tularensis* O-antigen yields a mixture of three types of saccharides. Biochemistry **50:**10941-10950.

90. **Wang, X., M. J. Karbarz, S. C. McGrath, R. J. Cotter, and C. R. Raetz.** 2004. MsbA transporter-dependent lipid A 1-dephosphorylation on the periplasmic surface of the inner membrane: topography of *Francisella novicida* LpxE expressed in *Escherichia coli*. J Biol Chem **279:**49470-49478.

91. **Wang, X., A. A. Ribeiro, Z. Guan, S. N. Abraham, and C. R. Raetz.** 2007. Attenuated virulence of a *Francisella* mutant lacking the lipid A 4'-phosphatase. Proc Natl Acad Sci U S A **104:**4136-4141.

92. **Wang, X., A. A. Ribeiro, Z. Guan, S. C. McGrath, R. J. Cotter, and C. R. Raetz.** 2006. Structure and biosynthesis of free lipid A molecules that replace lipopolysaccharide in *Francisella tularensis* subsp. *novicida*. Biochemistry **45:**14427-14440.

93. **Wehrly, T. D., A. Chong, K. Virtaneva, D. E. Sturdevant, R. Child, J. A. Edwards, D. Brouwer, V. Nair, E. R. Fischer, L. Wicke, A. J. Curda, J. J. Kupko, 3rd, C. Martens, D. D. Crane, C. M. Bosio, S. F. Porcella, and J. Celli.** 2009. Intracellular biology and virulence determinants of *Francisella tularensis* revealed by transcriptional profiling inside macrophages. Cell Microbiol **11:**1128-1150.

94. **Weiss, D. S., A. Brotcke, T. Henry, J. J. Margolis, K. Chan, and D. M. Monack.** 2007. In vivo negative selection screen identifies genes required for *Francisella* virulence. Proceedings of the National Academy of Sciences of the United States of America **104:**6037-6042.

95. **Whipp, M. J., J. M. Davis, G. Lum, J. de Boer, Y. Zhou, S. W. Bearden, J. M. Petersen, M. C. Chu, and G. Hogg.** 2003. Characterization of a *novicida*-like subspecies of *Francisella tularensis* isolated in Australia. J Med Microbiol **52:**839-842.

96. **White, J. D., J. R. Rooney, P. A. Prickett, E. B. Derrenbacher, C. W. Beard, and W. R. Griffith.** 1964. Pathogenesis of Experimental Respiratory Tularemia in Monkeys. J Infect Dis **114:**277-283.

97. **William B. Wherry, a. B. H. L.** 1914. Infection of man with *Bacterium tularense*. Public Health Bull. **43**.

98. **Woodward, J. M., M. L. Camblin, and M. H. Jobe.** 1969. Influence of bacterial infection on serum enzymes of white rats. Applied microbiology **17:**145-149.

## Chapter 2

## Effects of the putative transcriptional regulator IclR on *Francisella tularensis* pathogenesis[1][2]

### Overview

*Francisella tularensis* is a highly virulent Gram-negative bacterium and is the etiological agent of the disease tularemia. IclR, a presumed transcriptional regulator, is required for full virulence of the animal pathogen, *F. novicida* U112 (46). In this study, we investigated the contribution of IclR to the intracellular growth, virulence and gene regulation of human pathogenic *F. tularensis* subspecies. Deletion of *iclR* from the Live Vaccine and SchuS4 strains of *F. tularensis* subspecies *holarctica* and *tularensis*, respectively, did not affect their ability to replicate within macrophages or epithelial cells. In contrast to *F. novicida iclR* mutants, LVS and SchuS4 Δ*iclR* strains were equally virulent as their wild type parental strains in intranasal inoculation mouse models of

---

[1] Adapted for this dissertation from Mortensen BL, Fuller JR, Taft-Benz S, Kijek TM, Miller CN, Huang MT, and Kawula TH. Effects of the putative transcriptional regulator IclR on *Francisella tularensis* pathogenesis. 2010. Infection and Immunity. **78**:5022-5032.

[2] Attributions: Brittany Mortensen performed all the experiments in this chapter with the following exceptions. Cheryl Miller and Sharon Taft-Benz performed the mouse infections, organ collections, and organ burdens for Figure 3. Cheryl Miller, Sharon Taft-Benz, and Todd Kijek assisted with the mouse infections, organ collections, and organ burdens for Figures 2 and 5.

tularemia. Furthermore, wild type LVS and LVSΔ*iclR* were equally cytotoxic and induced equivalent levels of IL-1β expression by infected bone marrow-derived macrophages. Microarray analysis revealed that the relative expression of a limited number of genes differed significantly between LVS wild type and *iclR* strains. Interestingly, many of the identified genes were disrupted in LVS and SchuS4 but not in their corresponding *F. novicida* U112 homologs. Thus, in spite of the impact of *iclR* deletion on gene expression, and in contrast to the effects of *iclR* deletion on *F. novicida* virulence, IclR does not contribute significantly to the virulence or pathogenesis of *F. tularensis.*

## Introduction

*Francisella tularensis* is a Gram-negative bacterium and the etiological agent of tularemia or "rabbit fever". While zoonotic hosts include small mammals such as rabbits and voles, *F. tularensis* is also found in ticks, mosquitoes, and flies, and can replicate within amoebae as well (24). Human infection with *F. tularensis* can occur by several routes including bites by arthropod vectors (1, 2, 28), contact with contaminated tissues, ingestion of contaminated food or water (23, 37), or inhalation of aerosolized bacteria (15, 41). *F. tularensis* is considered a Select Agent by the Centers for Disease Control due to its low infectious dose (as few as 10 organisms) via the pulmonary route and its potential as a biological threat agent (12, 39).

There are two *F. tularensis* subspecies most commonly associated with disease in humans: *F. tularensis* subspecies *tularensis* (Type A) and *F. tularensis* subsp. *holarctica* (Type B). The Live Vaccine Strain (LVS) of subsp. *holarctica* is a useful model for studying the virulent *F. tularensis* subspecies, because it causes disease in mice, is

attenuated in humans (16), and shares genomic and proteomic similarity with *F. tularensis* subsp. *holarctica* and *tularensis* (44). *F. novicida*, which does not cause disease in healthy humans, has significant similarity with *F. tularensis* subsp. *holarctica* and *tularensis* and is also used as model organism for studying *F. tularensis* pathogenesis. Although there are reports of *F. novicida* causing disease, these cases are commonly associated with immunocompromised individuals (3, 8) However, *F. novicida* does cause a severe disease in *in vivo* mouse models (34).

*Francisella* is known to predominately infect and replicate within macrophages but also infects and replicates within neutrophils (31), dendritic cells (4) and Type II alveolar epithelial cells (19). After phagocytosis, *F. tularensis* escapes the phagosome and replicates within the cytoplasm of host cells (9). Numerous *in vitro* and *in vivo* screens have identified virulence factors required for this intracellular life cycle (11, 22, 25, 29, 35, 40, 42, 46); however, many of the identified virulence factors have little or no similarity to known proteins of other bacteria and their functions remain, for the most part, unknown.

Weiss et al. recently identified a locus (FTN_0720) in *F. novicida* U112 that is important for virulence in mice as determined by an *in vivo* competition assay between a FTN_0720 deletion mutant and wild type U112 (46). FTN_0720 encodes a protein with homology to the IclR family of transcriptional regulators. IclR family members activate and repress genes in a wide range of bacteria including genes involved in sporulation, metabolism, drug-efflux pumps and organic solvent tolerance, and phytopathogenicity (33). Given the close genetic relationship among *F. tularensis* and *F. novicida*, the phenotype of the *F. novicida iclR* deletion strain suggests that IclR may be involved in

the pathogenicity of the *F. tularensis* subspecies *holarctica* and *tularensis*. We investigated the contribution of IclR homologs in the pathogenicity of *F. tularensis* subsp. *holarctica* and *tularensis* by evaluating the role of IclR in gene expression, host cell interactions and virulence of *F. tularensis* subsp. *holarctica* LVS (FTL_1364) and subsp. *tularensis* SchuS4 (FTT_0748) strains.

## Materials And Methods

### *Bacterial strains*

*F. tularensis* subsp. *holarctica* LVS was obtained from the CDC, Atlanta, GA. *F. tularensis* subsp. *tularensis* SchuS4 was obtained from BEI Resources. *F. novicida* U112 was obtained from the American Type Culture 88 Collection (ATCC). An *iclR* transposon mutant was one of two mutants from the transposon mutant library (21) and was received as a gift from Colin Manoil. All strains were maintained on chocolate agar supplemented with 1% IsoVitaleX (Becton-Dickson), brain heart infusion (BHI) broth supplemented with 1% IsoVitaleX or Chamberlain's defined medium (CDM) (5). *Escherichia coli* TOP10 (Invitrogen) were used for cloning purposes. *E. coli* was propagated in Luria broth supplemented with hygromycin at 200 μg/ml or kanamycin at 20 μg/ml as necessary for antibiotic selection. All cultures were grown at 37°C.

### *Cell Culture*

J774A.1 (ATCC TIB-67) cells are a macrophage-like cell line derived from mouse sarcoma reticulum cells and were cultured in Dulbecco's minimal essential medium with 4.5 g/L glucose, 10% fetal bovine serum, and 2 mM L-glutamine. TC-1

(ATCC CRL-2785) cells are a tumor cell line derived from mouse primary lung epithelial cells and were cultured in RPMI 1640 supplemented with 10% fetal bovine serum, 2 mM L-glutamine, 1.5 g/L sodium bicarbonate, 10 mM HEPES and 0.1 mM nonessential amino acids. Bone marrow-derived macrophages were generated by flushing bone marrow cells from C57BL/6 mouse femurs and recovered cells were incubated for 6 days on 15 $cm^2$ non-tissue culture-treated dishes in L929 cell-conditioned DMEM. Nonadherent cells were removed by washing with phosphate-buffered saline (PBS) and bone marrow-derived macrophages were recovered from the dish using 1 mM EDTA in PBS.

***Molecular techniques and allelic exchange***

For both LVS and SchuS4 the *iclR* deletion was generated by splice overlap extension (SOE) PCR using primers designed to amplify the 5' and 3' regions of the *iclR* locus, which were then annealed to their complementary, homologous genomic DNA tags (17, 20). The subsequent deletion left only the first six amino acids and the stop codon of *iclR*. Each construct was cloned into the pCR-Blunt II TOPO vector (Invitrogen), verified by DNA sequence analysis, and subsequently cloned into pMP590 (*sacB* $Kan^r$) using BamHI and NotI restriction sites (17, 27). For allelic exchange, plasmids were electroporated into LVS or SchuS4 and integrants were selected on chocolate agar containing kanamycin (10 μg/ml). $Kan^r$ strains were grown overnight and plated on 10% sucrose for counterselection (loss of plasmid) (17, 27). Both the LVS and SchuS4 *iclR* deletion strains were confirmed for loss of *iclR* by PCR. For complementation of the *iclR* deletion in LVS, *iclR* and its predicted promoter were PCR-amplified and subcloned into the pCR-Blunt II TOPO vector (Invitrogen). After a

MluI/EcoRV restriction digest, the construct was ligated into the pMP633 low-copy *Francisella* shuttle vector (17) and electroporated into LVSΔ*iclR*. Complementation was determined by detection of *iclR* in the complementation strain via PCR as well as demonstration of increased *iclR* transcript levels via microarray analysis (data not shown).

***Gentamicin protection assays***

Gentamicin protection assays were performed as described (17, 19). Briefly, J774A.1 murine macrophages, TC-1 murine lung epithelial cells, or bone marrow-derived macrophages were infected with LVS or SchuS4 at an MOI of 100. Cells were incubated with the bacterial inoculum for 2 hr (J774A.1 and bone marrow-derived macrophages) or 4 hr (TC-1) and then incubated with media containing 25 μg/ml gentamicin for an additional 2 hr to kill extracellular bacteria. At time points of 4 hr (or 6 hr for TC-1) and 24 hr, medium was removed, cells were washed with PBS and then scraped from the dish, and the bacteria serially diluted and plated to determine the number of viable bacteria.

***Mouse infections***

6- to 8-week-old C57BL/6 mice were anesthetized intraperitoneally (i.p) with avertin and then inoculated intranasally (i.n.) with bacteria suspended in 50 μl PBS by application to the nares of each mouse or inoculated intradermally (i.d.) by injection into the tail using the same volume. Concentrations of LVS and U112 were determined by klett and concentrations of SchuS4 by spectrophotometer (OD600), and inocula were serially diluted and plated on chocolate agar to confirm the CFU administered. At the

designated time points, mice were euthanized and the lungs, liver and spleen of each mouse were removed and homogenized. Serial dilutions of the homogenates were plated on chocolate agar to enumerate the bacterial organ burdens. Statistical significance between strains in each organ and at each time point was determined by the Mann-Whitney nonparametric test using GraphPad Prism v.5 software. All animal experiments were performed according to the animal care and use guidelines as established by IACUC-approved protocols.

***IL-1β ELISAs and cytotoxicity assays***

Bone marrow-derived macrophages were seeded in 12-well dishes at $1x10^6$ cells per well, and infected with bacteria at an MOI of 500 in a final volume of 1 ml medium per well and incubated at 37°C. After 24 hr, the supernatants from each well were collected, centrifuged to pellet cellular debris, and stored at -20°C. The IL-1β ELISA was performed using the BD OptEIA mouse IL-1β ELISA kit (BD Biosciences) according to the manufacturer's protocol. The $OD_{450}$ was read using a TECAN Infinite M200 and analyzed using Magellan v6 software. Cytotoxicity assays were performed using the ToxiLight® BioAssay kit (Lonza) following the manufacturer's protocol for cytokine detection from supernatants, and the luminescence was read using a TECAN Infinite M200 and analyzed using Magellan v6 software. Statistical significance between each strain was determined by the student's t-test using GraphPad Prism v.5 software.

***Microarrays***

RNA was obtained using the RiboPure-Bacteria kit (Ambion) according to the manufacturer's protocol. Briefly, bacteria were grown to early mid-log phase in CDM

and pelleted. Cells were disrupted by suspension in Trizol and vortexing with 0.1 mm glass beads. Purified RNA was recovered by chloroform extraction followed by treatment with DNase I to remove DNA. Microarray analysis was performed following the guidelines provided by the Venter Institute for Genomic Research (SOP#M007, M008). Briefly, aminoallyl labeled cDNA was generated from 2 μg total RNA using SuperScript III reverse transcriptase (Invitrogen), random hexamers, and dNTPs containing aa-UTP. After removal of unincorporated aa-dUTP and free amines, labeled cDNA was coupled to Cy3 or Cy5 mono-reactive dye (GE Healthcare). The *Francisella* microarray slides (Pathogen Functional Genomics Resource Center; PFGRC) contained 2331 70mer oligonucleotides in quadruplicates of the *F. tularensis* SchuS4 genome and several LVS genes as well as quadruplicates of 70mer oligonucleotides for 500 *Arabidopsis thaliana* as controls. Slides were prehybridized in 5x SSC, 10% SDS and 1% BSA, washed and then hybridized with cDNA probes at 42°C. After post-hybridization washes, the slides were scanned using the GenePix 4000B scanner and GenePix Pro v6.0 software. The microarray data were normalized using the TIGR MIDAS v2.22 and analyzed using the TIGR Multiexperiment Viewer v 4.2.1 (MeV) as part of the TM4 Suite software (45). In MeV, pooled, normalized Cy5/Cy3 intensities from wild type LVS control arrays were compared to pooled, normalized Cy5/Cy3 intensities from LVSΔ*iclR* arrays. This list was filtered by statistical significance using Significance Analysis for Microarrays (SAM) provided on MeV after 179 an 80% cut-off filter and using a false discovery rate of 5%.

***Quantitative RT-PCR***

Quantitative RT-PCR was performed in a 96-well format using the SensiMix™ SYBR & Fluorescein One-Step kit (Bioline) following the manufacturer's protocol.

Briefly, 50 ng of RNA isolated from wild type or *iclR* mutant strains was mixed with SensiMix™ SYBR & Fluorescein, RNase inhibitors, and designated primers in a 20 µl volume. A genomic DNA ladder and a no reverse transcriptase control were analyzed using the SensiMix™ SYBR & Fluorescein kit following the manufacturer's protocol with primers to *gyrA*. Thermocycling and detection was performed using the iCycler Thermal Cycler (Bio-Rad). All starting quantity (SQ) values were normalized to the mean SQ value for *gyrA*.

***Antibiotic sensitivity assays***

*F. tularensis* LVS was grown to mid-log phase in BHI broth supplemented with 1% IsoVitaleX, the bacterial suspension was spread onto chocolate agar plates, and antibiotic-containing filter paper discs were placed in the center of each plate. The rafampin (5µg), tetracycline (30µg), and colistin (10µg) were purchased pre-loaded from Becton Dickinson. The ampicillin and polymyxin B discs were self-prepared by adding a 10 µl or 20 µl volume of antibiotic per disc at 10 µg ampicillin or 20 µg polymyxin B. Bacteria were grown for 36 hr and the diameter of the zone of inhibition was measured.

***Microarray data accession numbers***

The raw and normalized microarray 199 data is available on the GEO database under the following accession numbers: GSM574374, GSM574375, GSM574376, GSM574377, GSM574379, GSM574380, and GSE23454.

## Results

### *Comparison of iclR alleles among F. tularensis subspecies and construction of iclR deletion mutants*

The locus FTL_1364 is annotated as a hypothetical protein in NCBI; however, some of its homologs in other *Francisella* species are annotated as proteins belonging to the IclR family of transcriptional regulators. A search for conserved domains found within FTL_1364 resulted in several related hits including a helix-turn-helix (HTH) domain conserved among IclR family members. Additionally, *Francisella* IclR has a C-terminal domain with high similarity to the IclR family profile Pfam01614. A recent publication describes a highly specific IclR family member profile that lies outside the HTH domain and covers less than 100 amino acids in the central region towards the C-terminal end (26). These authors classify current Pfam01614 members as belonging to the IclR family based on the new profile. Furthermore, BLASTp analysis of *F. tularensis* LVS or SchuS4 IclR reveals high similarity to IclR family proteins found across many bacterial species. *F. tularensis* IclR proteins share considerable amino acid identity (30-40%) and amino acid similarity (60%) with non-*Francisella* IclR family proteins. Overall, the bioinformatic analysis strongly suggests that *Francisella* FTL_1364 and its homologous loci in other *Francisella* species encode a protein belonging 220 to the IclR family of transcriptional regulators.

Using NCBI and the *Francisella* genome browser (www.francisella.org) for annotations and synteny analysis, we found that the *iclR* locus has shared characteristics among *F. novicida* U112, *F. tularensis* subsp. *holarctica* LVS, and *F. tularensis* subsp. *tularensis* SchuS4 strains (FTN_0720, FTL_1364 and FTT_0748, respectively), (Figure 1A). On one side of *iclR* in each strain is a gene encoding a predicted protein with

similarity to an esterase lipase (FTL_1363, FTN_0721, and FTT_0749). On the other side of *iclR* is a gene encoding a predicted protein with similarity to the multidrug efflux protein EmrA (FTL_1365-66, FTN_0718, and FTT_0747). One difference is that EmrA is divided into two ORFs in LVS. There are other differences in the length and coding sequences of this genetic region, including an additional open reading frame in U112 that encodes a predicted protein of unknown function FTN_0719. Nevertheless, in each strain, *iclR* is located in a similar region of the genome.

Additionally, *iclR* itself is highly conserved among the three *F. tularensis* strains U112, LVS and SchuS4. SchuS4 *iclR* has three nucleotide differences compared to *iclR* from LVS that translate into two amino acid differences, S22G and H78Y, between LVS and SchuS4 IclR. U112 *iclR* has 95 nucleotide differences compared to LVS *iclR* and 94 nucleotide changes compared to SchuS4 *iclR*. Although this results in a three nucleotide truncation of U112 *iclR*, there is 80% amino acid identity between U112 IclR and SchuS4 and LVS IclR proteins (Figure 1B). While these similarities suggest that IclR is conserved among the U112, LVS, and SchuS4, there are a sufficient number of differences to account for possible functional deviations between these strains as well. Due to genetic similarity and the contribution of IclR to the virulence for *F. tularensis* subsp. *novicida*, we investigated the potential contribution of IclR to the virulence of *F. tularensis* subspecies *holarctica* and *tularensis*. To do this, we made a clean deletion of the *iclR* gene in the *F. tularensis* subspecies holarctica LVS (LVSΔ*iclR*) and SchuS4 (SchuS4Δ*iclR*) using SOE PCR and allelic exchange in LVS (FTL_1364). We also generated an *iclR* complementation strain by expression of *iclR* on a low-copy shuttle vector.

***LVS and SchuS4 iclR deletion mutants are competent for intracellular replication***

One method to assess the contribution of IclR to *F. tularensis* virulence is to determine what role IclR plays in intracellular replication. We used gentamicin protection assays in the J774A.1 murine macrophage-like cell line and the TC-1 murine lung epithelial cell-like cell line to assess intracellular replication by *iclR* deletion mutant strains. Both LVSΔ*iclR* and wild type LVS replicated approximately two logs by 24 hr in both J774A.1 and TC-1 cells (Figure 2A-B). We also performed these assays in bone marrow-derived macrophages, and both wild type LVS and LVSΔ*iclR* replicated intracellularly in these cells (Figure 2C). Similarly, the intracellular replication of SchuS4Δ*iclR* was similar to wild type SchuS4 in J774A.1 cells (Figure 2D). These results demonstrate that IclR is not required for intracellular replication of LVS or SchuS4 in these cell types.

***LVSΔiclR is not attenuated following intranasal or intradermal inoculation of mice***

Properties other than intracellular replication contribute to *F. tularensis* pathogenesis. We therefore determined whether IclR was required for LVS virulence *in vivo*. To test this, we used a mouse model of pulmonary tularemia in which we inoculated C57BL/6 mice i.n. with a lethal dose ($1x10^5$ CFU) of LVS or LVSΔ*iclR*. At 1, 3, 7 and 8 days post inoculation the lungs, liver and spleen were harvested to enumerate the bacterial organ burdens (Figure 3A). These initial experiments revealed that there were no differences in the organ burdens at 1 or 3 days post inoculation. At day 7, there appeared to be slight differences in the organ burdens in the liver and spleen, and by day 8 the organ burdens in the liver and spleen had not increased. These initial experiments suggested that LVSΔ*iclR* may demonstrate enhanced clearance in the mouse. This would

correlate with previously published data demonstrating a decrease in competitive index in the spleen at 48 hr for the *F. novicida* U112 *iclR* deletion mutant compared to wild type *F. novicida* U112 (46).

To further investigate the possibility of a subtle phenotype of enhanced clearance, we used a low dose ($1x10^3$ CFU) i.n. inoculation of groups of six wild type C57BL/6 mice with LVS or LVSΔ*iclR*. At days 1, 3, 7 and 10 post inoculation, we again harvested the lungs, liver and spleen to calculate the bacterial organ burdens. There were no significant differences between the bacterial organ burdens of LVSΔ*iclR* or wild type LVS at any time point (Figure 3B). This suggests that LVSΔ*iclR* is not attenuated in a mouse model of pulmonary tularemia.

Since the experiments with *F. novicida* U112 *iclR* deletion mutant were performed using subcutaneous (s.c.) and i.p. inoculation, we investigated whether a role for *iclR* in pathogenesis may be route-specific. Groups of 6 to 7 wild type C57BL/6 mice were infected i.d. with $3x10^5$ CFU of LVS or LVSΔ*iclR*. The i.d. route has a comparable $LD_{50}$ dose and is similar in nature to the s.c. route (14). At 1, 3, and 7 days post inoculation, we again harvested the lungs, liver and spleen and determined bacterial organ burdens. At each time point and in each organ, there was no significant difference in the bacterial burdens comparing LVS and LVSΔ*iclR* (Figure 3C). These data indicate that in LVS, *iclR* is not required for pathogenesis in the mouse via the i.n. or i.d. route.

***SchuS4ΔiclR is not attenuated following intranasal inoculation of mice***

Although *iclR* does not appear to be required for LVS pathogenesis, it is possible that *iclR* plays a role in SchuS4 pathogenesis. We inoculated groups of four wild type C57BL/6 mice i.n. with a lethal dose (100 CFU) of wild type SchuS4 or SchuS4Δ*iclR*. At

1 and 3 days post inoculation, the lungs, liver and spleen were harvested to enumerate the bacterial organ burdens of infected mice (Figure 4). At both time points and in each organ, there were no differences in bacterial burden between wild type SchuS4 and SchuS4Δ*iclR*. These data suggest that IclR does not play a role in the in vivo virulence of SchuS4 when assessed by the mouse model of pulmonary tularemia.

***F. novicida U112 iclR transposon mutant is attenuated following intranasal inoculation of mice***

As noted above, an *iclR* deletion mutant in *F. novicida* U112 displays decreased competitive index in the spleen following s.c. and i.p inoculation of mice (53). Therefore, we wanted to determine whether *iclR* is required for *F.* novicida U112 pathogenesis in a pulmonary mouse model. We inoculated groups of six wild type C57BL/6 mice i.n. with a dose of approximately 10 CFU of wild type U112 or a U112 *iclR* transposon mutant. At 1 and 5 days post inoculation, the lungs, liver and spleen were harvested and the bacterial organ burdens were enumerated. Each organ had reduced burdens of the *iclR* transposon mutant compared to wild type U112, and at day 5 these differences were statistically significant in the liver and spleen (Figure 5). These data suggest that *iclR* is required for U112 pathogenesis via the i.n. route and correlates with the previously published data using the s.c. and i.p. routes.

***Deletion of iclR does not affect IL-1β expression or cytotoxicity of infected cells***

To determine if there is an altered cellular response to LVSΔ*iclR* compared to wild type LVS, we measured the production of pro-inflammatory cytokines by infected cells. Bone marrow-derived macrophages were infected at an MOI of 500 with LVS or LVSΔ*iclR* and the supernatants were analyzed for IL-1β at 24 hr post infection (Figure

6A). The levels of IL-1β measured in the supernatants of LVSΔ*iclR*-infected cells was similar to that of cells infected with wild type LVS, and no differences between strains were statistically significant.

*F. tularensis* is also reported to induce cytotoxicity of infected macrophages. To determine whether there was a change in cytotoxicity induced by LVSΔ*iclR*, we infected murine bone marrow-derived macrophages with LVS or LVSΔ*iclR* at an MOI of 500 and performed cytotoxicity assays on supernatants collected at 24 hr post infection. As shown in Figure 6B, LVSΔ*iclR* induces cytotoxicity in infected cells to a level similar to that of wild type LVS, and no differences between strains were statistically significant.

***The effects of IclR on gene expression***

Due to its homology to transcriptional regulators, we used microarray analysis to determine what genes in LVS were affected by IclR by comparing gene expression between the LVSΔ*iclR* mutant and wild type LVS. We grew LVS and LVSΔ*iclR* to mid-log phase to harvest RNA for reverse transcription and amino-allyl labeling of cDNA, and the labeled cDNA was hybridized to microarray slides. The slides are printed for every annotated ORF for SchuS4, plus LVS alleles that are either not present or are variant in SchuS4, but they are not tailored to *F. novicida*. Three separate microarrays from independent RNA samples were pooled and statistically significant gene expression differences between LVSΔ*iclR* and wild type LVS were determined by SAM (Table 1). Genes exhibiting significant changes in expression are listed by the provided locus annotations, LVS or SchuS4, as printed on the slides.

Using the above criteria, we identified 13 downregulated and 4 upregulated genes in LVSΔ*iclR*. The list of genes identified comprises diverse functional groups suggesting

that IclR does not impact expression of one specific functional group of proteins. There were several IclR-affected genes annotated as encoding hypothetical proteins. To get a better idea of what types of proteins these genes may be encoding and possibly obtain insight on IclR function, we performed BLASTp analyses. Many of the proteins were only conserved in *Francisella* with no similarity to proteins or conserved domains in other bacteria. However, there were several with similarity to known proteins in other bacteria and these are described in Table 1. Although most of the genes were represented exclusively by the SchuS4 allele, there were two cases where the SchuS4 and LVS homologs were both printed on the microarray slide and also appeared on the gene list as having significant expression changes in the absence of IclR. FTT_0741c and its FTL_1373 homolog were both upregulated in LVSΔ*iclR*, and both FTL_0388 and its homolog FTT_0885 were downregulated in LVSΔ*iclR*. Overall, although further studies need to be performed to demonstrate a function of IclR, both bioinformatic and microarray data suggest that *Francisella* IclR could function as a transcriptional regulator.

***Comparison of IclR-regulated genes between LVS, SchuS4 and U112***

One explanation for the phenotypic differences observed for *iclR* mutants among the *F. novicida* U112*, F. tularensis,* LVS and SchuS4 strains could be due to differences in the genes affected by IclR among the strains. To address this we performed a more detailed examination of the genes on our microarray list. First, we performed synteny analysis using the genome synteny tool at www.francisella.org to determine whether each gene was annotated in SchuS4, LVS and U112. We observed that there were a few genes that were not annotated or not present in all three strains, as shown in Table 1. Secondly,

we generated alignments and protein translations of the genes using Vector NTI software based on the NCBI annotation or the putative loci of non-annotated genes from the synteny analysis, if they were found. For example, sequence alignments revealed that in LVS there is an unannotated ORF between FTL_1120 and FTL_1121 bearing homology to FTT_1082. Nearly half of the genes were similarly annotated and encoded one intact open reading frame (ORF) in SchuS4, LVS and U112. However, a significant percentage of genes displayed considerable sequence differences between strains as described in Table 1.

Of these genes, many were not intact in the virulent strains LVS and/or SchuS4, whereas the homologous genes in U112 were intact. For example, FTL_1506 and FTL_1507 are pseudogenes because they encode two ORFs while their SchuS4 (FTT_0723c) and U112 (FTN_0634) encode only one ORF. One special case is FTT0715, which along with its LVS homolog FTL_1521, has two large deletions, 131bp (119bp in LVS) and 197bp, when compared to the U112 homolog FTN_0627. The significance of these deletions cannot be inferred, and though these genes are not pseudogenes, the fact that these large deletions are present only in SchuS4 and LVS is noteworthy. This also highlights the fact that many of the intact genes on the microarray list have greater overall sequence differences between U112 and LVS or SchuS4 when compared to that of the differences between LVS and SchuS4.

We next wanted to determine whether the set of genes that were changed in expression in LVSΔ*iclR* were also changed in the absence of IclR in U112. First, we performed quantitative RT-PCR on six genes that were differentially-regulated in the microarray for LVS versus LVSΔ*iclR* (Figure 7A) and normalized to the housekeeping

gene *gyrA*. We also included *iclR*. As expected, we detected a dramatic decrease in *iclR* transcript in LVSΔ*iclR* and negligible change in *gyrA*. Of the six genes analyzed, four repeated the trend seen in the microarray analysis. For the two genes that did not, the primers appeared to amplify with similar efficiencies to other primers (data not shown). Overall, the qRT-PCR data supports the fact that the genes identified in our microarray are changed in expression in the absence of IclR using a different method. We then tested the same set of gene homologs on RNA isolated from wild type U112 and the U112 *iclR* transposon mutant (Figure 7B). Quantitative RT-PCR first verified that *iclR* transcripts were substantially lower in the transposon mutant. Overall, the six selected genes appear to be changed similarly to their LVS homologs, suggesting a similar set of genes affected by IclR in U112. These analyses do not account for any additional genes affected by U112 IclR that were not affected by LVS IclR as detected by microarray. Furthermore, these analyses alone are not sufficient to extrapolate any correlations in terms of IclR function or which of the IclR-affected genes are likewise impacted at the protein level or functional.

***The effects of IclR on antibiotic resistance***

Other IclR family proteins are known to be involved in the regulation of multi-drug efflux pumps (33). In *F. novicida* and *F. tularensis* subspecies, *iclR* is located near ORFs encoding hypothetical proteins that have homology to the EmrA multidrug efflux pump. In LVS, the two ORFs encoding proteins with EmrA homology that are found upstream of *iclR* were not changed in expression as determined by our microarray analysis. Nevertheless, the microarray data for LVSΔ*iclR* showed increased expression of

a gene encoding a protein with homology to organic solvent tolerance proteins, suggesting that IclR may be involved in repression of some genes involved in drug efflux. Organic solvent tolerance is often associated with multi-drug efflux pumps, most notably in *Escherichia coli* and *Pseudomonas putida* (36). Furthermore, our BLASTp analyses of hypothetical genes that appear in the LVSΔ*iclR* microarray gene list also reveal proteins with homology to other transporter proteins. To determine whether *iclR* is involved with drug efflux, we performed disc diffusion assays using a panel of antibiotics. Antibiotics selected for analysis were chosen as representatives from several classes of antibiotics targeting cell wall synthesis, protein synthesis, nucleic acid synthesis, and cell membrane integrity. There was no difference in antibiotic sensitivity between wild type LVS and LVSΔ*iclR* using this method (Figure 8).

## Discussion

Herein we investigated the contribution of the putative transcriptional regulator IclR to *F. tularensis* pathogenicity. In this study, we found that the LVSΔ*iclR* was not attenuated for intracellular replication in J774A.1 macrophage-like cells, TC-1 epithelial cells, or bone marrow-derived macrophages. Similarly, SchuS4Δ*iclR* was not attenuated for replication in J774A.1 cells. These data are consistent with published data by Weiss et al. for the *F. novicida* U112 *iclR* deletion mutant strain in bone-marrow derived macrophages (46).

When compared to wild type LVS, LVSΔ*iclR* did not impact IL-1β induction or cytotoxicity of infected cells, which is different from that of the published *F. novicida* studies (46). It is important to note that the methods used for these analyses were

different between the two studies. The levels of IL-1β that we reported in this study are near but not below the limit of detection for the ELISA. The fact that the levels of IL-1β induced are low is consistent with other studies evidencing that LVS suppresses the inflammatory response (21, 43). Furthermore, Weiss et al. used pre-stimulated bone marrow-derived macrophages, whereas we used naïve bone marrow-derived macrophages. Macrophages pre-treated with LPS or heat-killed *F. novicida* as well as thioglycolate-elicited macrophages produce higher levels of IL-1β in response to infection (9, 10, 30, 45). Another possibility is that there are strain-specific differences in the role of IclR, as evidenced by the results of the in vivo studies discussed below.

Unlike the *F. novicida iclR* deletion mutant, neither LVSΔ*iclR* nor SchuS4Δ*iclR* were attenuated in mice following i.n. inoculation. There were differences in the experimental design between our studies and the *novicida* study. We initially inoculated mice i.n. and monitored lung, liver, and spleen over several days post infection. Weiss et al. used s.c. and i.p. inoculations in competition assays examining the spleen at 2 days post infection. It is possible that inoculation route may have an impact on the importance of IclR on establishing infection. To address the possibility that the phenotype is route-specific, we performed a reciprocal analysis by evaluating the virulence of LVS and U112 *iclR* mutants in i.d. and i.n. infection models, respectively. The results confirmed that the *Francisella* virulence-specific properties of IclR are restricted to *F. novicida*.

It is not clear why IclR is required for virulence in U112 but not LVS and SchuS4. Based on our microarray analysis, the species-specific sequence differences among IclR-affected genes could contribute to the functional differences we observe for IclR between species. Many of the genes are intact in U112, but in LVS and/or SchuS4,

the homologous genes are pseudogenes or displayed significant sequence variation (e.g. two large deletions in FTT0715/FTL_1521). The virulent subspecies of *F. tularensis* are noted for their genome decay as characterized by smaller genomes as well as increased numbers of pseudogenes, transposases and gene rearrangements (44). Genome-wide analyses of *Francisella* strains support this idea and many of the genes changed in LVSΔ*iclR* that we identified to be pseudogenes correlate with those found in other studies (6, 38). It is possible that IclR in *F. novicida* exerts its effects on genes that are intact whereas in LVS and SchuS4, IclR affects genes that are similar to those in *F. novicida* but because of disruptions or changes to the ORFs, many of these genes are transcribed but do not encode functional proteins. We must also consider that there are two genes in the list that are absent in U112 that are present in LVS and SchuS4, and the absence of a gene affected by IclR in *novicida* could also contribute to the different phenotypes. Overall, analysis of the genes identified in our microarray suggest that the majority of genes affected by IclR have differences in sequence between the three species and that this variation could contribute to the phenotypic disparities observed.

Taken together, our data suggest that IclR contributes to the virulence of U112 but not to that of LVS or SchuS4, highlighting the fact that there are significant differences among these strains. Another example of differences among strains is seen in the conserved acid phosphatases AcpA, AcpB, and AcpC. These proteins were shown to be required for the virulence of *F. novicida*, but not for the virulence of SchuS4 (7, 32). Even though IclR may not play a major role in SchuS4 or LVS virulence, there are other potential roles that IclR could be have as a functional transcriptional regulator. Quite a few of the microarray-identified genes encode hypothetical proteins, but there are others

that encode proteins with known functions or are homologous to proteins with known functions. Investigation into these proteins may provide an additional understanding of the function of IclR in *F. tularensis*. For example, in *Pseudomonas putida*, the IclR family proteins TtgT and TtgV regulate operons encoding genes that form efflux pumps for organic solvent extrusion (13, 18). Although our antibiotic sensitivity assays showed no role for IclR in drug efflux by LVS, we cannot rule out the involvement of IclR in the regulation of a system specific for organic solvent efflux or the role of IclR in drug efflux in other *Francisella* species. Finally, direct comparison of the complete transcriptional profiles of *F. novicida*, and *F. tularensis iclR* deletion strains might reveal some clues to the properties that are responsible for the phenotypic differences. Unfortunately, the currently available microarrays do not contain targets for genes found exclusively in *F. novicida*.

# Figures

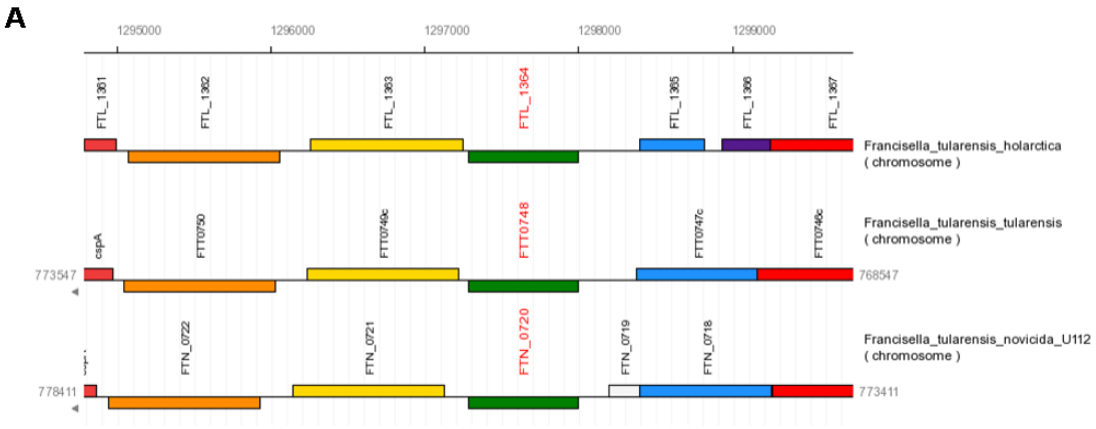


B

```
                1                                                  50
FTN_0720    (1) MSEDKRIQVISRAVNVLKSIGSKPDGMSLGEIAKQIYLPRSTVQRIVAAL
FTL_1364    (1) MSEDKRIQVISRAVNVLKSIGSKPDGMSLGEIAKQIYLPRSTVQRIVAAL
FTT_0748    (1) MSEDKRIQVISRAVNVLKSIGGKPDGMSLGEIAKQIYLPRSTVQRIVAAL
                51                                                 100
FTN_0720   (51) EEEGFIRSEGAGKILLGPGIFKLISSCYVDIITLTQDSLSKLSEKVQETV
FTL_1364   (51) EEEGFIKSEGAGKILLGPGIFKLISSSHADIISLTQDSLSKLSAKIQETV
FTT_0748   (51) EEEGFIKSEGAGKILLGPGIFKLISSSYADIISLTQDSLSKLSAKIQETV
                101                                                150
FTN_0720  (101) SLTQSYDKNLLVLHRFVVNRELQIIPRVGALVPLHKTAAGRALLSLHTDD
FTL_1364  (101) VITQPYDSDLLIVHRFIINRELQVLPRVGALIPIYNSSSGRAILALHTDD
FTT_0748  (101) VITQPYDSDLLIVHRFIINRELQVLPRVGALIPIYNSSSGRAILALHTDD
                151                                                200
FTN_0720  (151) KIIKILGEQITDDKELFEKIAKIRVKGIDIDYSQTIKGIVTIGVAIKSFL
FTL_1364  (151) KIIEILGEQIPDDKELFEKIAKIRADGIEFDYGKVIKGIVSIGVAINTFL
FTT_0748  (151) KIIEILGEQIPDDKELFEKIAKIRADGIEFDYGKVIKGIVSIGVAINTFL
                201                                240
FTN_0720  (201) GDFGVSILAPQHRFDQNKDLYVDELLKVKSKIIDEIGV--
FTL_1364  (201) GTFGISILTPQHRFDKYKEFYVNELLKTKSKIIDEIGIK-
FTT_0748  (201) GTFGISILTPQHRFDKYKEFYVNELLKTKSKIIDEIGIK-
```

**Figure 2.1. Comparison of iclR in three *Francisella* strains**

(A) Synteny diagram of the genomic organization of the *iclR* locus in *F. novicida* U112 (FTN_0720), *F. tularensis* subspecies *holarctica* LVS (FTL_1364), and *F. tularensis* subspecies *tularensis* SchuS4 (FTT_0748). (B) Amino acid sequence alignment of *F. novicida* U112, *F. tularensis* subspecies *holarctica* LVS, and *F. tularensis* subspecies *tularensis* SchuS4 IclR. Alignment was created using VectorNTI software and *iclR* sequences uploaded from NCBI annotated genomes of each strain and translated using VectorNTI. Red letters highlight residues conserved between all three strains. Blue letters highlight the residues conserved between two strains.

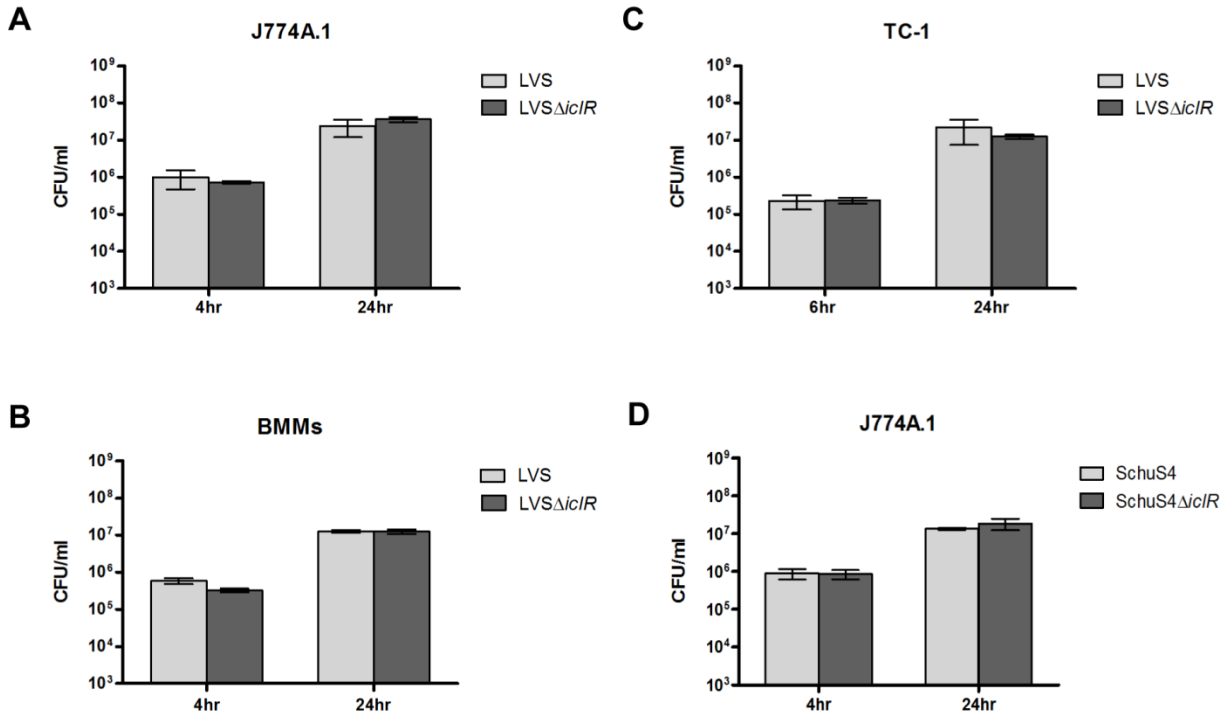


**Figure 2.2. Intracellular replication of LVSΔ*iclR* and SchuS4Δ*iclR***

Gentamicin protection assays were performed by infecting (A) J774A.1 murine macrophages, (B) TC-1 murine lung epithelial cells, and (C) bone marrow-derived macrophages with wild type LVS or LVSΔ*iclR* at an MOI of 100. (D) Gentamicin protection assay was performed using J774A.1 cells infected with wild type SchuS4 or SchuS4Δ*iclR*. Bars represent the standard deviation of three replicate wells and each graph is representative of two separate experiments.

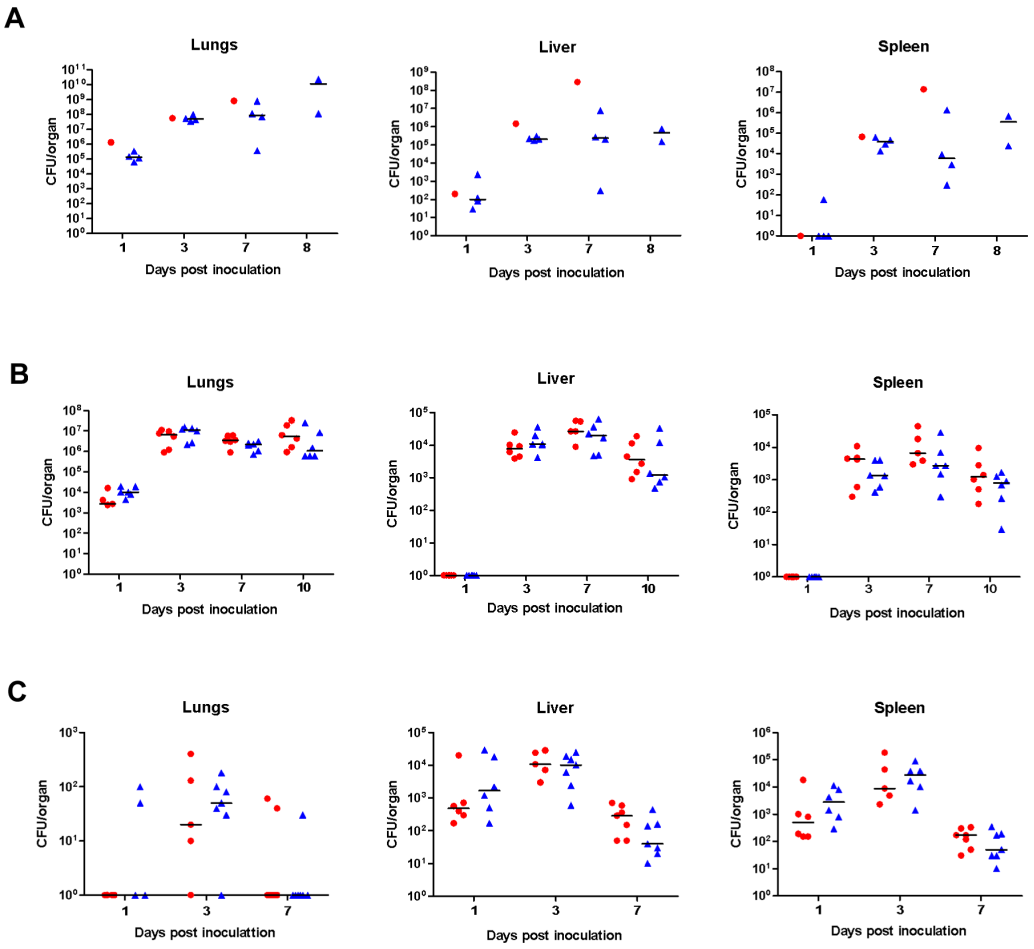


**Figure 2.3.** Recovery of LVSΔ*iclR* mutant in mice following i.n. or i.d. inoculation

C57BL/6 mice were inoculated with either wild type LVS (circles) or LVSΔ*iclR* (triangles) i.n. at (A) a lethal dose of ~1x10$^5$ CFU or (B) a low dose of ~1x10$^3$ CFU. (C) C57BL/6 mice were inoculated with either wild type LVS (circles) or LVSΔ*iclR* (triangles) i.d. at a dose of ~3x10$^5$ CFU. Each symbol represents data from a single mouse. There were no significant differences in recovery of mutant versus wild type organisms from any organ at any time point as determined by the Mann-Whitney nonparametric test in the low dose (B) and i.d. (C) experiments.

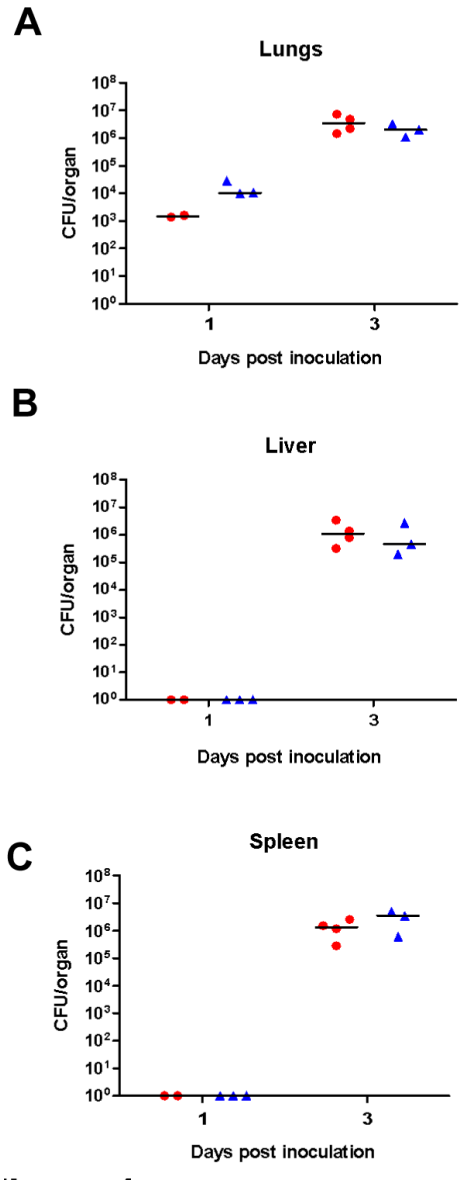


**Figure 2.4.** Recovery of SchuS4Δ*iclR* mutant in mice following i.n. inoculation

C57BL/6 mice were inoculated with either wild type SchuS4 (circles) or SchuS4Δ*iclR* (triangles) i.n. at a dose of ~100 CFU. No differences in recovery of mutant versus wild type organisms from any organ at any time point were significant using the Mann-Whitney nonparametric test.

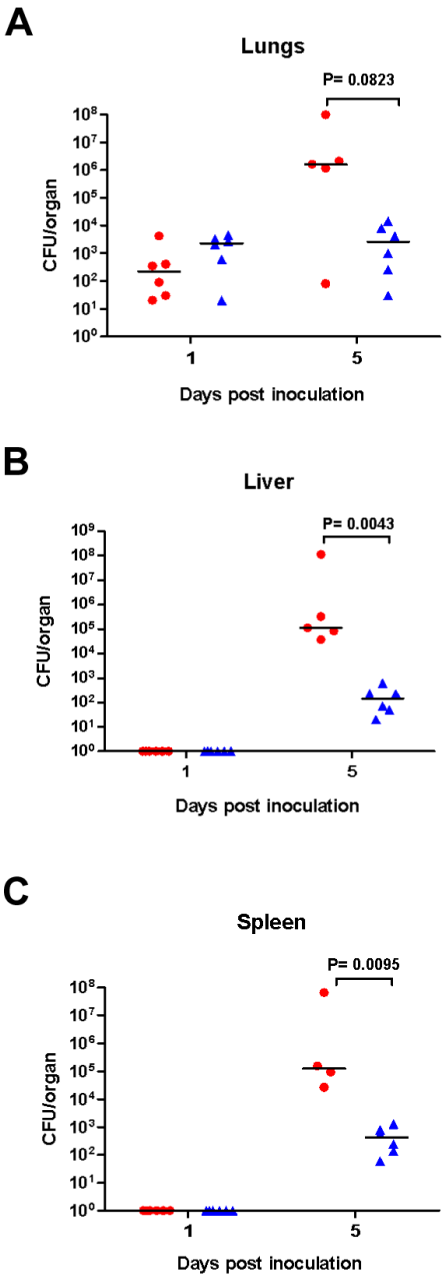


**Figure 2.5. Recovery of U112 *iclR* transposon mutant in mice following i.n. inoculation**

C57BL/6 mice were inoculated with either wild type U112 (circles) or U112 *iclR* mutant (triangles) i.n. at a dose of ~10 CFU. Differences in recovery of mutant versus wild type organisms at day 5 for the liver and spleen were significant using the Mann-Whitney nonparametric test.

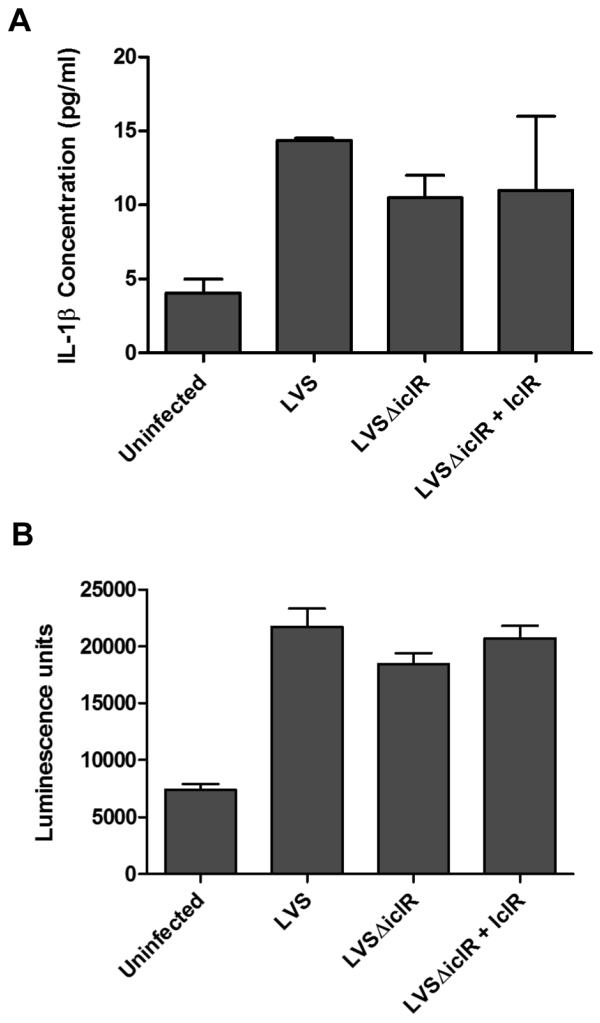


Figure 2.6. IL-1β release and cytotoxicity in macrophages infection with LVSΔ*iclR*

Infections were carried out at an MOI of 500 for wild type LVS, LVSΔ*iclR*, and LVSΔ*iclR* + IclR (complementation). (A) IL-1β was quantified via ELISA and (B) cytotoxicity was quantified via ToxiLight bioassay (Lonza), both at 24 hr post infection. Graphs are representative of at least three separate experiments, with duplicate or triplicate wells for each strain per experiment. No differences were significant by any strain comparison using the student's t-test.

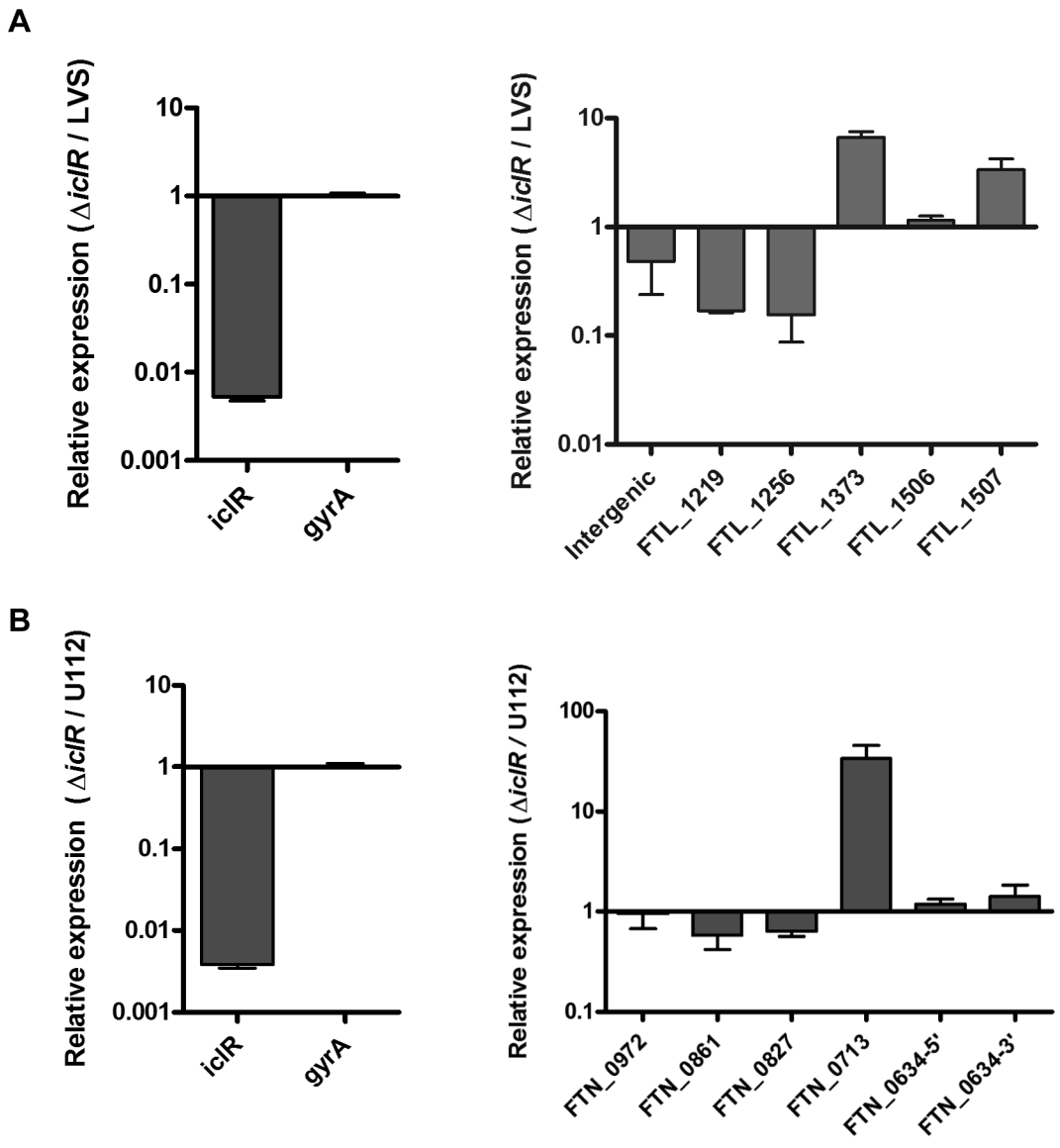


Figure 2.7. Differences in transcript levels of genes in LVS versus LVSΔ*iclR*

RNA was isolated from (A) wild type *F. tularensis* subsp. *holarctica* LVS and LVSΔ*iclR* or (B) wild type *F. novicida* U112 and a U112 *iclR* transposon mutant and used in qRT-PCR analysis for several genes that were significantly changed in the microarray. Data is presented as relative expression of log change in wild type over the respective *iclR* mutant after normalization to *gyrA*. Graph is representative of two or three experiments.

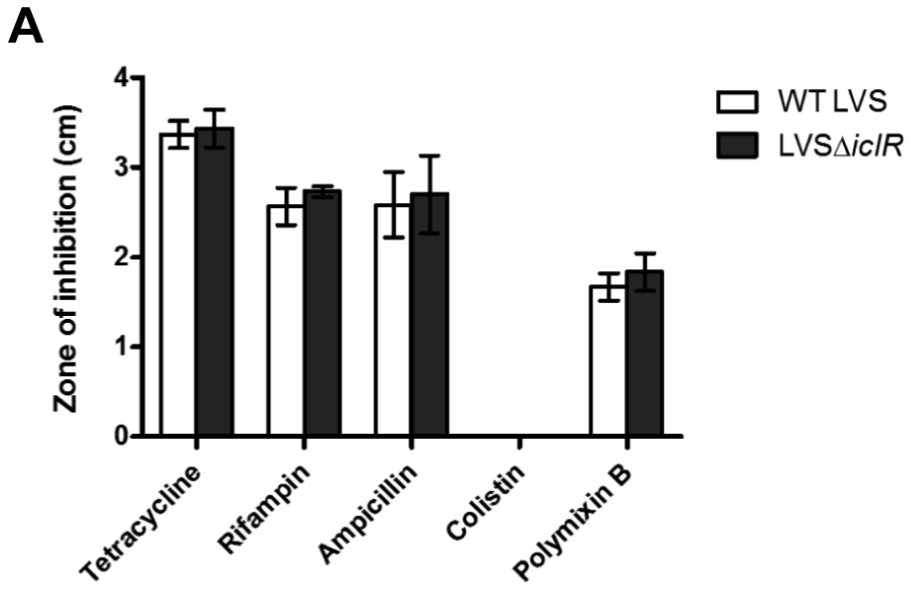


**Figure 2.8. Antibiotic sensitivity** of LVSΔ*iclR*

Wild type LVS and LVSΔ*iclR* were grown to mid-log phase, bacteria spread on chocolate agar, and an antibiotic-containing paper disc was added to the center. Bacteria were grown for 36 hr and the diameter of the zone of inhibition was measured. Experiment was performed in triplicate and the averages and standard deviations were calculated.

# Tables

## Table 2.1. Microarray gene expression in LVSΔ*iclR*

TABLE 1. Microarray gene expression in LVSΔ*iclR*

| Gene regulation and locus | Fold change | Description or annotation (BLASTp)[a] | Result of gene comparison between strains[b] | | |
|---|---|---|---|---|---|
| | | | SchuS4 | LVS | U112 |
| Downregulated | | | | | |
| FTT0748 | 34.57 | *iclR* | Intact | Intact | Intact |
| FTT0980 | 5.02 | Hypothetical protein (aminotransferase class II) | Intact | Intact | Intact |
| FTT0987 | 2.84 | Hypothetical protein (membrane protein of unknown function) | Pseudogene | Pseudogene | Intact |
| FTL_1506 | 2.82 | Short-chain dehydrogenase (reductase family protein) | Intact | Pseudogene | Intact |
| FTT1082 | 2.64 | T1082 protein | Intact | Intact | Intact |
| FTL_0388/FTT0885 | 2.63/2.18 | Cation transporter (cobalt zinc cadmium cation transporter) | Pseudogene | Intact | Intact |
| FTL_1256 | 2.62 | Pseudogene (carbon-nitrogen hydrolase family protein) | Pseudogene | Pseudogene | Intact |
| FTL_1507 | 2.57 | 3-Oxoacyl-[acyl-carrier protein] reductase | Intact | Pseudogene | Intact |
| FTT1081 | 2.53 | Hypothetical protein (hemolysin-type binding protein) | Intact | Intact | Absent |
| FTT1507 | 2.37 | Hypothetical protein (thymosin beta-4 family protein) | Intact | Absent | Intact |
| FTL_1122 | 2.19 | Hypothetical membrane protein | Intact | Pseudogene | Absent |
| FTT0715 | 2.19 | Chitinase family 18 protein | Two large deletions | Two large deletions | Intact |
| FTT0389 | 2.16 | Acetyltransferase | Intact[c] | Intact[c] | Intact[c] |
| FTT0203 | 1.97 | Bifunctional purine biosynthesis protein (*purH*) | Intact | Intact | Intact |
| Upregulated | | | | | |
| FTL_1373/FTT0741 | 4.28/6.40 | Organic solvent tolerance protein | Pseudogene | Pseudogene | Intact |
| FTT1555 | 1.93 | RNase III (*mc*) | Intact | Intact | Intact |
| FTT1554 | 1.88 | tRNA pseudouridine synthetase B (*truB*) | Intact | Intact | Intact |
| FTT0554 | 1.59 | Hypothetical protein | Intact | Intact | Intact |

[a] Annotation based on the microarray; BLASTp results (shown in parentheses), when included, provided additional information.
[b] Following alignments, genes were designated as intact, absent, or a pseudogene (introduced stop codon and two shorter predicted ORFs); genes those without such designations are discussed in the text.
[c] Possible alternative start site (see text for details).

## References


1. **(CDC), C. f. D. C. a. P.** 2005. Tularemia transmitted by insect bites--Wyoming, 2001-2003. MMWR Morb. Mortal. Wkly. Rep. 54:170-173.

2. **(CDC)., C. f. D. C. a. P.** 2009. Tularemia - Missouri, 2000-2007. MMWR Morb. Mortal. Wkly. Rep. 58:744-748.

3. **Birdsell, D. N., T. Stewart, A. J. Vogler, E. Lawaczeck, A. Diggs, T. L. Sylvester, J. L. Buchhagen, R. K. Auerbach, P. Keim, and D. M. Wagner.** 2009. *Francisella tularensis* subsp. *novicida* isolated from a human in Arizona. BMC Res Notes **2:**223.

4. **Bosio, C. M., and S. W. Dow.** 2005. *Francisella tularensis* induces aberrant activation of pulmonary dendritic cells. J Immunol **175:**6792-6801.

5. **Chamberlain, R. E.** 1965. Evaluation of Live Tularemia Vaccine Prepared in a Chemically Defined Medium. Applied microbiology **13:**232-235.

6. **Champion, M. D., Q. Zeng, E. B. Nix, F. E. Nano, P. Keim, C. D. Kodira, M. Borowsky, S. Young, M. Koehrsen, R. Engels, M. Pearson, C. Howarth, L. Larson, J. White, L. Alvarado, M. Forsman, S. W. Bearden, A. Sjostedt, R. Titball, S. L. Michell, B. Birren, and J. Galagan.** 2009. Comparative genomic characterization of *Francisella tularensis* strains belonging to low and high virulence subspecies. PLoS Pathog **5:**e1000459.

7. **Child, R., T. D. Wehrly, D. Rockx-Brouwer, D. W. Dorward, and J. Celli.** 2010. Acid phosphatases do not contribute to the pathogenesis of type A *Francisella tularensis*. Infect Immun **78:**59-67.

8. **Clarridge, J. E., 3rd, T. J. Raich, A. Sjosted, G. Sandstrom, R. O. Darouiche, R. M. Shawar, P. R. Georghiou, C. Osting, and L. Vo.** 1996. Characterization of two unusual clinically significant *Francisella* strains. J Clin Microbiol **34:**1995-2000.

9. **Cole, L. E., K. L. Elkins, S. M. Michalek, N. Qureshi, L. J. Eaton, P. Rallabhandi, N. Cuesta, and S. N. Vogel.** 2006. Immunologic consequences of *Francisella tularensis* live vaccine strain infection: role of the innate immune response in infection and immunity. J Immunol **176:**6888-6899.

10. **Cole, L. E., A. Santiago, E. Barry, T. J. Kang, K. A. Shirey, Z. J. Roberts, K. L. Elkins, A. S. Cross, and S. N. Vogel.** 2008. Macrophage proinflammatory response to *Francisella tularensis* live vaccine strain requires coordination of multiple signaling pathways. J Immunol **180:**6885-6891.

11. **Deng, K., R. J. Blick, W. Liu, and E. J. Hansen.** 2006. Identification of *Francisella tularensis* genes affected by iron limitation. Infect Immun **74:**4224-4236.

12. **Dennis, D. T., T. V. Inglesby, D. A. Henderson, J. G. Bartlett, M. S. Ascher, E. Eitzen, A. D. Fine, A. M. Friedlander, J. Hauer, M. Layton, S. R. Lillibridge, J. E. McDade, M. T. Osterholm, T. O'Toole, G. Parker, T. M. Perl, P. K. Russell, and K. Tonat.** 2001. Tularemia as a biological weapon: medical and public health management. Jama **285:**2763-2773.

13. **Duque, E., A. Segura, G. Mosqueda, and J. L. Ramos.** 2001. Global and cognate regulators control the expression of the organic solvent efflux pumps TtgABC and TtgDEF of *Pseudomonas putida*. Molecular microbiology **39:**1100-1106.

14. **Elkins, K. L., R. K. Winegar, C. A. Nacy, and A. H. Fortier.** 1992. Introduction of *Francisella tularensis* at skin sites induces resistance to infection and generation of protective immunity. Microb Pathog **13:**417-421.

15. **Feldman, K. A., R. E. Enscore, S. L. Lathrop, B. T. Matyas, M. McGuill, M. E. Schriefer, D. Stiles-Enos, D. T. Dennis, L. R. Petersen, and E. B. Hayes.** 2001. An outbreak of primary pneumonic tularemia on Martha's Vineyard. N Engl J Med **345:**1601-1606.

16. **Fortier, A. H., M. V. Slayter, R. Ziemba, M. S. Meltzer, and C. A. Nacy.** 1991. Live vaccine strain of *Francisella tularensis*: infection and immunity in mice. Infect Immun **59:**2922-2928.

17. **Fuller, J. R., R. R. Craven, J. D. Hall, T. M. Kijek, S. Taft-Benz, and T. H. Kawula.** 2008. RipA, a cytoplasmic membrane protein conserved among *Francisella* species, is required for intracellular survival. Infect Immun **76:**4934-4943.

18. **Guazzaroni, M. E., W. Teran, X. Zhang, M. T. Gallegos, and J. L. Ramos.** 2004. TtgV bound to a complex operator site represses transcription of the promoter for the multidrug and solvent extrusion TtgGHI pump. Journal of bacteriology **186:**2921-2927.

19. **Hall, J. D., R. R. Craven, J. R. Fuller, R. J. Pickles, and T. H. Kawula.** 2007. *Francisella tularensis* replicates within alveolar type II epithelial cells in vitro and in vivo following inhalation. Infect Immun **75:**1034-1039.

20. **Horton, R. M., H. D. Hunt, S. N. Ho, J. K. Pullen, and L. R. Pease.** 1989. Engineering hybrid genes without the use of restriction enzymes: gene splicing by overlap extension. Gene **77:**61-68.

21. **Huang, M. T., B. L. Mortensen, D. J. Taxman, R. R. Craven, S. Taft-Benz, T. M. Kijek, J. R. Fuller, B. K. Davis, I. C. Allen, W. J. Brickey, D. Gris, H. Wen, T. H. Kawula, and J. P. Ting.** 2010. Deletion of *ripA* alleviates suppression of the inflammasome and MAPK by *Francisella tularensis*. J Immunol **185:**5476-5485.

22. **Kadzhaev, K., C. Zingmark, I. Golovliov, M. Bolanowski, H. Shen, W. Conlan, and A. Sjostedt.** 2009. Identification of genes contributing to the virulence of *Francisella tularensis* SCHU S4 in a mouse intradermal infection model. PLoS One **4:**e5463.

23. **Kandemir, B., I. Erayman, M. Bitirgen, E. T. Aribas, and S. Guler.** 2007. Tularemia presenting with tonsillopharyngitis and cervical lymphadenitis: report of two cases. Scand J Infect Dis **39:**620-622.

24. **Keim, P., A. Johansson, and D. M. Wagner.** 2007. Molecular epidemiology, evolution, and ecology of *Francisella*. Ann N Y Acad Sci **1105:**30-66.

25. **Kraemer, P. S., A. Mitchell, M. R. Pelletier, L. A. Gallagher, M. Wasnick, L. Rohmer, M. J. Brittnacher, C. Manoil, S. J. Skerett, and N. R. Salama.** 2009. Genome-wide screen in *Francisella novicida* for genes required for pulmonary and systemic infection in mice. Infect Immun **77:**232-244.

26. **Krell, T., A. J. Molina-Henares, and J. L. Ramos.** 2006. The IclR family of transcriptional activators and repressors can be defined by a single profile. Protein Sci **15:**1207-1213.

27. **LoVullo, E. D., L. A. Sherrill, L. L. Perez, and M. S. Pavelka, Jr.** 2006. Genetic tools for highly pathogenic *Francisella tularensis* subsp. *tularensis*. Microbiology (Reading, England) **152:**3425-3435.

28. **Lubbert, C., C. Taege, T. Seufferlein, and R. Grunow.** 2009. [Prolonged course of tick-borne ulceroglandular tularemia in a 20-year-old patient in Germany--case report and review of the literature]. Dtsch Med Wochenschr **134:**1405-1410.

29. **Maier, T. M., M. S. Casey, R. H. Becker, C. W. Dorsey, E. M. Glass, N. Maltsev, T. C. Zahrt, and D. W. Frank.** 2007. Identification of *Francisella tularensis* Himar1-based transposon mutants defective for replication in macrophages. Infect Immun **75:**5376-5389.

30. **Mariathasan, S., D. S. Weiss, V. M. Dixit, and D. M. Monack.** 2005. Innate immunity against *Francisella tularensis* is dependent on the ASC/caspase-1 axis. J Exp Med **202:**1043-1049.

31. **McCaffrey, R. L., and L. A. Allen.** 2006. *Francisella tularensis* LVS evades killing by human neutrophils via inhibition of the respiratory burst and phagosome escape. J Leukoc Biol **80:**1224-1230.

32. **Mohapatra, N. P., S. Soni, T. J. Reilly, J. Liu, K. E. Klose, and J. S. Gunn.** 2008. Combined deletion of four *Francisella novicida* acid phosphatases attenuates virulence and macrophage vacuolar escape. Infect Immun **76:**3690-3699.

33. **Molina-Henares, A. J., T. Krell, M. Eugenia Guazzaroni, A. Segura, and J. L. Ramos.** 2006. Members of the IclR family of bacterial transcriptional regulators function as activators and/or repressors. FEMS Microbiol Rev **30:**157-186.

34. **Ojeda, S. S., Z. J. Wang, C. A. Mares, T. A. Chang, Q. Li, E. G. Morris, P. A. Jerabek, and J. M. Teale.** 2008. Rapid dissemination of *Francisella tularensis* and the effect of route of infection. BMC microbiology **8:**215.

35. **Qin, A., and B. J. Mann.** 2006. Identification of transposon insertion mutants of *Francisella tularensis tularensis* strain Schu S4 deficient in intracellular replication in the hepatic cell line HepG2. BMC microbiology **6:**69.

36. **Ramos, J. L., E. Duque, M. T. Gallegos, P. Godoy, M. I. Ramos-Gonzalez, A. Rojas, W. Teran, and A. Segura.** 2002. Mechanisms of solvent tolerance in gram-negative bacteria. Annu Rev Microbiol **56:**743-768.

37. **Reintjes, R., I. Dedushaj, A. Gjini, T. R. Jorgensen, B. Cotter, A. Lieftucht, F. D'Ancona, D. T. Dennis, M. A. Kosoy, G. Mulliqi-Osmani, R. Grunow, A. Kalaveshi, L. Gashi, and I. Humolli.** 2002. Tularemia outbreak investigation in Kosovo: case control and environmental studies. Emerg Infect Dis **8:**69-73.

38. **Rohmer, L., C. Fong, S. Abmayr, M. Wasnick, T. J. Larson Freeman, M. Radey, T. Guina, K. Svensson, H. S. Hayden, M. Jacobs, L. A. Gallagher, C. Manoil, R. K. Ernst, B. Drees, D. Buckley, E. Haugen, D. Bovee, Y. Zhou, J. Chang, R. Levy, R. Lim, W. Gillett, D. Guenthener, A. Kang, S. A. Shaffer, G. Taylor, J. Chen, B. Gallis, D. A. D'Argenio, M. Forsman, M. V. Olson, D. R. Goodlett, R. Kaul, S. I. Miller, and M. J. Brittnacher.** 2007. Comparison of *Francisella tularensis* genomes reveals evolutionary events associated with the emergence of human pathogenic strains. Genome Biol **8:**R102.

39. **Saslaw, S., H. T. Eigelsbach, J. A. Prior, H. E. Wilson, and S. Carhart.** 1961. Tularemia vaccine study. II. Respiratory challenge. Arch Intern Med **107:**702-714.

40. **Schulert, G. S., R. L. McCaffrey, B. W. Buchan, S. R. Lindemann, C. Hollenback, B. D. Jones, and L. A. Allen.** 2009. *Francisella tularensis* genes required for inhibition of the neutrophil respiratory burst and intramacrophage growth identified by random transposon mutagenesis of strain LVS. Infect Immun **77:**1324-1336.

41. **Siret, V., D. Barataud, M. Prat, V. Vaillant, S. Ansart, A. Le Coustumier, J. Vaissaire, F. Raffi, M. Garre, and I. Capek.** 2006. An outbreak of airborne tularaemia in France, August 2004. Euro Surveill **11:**58-60.

42. **Su, J., J. Yang, D. Zhao, T. H. Kawula, J. A. Banas, and J. R. Zhang.** 2007. Genome-wide identification of *Francisella tularensis* virulence determinants. Infect Immun **75:**3089-3101.

43. **Telepnev, M., I. Golovliov, T. Grundstrom, A. Tarnvik, and A. Sjostedt.** 2003. *Francisella tularensis* inhibits Toll-like receptor-mediated activation of intracellular signalling and secretion of TNF-alpha and IL-1 from murine macrophages. Cell Microbiol **5:**41-51.

44. **Titball, R. W., and J. F. Petrosino.** 2007. *Francisella tularensis* genomics and proteomics. Ann N Y Acad Sci **1105:**98-121.

45. **Ulland, T. K., B. W. Buchan, M. R. Ketterer, T. Fernandes-Alnemri, D. K. Meyerholz, M. A. Apicella, E. S. Alnemri, B. D. Jones, W. M. Nauseef, and F. S. Sutterwala.** 2010. Cutting edge: mutation of *Francisella tularensis mviN* leads to increased macrophage absent in melanoma 2 inflammasome activation and a loss of virulence. J Immunol **185:**2670-2674.

46. **Weiss, D. S., A. Brotcke, T. Henry, J. J. Margolis, K. Chan, and D. M. Monack.** 2007. In vivo negative selection screen identifies genes required for *Francisella* virulence. Proceedings of the National Academy of Sciences of the United States of America **104:**6037-6042.

# Chapter 3

## TetR-based Gene Regulation Systems for *Francisella tularensis*[1,2]

### Overview

There are a number of genetic tools available for *Francisella tularensis*, the etiological agent of tularemia, however there is not an effective inducible or repressible gene expression system. Herein we describe inducible and repressible gene expression systems for *F. tularensis* based on the Tet repressor, TetR. For the inducible system a tet operator sequence was cloned into a modified *F. tularensis groESL* promoter sequence and carried in a plasmid that constitutively expressed TetR. To monitor regulation the luminescence operon, *luxCDABE* was cloned under the hybrid Francisella Tetracycline Regulated promoter (*FTRp*) and transcription was initiated with addition of anhydrotetracycline (ATc), which binds TetR and alleviates TetR association with *tetAo*. Expression levels measured by luminescence correlated with ATc inducer concentrations ranging from 20 – 250 ng $ml^{-1}$. In the absence of ATc luminescence was below the level

---

[1] Adapted for this dissertation from Eric D. LoVullo, Cheryl N. Miller, Martin S. Pavelka, Jr. and Thomas H. Kawula. TetR-based Gene Regulation Systems for *Francisella tularensis*. *Appl. Environ. Microbiol*. 2012, 78(19):6883-6889.

[2] Attributions: Eric LoVullo performed all the experiments in this chapter with the following exceptions. Cheryl Miller helped design and performed the TetR intracellular growth rescue experiment with LVSΔ*ripA* (Figure 4). Cheryl also helped design and perform the essentiality test with SecA using the TetR and revTetR systems.

of detection. The inducible system was also functional during the infection of J774A.1 macrophages as determined by both luminescence and rescue of a mutant strain with an intracellular growth defect. The repressible system consists of *FTRp* regulated by the revTetR, TetR r1.7. Using this system with the *lux* reporter addition of ATc resulted in decreased luminescence, while in the absence of ATc the level of luminescence was not significantly different than a construct lacking TetR r1.7. Utilizing both systems the essentiality of SecA, the protein translocase ATPase, was confirmed establishing that they can effectively regulate gene expression. These two systems will be invaluable in exploring *F. tularensis* protein function.

## Introduction

Regulated expression systems are important tools for the manipulation of gene transcription for the study of organismal biology. Currently, there are no suitable genetic control systems for *Francisella tularensis*, a Gram-negative bacterium which is the etiological agent of tularemia (13). A conditional expression system was developed for *F. tularensis* that relies on the *F. tularensis* glucose repressible promoter, *FGRp* (26). However, this system relies on a ubiquitous carbon source and is not flexible. Hence, we developed regulated gene expression systems for *F. tularensis* based upon tetracycline that can be used for both induction and repression.

Tetracycline-regulated systems have become an useful tool in analyzing gene function in prokaryotes (6). Such systems, derived from Tn*10,* involve a constitutively expressed tetracycline repressor, TetR, which binds the tetracycline operator, *tetAo*, of the tetracycline promoter, *tetAp*, blocking transcription. TetR is released from *tetAo* in the presence of tetracycline allowing transcription from *tetAp*. The tetracycline analog

anhydrotetacyline (ATc) is significantly less toxic and binds more avidly to TetR making it a useful chemical for modulating TetR mediated gene expression in bacteria (21). The TetR system has been used with a diverse group of bacteria including other respiratory pathogens such as *Yersinia pestis*, *Brucella abortus*, *Coxiella burnetii*, and *Mycobacterium tuberculosis* (4, 14, 27, 37). In addition, a mutant derivative, revTetR, acts as a corepressor binding *tetAo* only when associated with ATc and can thus function to silence gene expression (34). Herein we describe TetR and revTetR plasmid systems for the regulation of target gene(s) in *Francisella tularensis*.

## Materials And Methods

### *Bacterial strains, transformation and cell culture*

*Escherichia coli* strains (Table 1) were grown in Luria-Bertani (LB) broth (BD Biosciences) or on LB agar. *F. tularensis* strains (Table 1) were grown at 37°C on chocolate agar (25 g BHI $l^{-1}$, 10 μg hemoglobin $ml^{-1}$, 15 g agarose $l^{-1}$) supplemented with 1% IsoVitaleX (Becton-Dickson) or in Chamberlain's Defined Medium (CDM) (10) When necessary kanamycin (Km; Sigma-Aldrich) was used at 50 μg $ml^{-1}$ for *E. coli*, 10 μg $ml^{-1}$ for *F. tularensis* and Hygromycin B (Hyg; Roche Applied Science) was used at 200 μg $ml^{-1}$ for both species. Sucrose was used at a final concentration of 10% (w/v). Anhydrotetracycline (ATc; Sigma-Aldrich) was used at the concentrations stated.

*E. coli – F. tularensis* shuttle vectors were introduced into *F. tularensis* strains via electroporation as described (30). Transformants were selected on chocolate agar supplemented with the appropriate antibiotics.

J774A.1 (ATCC# TIB-67) is a mouse macrophage-like cell line that was cultured in Dulbecco's minimal essential medium with 4.5 g $l^{-1}$ glucose, 2 mM L-glutamine, and 10% heat-inactivated fetal bovine serum. Cell lines were maintained at 37°C in 5% $CO_2$.

***secA mutagenesis and allelic exchange***

A DNA fragment containing *secA* was obtained from LVS genomic DNA (GenBank accession no. AM233362.1) using PCR and cloned into the SacB/oriT vector pEDL50, which was used as a template for PCR to generate an in-frame deletion of 2703 bp within *secA*. There is 761 bp of DNA upstream and 836 bp downstream of the Δ*secA1* allele in the deletion construct, pEDL55.

Conjugation and allelic exchange was performed similar to the previous described method (24) except pEDL55 was mobilized into *F. tularensis* using *E. coli* S17-1 λpir and primary recombinants were selected on chocolate plates supplemented with polymyxin B at 200 μg $ml^{-1}$ and kanamycin at 10 μg $ml^{-1}$.

***DNA manipulation***

Recombinant DNA methods were performed essentially as described (2). DNA fragments were isolated using agarose gel electrophoresis and QIAquick spin columns (Qiagen Inc.). Oligonucleotides were synthesized by Invitrogen Life Technologies. All restriction endonucleases were from New England Biolabs (NEB). DNA ligations were performed with the Fast-Link DNA ligation kit (Epicentre). PCR reactions were performed with Phusion High-Fidelity DNA Polymerase (NEB) according to the manufacturer's recommendations.

***Plasmid construction***

Plasmids pertinent to this study are listed in Table 1. Detailed descriptions of the construction of the plasmids can be obtained from the corresponding author.

***Broth culture luminescence assay and SecA depletion assay***

Bacteria were grown shaking at 37°C in 96 well flat clear bottom black polystyrene plates (Corning) in CDM in an Infinite 200 microplate reader (TECAN) with luminescence and absorbance ($OD_{600}$) monitored every fifteen minutes. The SecA depletion assay was performed similarly except growth was in 96 well flat clear polystyrene plates (Corning) and only the absorbance ($OD_{600}$) monitored.

***Intracellular induction and ripA growth rescue***

To determine the rate of intracellular induction by ATc *F. tularensis* LVS strains harboring luminescent *FTRp* constructs were cultured to mid-exponential phase in CDM and then added to J774A.1 cells at a multiplicity of infection (MOI) of 100. Wells were washed 2 hours post infection and 50 μg $ml^{-1}$ gentamicin was added to inhibit any remaining extracellular bacteria. As peak luminescence of a LVS J774A.1 gentamicin protection assay is ~24-30 hours post infection, the strains were induced with ATc at 23 hours and placed in an Infinite 200 Pro microplate reader (Tecan) equipped with a gas control module set at 5% $CO_2$ and luminescence was monitored every fifteen minutes.

We used the gentamicin protection assay described above for the *ripA* intracellular growth rescue experiments, except that ATc was added at 12 hours post infection and CFU's were enumerated at 12 hours and 36 hours post infection. Assays were performed in sextuplicate and statistical significance was determined using unpaired

*t* tests on the fold change of recovered CFU to compare the difference in growth between rescued strains and the *ripA* deletion strains.

## Results

As *Francisella tularensis* does not recognize the Tn*10 tetA* promoter (data not shown) we chose to modify the well characterized *Francisella groESL* promoter (15, 22), which drives strong gene expression *in vitro* and *in vivo* (7, 30). The *groESLp* was modified by inserting a *tetAo* sequence immediately downstream of the predicted transcriptional start site creating the *Francisella* Tetracycline Regulated promoter (*FTRp*) (Fig. 1). A *Mlu*I restriction site was added to facilitate cloning open reading frames and also to allow for changing the 5' UTR or start codon (e.g. a GTG start has been found to decrease expression in *F. tularensis* (3)). The *tetR* gene encoding the repressor TetR was placed under the constitutively active *Francisella rpsL* promoter and cloned divergent to *FTRp* (28).

We used the bacterial luminescence operon *luxCDABE* from *Photorhabdus luminescens,* which has been shown to function in *F. tularensis* (7), to assess our ability to regulate transcription of the hybrid promoter. We created two separate constructs; pEDL40 (Fig. 2A), an *E. coli – F. tularensis* shuttle vector bearing *FTRp* driving the *lux* operon and a *rpsLp-tetR* cassette, and pEDL41 (Fig. 2B), which is pEDL40 with *tetR* deleted allowing for constitutive *FTRp-luxCDABE* expression. As the *groESL* promoter is strong we specifically chose the low copy hygromycin resistant vector platform (29). The plasmids were introduced into *F. tularensis* LVS and growth curves in Chamberlain's defined medium (CDM) were performed in the presence of ATc at 0, 100

or 250 ng $ml^{-1}$ while monitoring luminescence and absorbance ($OD_{600}$) (Fig. 3A). The constitutive Δ*tetR* strain was not supplemented; however we found ATc had no effect on luminescence except at high levels (> 250 ng $ml^{-1}$ ATc) becoming increasingly bacteriostatic causing an overall reduction in $RLU/OD_{600}$ (data not shown). No luminescence was detected at 0 ng $ml^{-1}$ suggesting the system is effectively silenced by TetR, while the 100 and 250 ng $ml^{-1}$ concentrations were similar to the constitutive promoter suggesting that at these levels the system was fully induced. LVS exhibits diauxie in CDM, which leads to the two peak luminescence curve. The system was titrated with concentrations of 20 to 50 ng $ml^{-1}$ ATc and as the concentration increased so did the luminescence, although concentrations less than 20 ng $ml^{-1}$ were below the level of luminescence detection (Fig. 3B). Thus by luminescence the TetR system has a useable range of 20 – 250 ng $ml^{-1}$ ATc in broth culture. To determine the speed of induction, a midlog culture was induced with 250 ng $ml^{-1}$ ATc and measured over time (Fig. 3C). Luminescence exceeded the limit of detection within 18 minutes showing that induction of transcription and subsequent translation is rapid.

These results confirm that the system is useful in broth culture; however as *F. tularensis* is a facultative intracellular bacterium we wanted to determine if induction of the TetR system was possible in cell culture. A J774A.1 mouse macrophage-like cell line was infected with LVS bearing pEDL40 or pEDL41. Since peak luminescence in a J774A.1 infection is ~24-30 hours post infection (Data not shown) ATc was added at 23 hours post infection at 0, 100 or 250 ng $ml^{-1}$. With addition of ATc at 100 or 250 ng $ml^{-1}$ the luminescence was above background within 45 minutes and reached the level of the

constitutive promoter within 3 hours (Fig. 3D). The bacteriostatic concentration of ATc in cell culture was found to be greater than 500 ng $ml^{-1}$.

We wanted to establish if the TetR system was suitable for rescuing a mutant defective for intracellular replication. RipA is a cytoplasmic transmembrane protein essential for *Francisella tularensis* intracellular growth in host macrophage cells and for growth at the neutral pH found in the host cell's cytoplasmic environment (19, 38). The *F. tularensis* Δ*ripA* mutant can infect host macrophages and escape the phagosome at the same frequency as wild type, but fails to replicate inside host cells and is impaired in its ability to colonize and disseminate in a mouse model of tularemia (18). A gentamicin protection assay was performed with LVS bearing the TetR control plasmid pEDL17 in which *FTRp* drives production of a RFP, mOrange2 (36), LVSΔ*ripA* bearing pEDL17, and LVSΔ*ripA* containing the plasmid pEDL20 with *ripA* under the control of *FTRp*. J774A.1 macrophages were infected and 100 ng $ml^{-1}$ ATc was added at 12 hours post infection, to determine if the LVSΔ*ripA* strain could be rescued after such a long period of stasis. As expected, the control strains LVS/pEDL17 replicated inside host macrophages, increasing in numbers by 3 to 5 fold between 12 and 36 hours post infection, while the *ripA*/pEDL17 failed to replicate inside macrophages. Furthermore the addition of 100 ng $ml^{-1}$ ATc did not change the intracellular growth of LVS or the *ripA* deletion mutant (Fig. 4). In contrast, the Δ*ripA*/pEDL20 strain was rescued for growth when 100 ng $ml^{-1}$ of ATc was added to the cells, increasing in viable counts by 50 fold in the subsequent 24 hours ($P<0.0001$) (Fig. 4). The rescue of Δ*ripA*/pEDL20 by addition of ATc confirmed that the system works intracellularly and suggests that

although the *ripA* deletion strain is unable to replicate, it is still viable at 12 hours post infection.

To create a repressible TetR system in *Francisella* we chose a highly efficient revTetR, TetR r1.7 (23, 34). We replaced the *tetR* gene in pEDL40 with *tetR* r1.7 to create pEDL47 (Fig. 2C). The plasmid pEDL47 was introduced into LVS and growth curves were performed in the presence of ATc at 0, 100 or 250 ng $ml^{-1}$ (Fig. 5). There was no significant difference between 0 ng $ml^{-1}$ ATc and the constitutive Δ*tetR* strain, which suggests that there is no binding of TetR r1.7 to *tetAo* in the absence of ATc. Both the 100 and 250 ng $ml^{-1}$ ATc levels tested inhibited transcription of the operon and while it took over 20 hours to reach baseline it was significantly different than 0 ng $ml^{-1}$ ATc. This slow decline in luminescence is likely due to the time it takes for depletion of the Lux proteins after transcriptional silencing by TetR r1.7.

To determine if the TetR and revTetR systems were suitable for silencing gene expression an essentiality test was performed on SecA, the protein translocase ATPase. SecA is a component of the general secretory pathway (Sec). The Sec pathway consists of three integral membrane proteins SecY, SecE, and SecG and two cytosolic proteins SecA and SecB. The SecYEG complex forms a heterotrimeric channel in the cytoplasmic membrane where the unfolded substrates pass through (32). SecB is a cytosolic chaperone that specifically targets preproteins to SecA (39). SecA is central to the pathway as it is the ATPase that energizes the transport through SecYEG, as well as recognizing and delivering preproteins to the SecYEG channel (8, 11). In a transposon screen in the closely related *Francisella novicida* there are two hits in the 3' end of the *secA* gene (20) and a study by Margolis et al 2009 found that these *secA* mutants were

defective in biofilm formation, suggesting a defect in protein secretion, however they were unable to delete the full length *F. novicida secA* (31) as SecA is likely essential in all prokaryotes (1, 5, 9, 16, 17, 23). To silence expression of SecA in LVS we deleted the chromosomal copy of *secA* in strains bearing either plasmid pEDL54 (*FTRp-secA*, TetR) or pEDL58 (*FTRp-secA,* revTetR) which will be referred to as the TetOn and TetOff strains, respectively. We streaked LVS, TetOn, and TetOff on plates containing 0 or 500 ng $ml^{-1}$ ATc. The LVS control grew normally in both conditions, and as expected TetOn grew only in the presence of ATc and TetOff in the absence of ATc (Fig. 6A). There were a few colonies in the primary streak of the silenced strains, suggesting the selection of suppressors. To resolve the nature of the suppression three overnight cultures of the TetOn strain, grown in 50 ng $ml^{-1}$ ATc, were plated onto chocolate agar lacking ATc and 15 colonies were chosen for further analysis. Each strain that grew without ATc was found to harbor a mutation in *tetR* or *tetAo* allowing constitutive production of SecA. These results established SecA as essential; however the growth kinetics of the two strains on depletion of SecA in CDM might explain whether depletion was bacteriostatic or bactericidal. As expected TetOn grew without ATc until SecA was depleted but grew to WT levels with ATc present ($P<0.01$) and TetOff followed the opposite pattern ($P<0.01$) (Fig. 6B). Even though it has been suggested that lack of SecA or inhibition of SecA is bactericidal (35) these results suggest that depletion was bacteriostatic in LVS, however at late time points suppression of the *secA* deletion did occur in both strains which obfuscates the results. As it was difficult to maintain a clean population of the TetOn strain, because of constant selective pressure, the revTetR system would likely be a better system to use when studying a potentially essential gene.

## Discussion

In this study, we developed TetR-based gene regulation systems for *Francisella tularensis* that allow for inducible or repressible gene expression with addition of ATc and demonstrated that the systems are useful in both broth and cell culture. We further established that the systems can be used effectively for gene silencing. We anticipate these systems will be useful for studies investigating gene dosage, gene timing, essentiality testing, as well as for expression of toxic proteins. Thus these systems will be invaluable in addressing protein function in *Francisella tularensis*.

## Figures

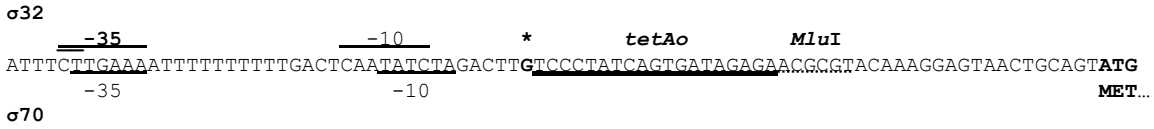


**Figure 3.1. *Francisella* Tetracycline Regulated Promoter**

*FTRp* has both sigma 32 and sigma 70 recognition delineated by the underlined -35 and -10 sequences. The asterisk* signifies the transcriptional start. Following in the 5' UTR is the tet operator, *tetAo*, as well as a *Mlu*I site to facilitate cloning. The ATG represents the translational start.

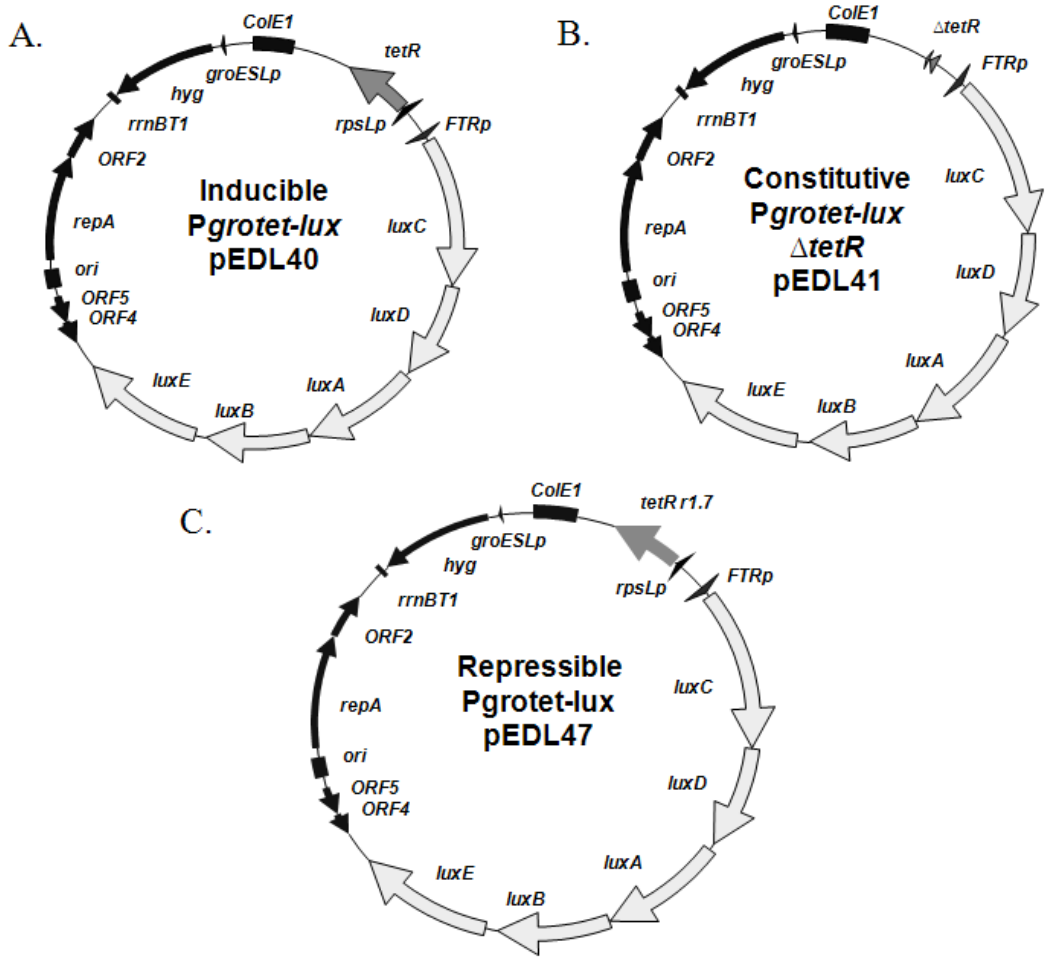


**Figure 3.2. Maps of the *FTRp-luxCDABE* vectors**

(A) The inducible vector, pEDL40, is a stable HygR *E. coli – F. tularensis* shuttle vector that contains the hybrid *Francisella FTR* promoter driving the luminescence operon, *luxCDABE*. Divergently transcribed is the *tetR* gene constitutively expressed from the *Francisella rpsL* promoter. (B) The vector, pEDL41, is pEDL40 with the *tetR* gene deleted. This allows constitutive expression of the lux operon from *FTRp*. (C) The repressible vector, pEDL47, is a HygR stable *E. coli – F. tularensis* shuttle vector that contains *FTRp-luxCDABE*. Divergently transcribed is the revTetR *tetR* r1.7 gene constitutively expressed from the *Francisella rpsL* promoter.

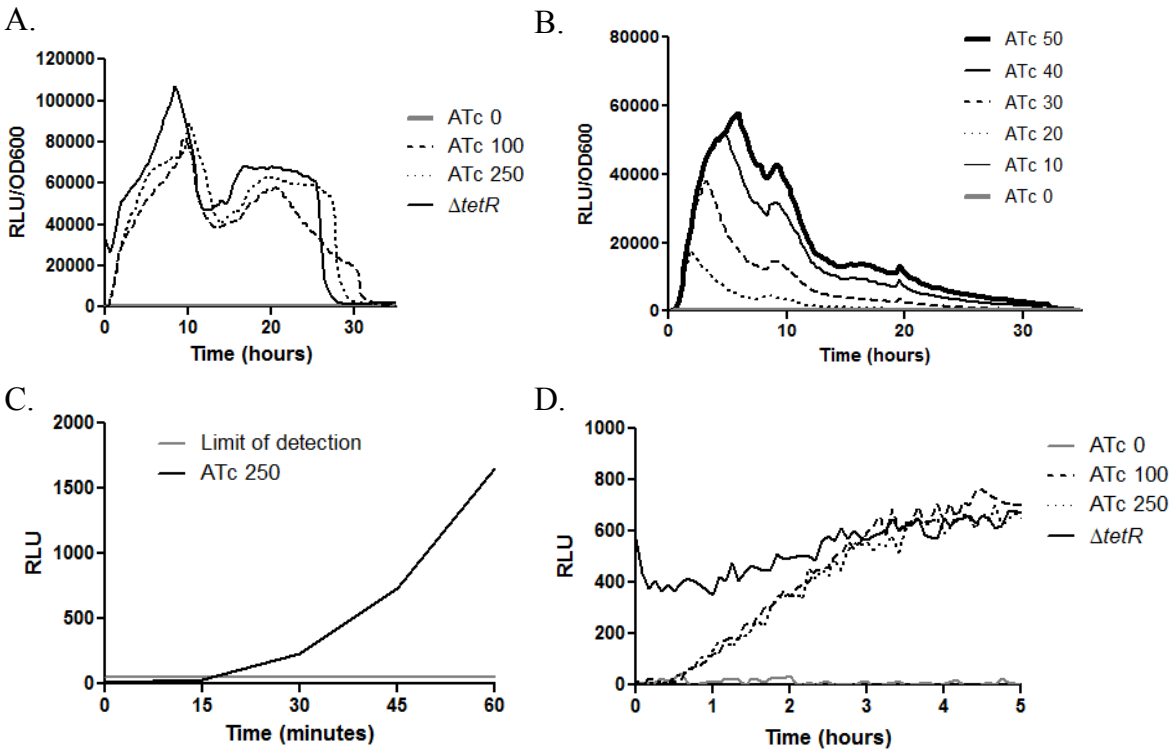


**Figure 3.3. The TetR system**

(A) Growth curves were performed in Chamberlain's Defined Medium (CDM) with LVS bearing plasmid pEDL40 in the presence of ATc concentrations of 0, 100 and 250 ng $ml^{-1}$ and LVS bearing pEDL41 Δ*tetR* as the constitutive control. The absorbance at $OD_{600}$ and luminescence were monitored every fifteen minutes for 36 hours. To determine the relative light produced per bacterium the luminescence was divided by the absorbance and represented as $RLU/OD_{600}$. (B) Growth curves were performed in CDM utilizing ATc concentrations from 0 - 50 ng $ml^{-1}$ in 10 ng $ml^{-1}$ increments and luminescence per bacterium was followed as above. (C) A midlog culture of LVS/pEDL40 was induced with 250 ng $ml^{-1}$ ATc to test induction time. Luminescence was monitored every fifteen minutes to ascertain the time it took to increase above 50 RLU, which represents the limit of detection. (D) A gentamicin protection assay was

performed with LVS bearing plasmid pEDL40 LVS bearing pEDL41 Δ*tetR* as the constitutive control. Induction was at 23 hours post infection with ATc concentrations of 0, 100 and 250 ng $ml^{-1}$. Luminescence was measured every fifteen minutes for 5 hours after induction.

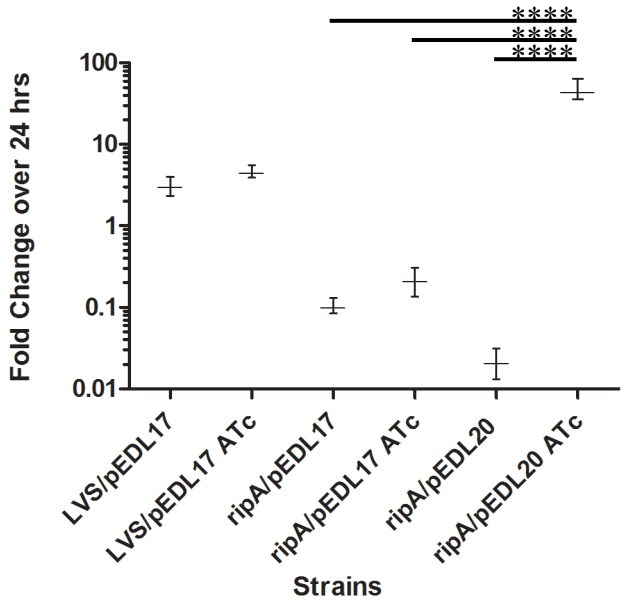


**Figure 3.4. The TetR system rescues LVSΔ*ripA* intracellular growth in J774A.1 macrophages**

Fold change in growth was measured after 24 hours during a gentamicin protection assay with LVS bearing the TetR control plasmid pEDL17, LVSΔ*ripA* bearing pEDL17, and LVSΔ*ripA* containing pEDL20 with P*grotet-ripA*. All strains were added to J774A.1 cells at a multiplicity of infection of 100. Gentamicin was added at 2 hours post infection. At 12 hours 100 ng $ml^{-1}$ ATc was added to wells. CFU's were enumerated at 12 hours and 36 hours post infection. Data are represented as average fold change in growth (n=6) between 12 and 36 hours post infection. Error bars represent standard deviation. **** $P < 0.0001$.

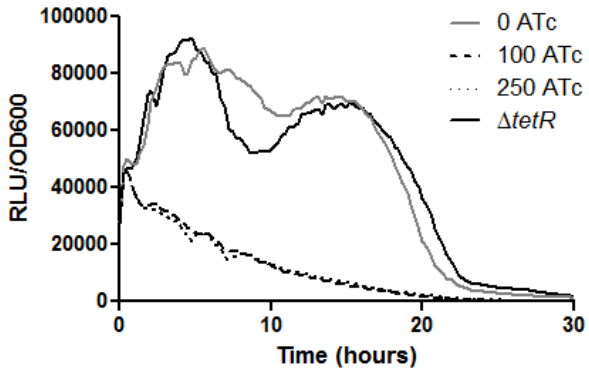


**Figure 3.5. The revTetR system**

Growth curves were performed with LVS bearing plasmid pEDL47 in the presence of ATc concentrations of 0, 100 and 250 ng $ml^{-1}$ and LVS bearing pEDL41 Δ*tetR* as the constitutive control. The absorbance at $OD_{600}$ and luminescence were monitored every fifteen minutes for 36 hours. To determine the relative light produced per bacterium the luminescence was divided by the absorbance.

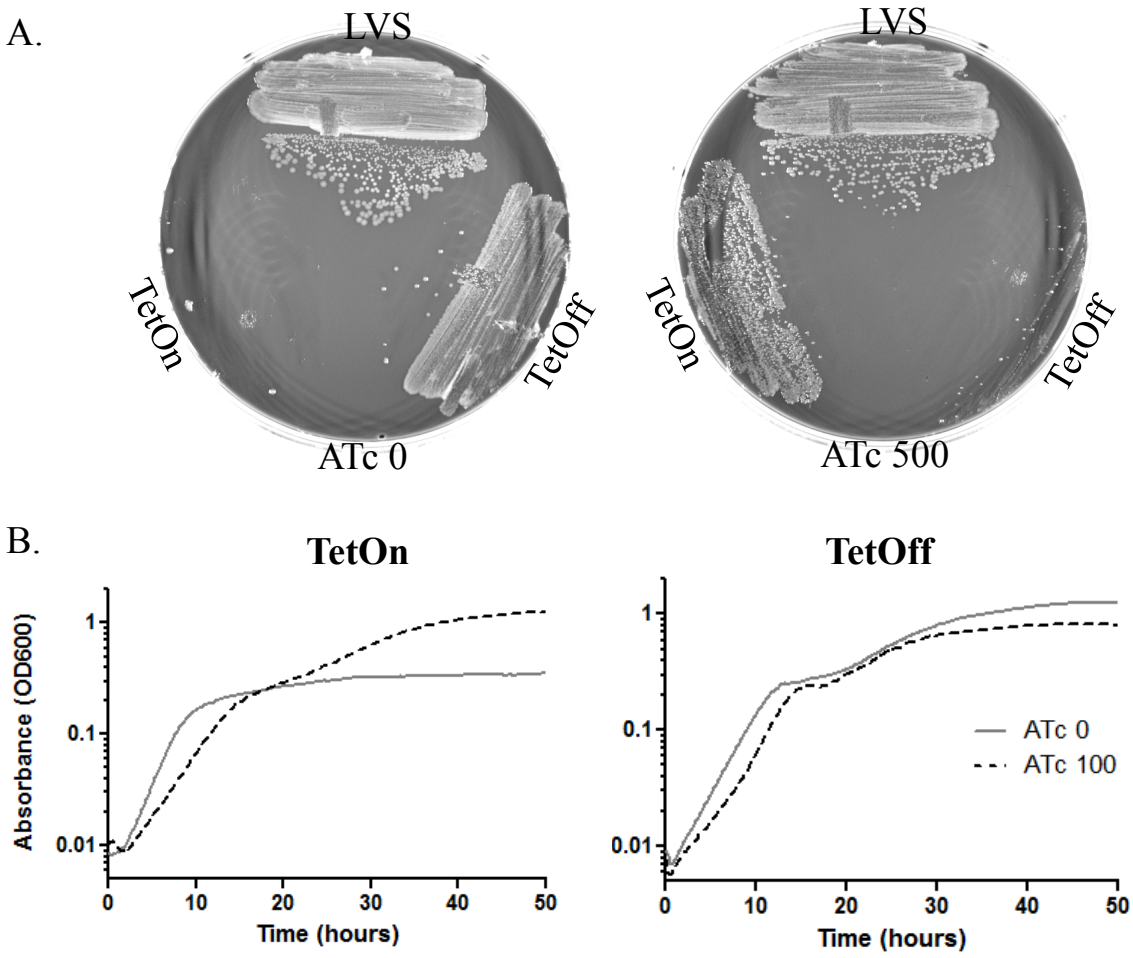


**Figure 3.6. SecA is essential**

(A) The strains LVS, TetOn (*FTRp-secA*, TetR), and TetOff (*FTRp-secA*, revTetR) were streaked onto chocolate agar plates that either contain 0 or 500 ng $ml^{-1}$ ATc. The plates were allowed to incubate for 72 hours at 37 °C. (B) Growth curves of either TetOn or TetOff were performed in media containing 0 or 100 ng $ml^{-1}$ ATc. The absorbance at $OD_{600}$ was measured every 15 minutes for 50 hours. The growth curves were plotted onto a $\log_{10}$ scale. There was a significant difference in final growth as measured by absorbance at $OD_{600}$ with TetON unable to reach WT levels without ATc $P<0.01$ and TetOff unable to reach WT levels of growth with ATc $P<0.01$.

# Tables

## Table 3.1. Bacterial strains and plasmids

| Strains or Plasmids | Description | Reference or Source |
|---|---|---|
| **Strains** | | |
| *E. coli* | | |
| DH10B | F- *mcrA* Δ(*mcrBC-hsdRMS-mrr*) [φ80dΔ*lacZ*ΔM15] Δ*lacX74 deoR recA1 endA1 araD139* Δ*(ara,leu)7697 galU galK* λ*- rpsL nupG* | Invitrogen |
| S17-1 λpir | $Tp^r$ $Sm^r$ *hsdR pro recA*RP4-2-Tc::Mu-Km::Tn*7* λ *pir* | (12) |
| NK7402 | *trpC83::Tn10*, *IN(rrnD-rrnE)1* source of *tetR* | CGSC Strain #6688 |
| *F. tularensis* | | |
| LVS | *F. tularensis* subsp. *holarctica* live vaccine strain | CDC |
| LVSΔ*ripA* | LVSΔ*ripA* | (18) |
| LE149/TetOn | LVSΔ*secA* pEDL54 *in trans* | This work |
| LE150/TetOff | LVSΔ*secA* pEDL58 *in trans* | This work |
| **Plasmids** | | |
| pcDNA3-mOrange2 | ApR, NeoR source of mOrange2 | (36) |
| pJH1 | HygR, source of *oriT* | (25) |
| pMP812 | KmR, SacB suicide vector | (28) |
| pNR55 | KmR, source of the revTetR, *tetR* r1.7 | (33) |
| pXB173-lux | KmR, *E. coli-F.tularensis* shuttle vector containing the *luxCDABE* operon | (7) |
| pEDL17 | HygR, *FTRp*-mOrange2, *rpsLp-tetR* | This work |
| pEDL20 | HygR, *FTRp-ripA*, *rpsLp-tetR* | This work |
| pEDL40 | HygR, *FTRp-luxCDABE, rpsLp-tetR* | This work |
| pEDL41 | HygR, *FTRp-luxCDABE* with deletion of *tetR* | This work |
| pEDL47 | HygR, *FTRp-luxCDABE, rpsLp- tetR* r1.7 | This work |
| pEDL50 | KmR, pMP812 SacB suicide vector with *oriT* from pJH1 | This work |
| pEDL54 | HygR, *FTRp-secA, rpsLp-tetR* | This work |
| pEDL55 | pEDL50 with LVS Δ*secA* region | This work |
| pEDL58 | HygR, *FTRp-secA, rpsLp-tetR* r1.7 | This work |

## References


1. **Akerley, B. J., E. J. Rubin, A. Camilli, D. J. Lampe, H. M. Robertson, and J. J. Mekalanos.** 1998. Systematic identification of essential genes by in vitro mariner mutagenesis. Proceedings of the National Academy of Sciences of the United States of America **95:**8927-8932.

2. **Ausubel, F. M., R. Brent, R. E. Kingston, D. D. Moore, J. G. Seidman, J. A. Smith, and K. Struhl.** 1987. Current Protocols in Molecular Biology. Greene Publishing Associates and Wiley-Interscience.

3. **Bakshi, C. S., M. Malik, K. Regan, J. A. Melendez, D. W. Metzger, V. M. Pavlov, and T. J. Sellati.** 2006. Superoxide dismutase B gene (*sodB*)-deficient mutants of *Francisella tularensis* demonstrate hypersensitivity to oxidative stress and attenuated virulence. Journal of bacteriology **188:**6443-6448.

4. **Beare, P. A., S. D. Gilk, C. L. Larson, J. Hill, C. M. Stead, A. Omsland, D. C. Cockrell, D. Howe, D. E. Voth, and R. A. Heinzen.** 2011. Dot/Icm type IVB secretion system requirements for *Coxiella burnetii* growth in human macrophages. mBio **2:**e00175-00111.

5. **Benson, R. E., E. B. Gottlin, D. J. Christensen, and P. T. Hamilton.** 2003. Intracellular expression of Peptide fusions for demonstration of protein essentiality in bacteria. Antimicrobial agents and chemotherapy **47:**2875-2881.

6. **Bertram, R., and W. Hillen.** 2008. The application of Tet repressor in prokaryotic gene regulation and expression. Microbial biotechnology **1:**2-16.

7. **Bina, X. R., M. A. Miller, and J. E. Bina.** 2010. Construction of a bioluminescence reporter plasmid for Francisella tularensis. Plasmid **64:**156-161.

8. **Cabelli, R. J., L. Chen, P. C. Tai, and D. B. Oliver.** 1988. SecA protein is required for secretory protein translocation into *E. coli* membrane vesicles. Cell **55:**683-692.

9. **Caspers, M., and R. Freudl.** 2008. *Corynebacterium glutamicum* possesses two *secA* homologous genes that are essential for viability. Archives of microbiology **189:**605-610.

10. **Chamberlain, R. E.** 1965. Evaluation of live Tularemia vaccine prepared in a chemically defined medium. Applied microbiology **13:**232-235.

11. **Cunningham, K., and W. Wickner.** 1989. Specific recognition of the leader region of precursor proteins is required for the activation of translocation ATPase

of *Escherichia coli*. Proceedings of the National Academy of Sciences of the United States of America **86:**8630-8634.

12. **de Lorenzo, V., and K. N. Timmis.** 1994. Analysis and construction of stable phenotypes in gram-negative bacteria with Tn5- and Tn10-derived minitransposons. Methods in enzymology **235:**386-405.

13. **Dennis, D. T., T. V. Inglesby, D. A. Henderson, J. G. Bartlett, M. S. Ascher, E. Eitzen, A. D. Fine, A. M. Friedlander, J. Hauer, M. Layton, S. R. Lillibridge, J. E. McDade, M. T. Osterholm, T. O'Toole, G. Parker, T. M. Perl, P. K. Russell, and K. Tonat.** 2001. Tularemia as a biological weapon: medical and public health management. Jama **285:**2763-2773.

14. **Ehrt, S., X. V. Guo, C. M. Hickey, M. Ryou, M. Monteleone, L. W. Riley, and D. Schnappinger.** 2005. Controlling gene expression in mycobacteria with anhydrotetracycline and Tet repressor. Nucleic acids research **33:**e21.

15. **Ericsson, M., I. Golovliov, G. Sandstrom, A. Tarnvik, and A. Sjostedt.** 1997. Characterization of the nucleotide sequence of the *groE* operon encoding heat shock proteins chaperone-60 and -10 of *Francisella tularensis* and determination of the T-cell response to the proteins in individuals vaccinated with *F. tularensis*. Infect Immun **65:**1824-1829.

16. **Fagan, R. P., and N. F. Fairweather.** 2011. *Clostridium difficile* has two parallel and essential Sec secretion systems. The Journal of biological chemistry **286:**27483-27493.

17. **Forsyth, R. A., R. J. Haselbeck, K. L. Ohlsen, R. T. Yamamoto, H. Xu, J. D. Trawick, D. Wall, L. Wang, V. Brown-Driver, J. M. Froelich, K. G. C, P. King, M. McCarthy, C. Malone, B. Misiner, D. Robbins, Z. Tan, Z. Y. Zhu Zy, G. Carr, D. A. Mosca, C. Zamudio, J. G. Foulkes, and J. W. Zyskind.** 2002. A genome-wide strategy for the identification of essential genes in *Staphylococcus aureus*. Molecular microbiology **43:**1387-1400.

18. **Fuller, J. R., R. R. Craven, J. D. Hall, T. M. Kijek, S. Taft-Benz, and T. H. Kawula.** 2008. RipA, a cytoplasmic membrane protein conserved among *Francisella* species, is required for intracellular survival. Infect Immun **76:**4934-4943.

19. **Fuller, J. R., T. M. Kijek, S. Taft-Benz, and T. H. Kawula.** 2009. Environmental and intracellular regulation of *Francisella tularensis ripA*. BMC microbiology **9:**216.

20. **Gallagher, L. A., E. Ramage, M. A. Jacobs, R. Kaul, M. Brittnacher, and C. Manoil.** 2007. A comprehensive transposon mutant library of *Francisella*

*novicida*, a bioweapon surrogate. Proceedings of the National Academy of Sciences of the United States of America **104:**1009-1014.

21. **Gossen, M., and H. Bujard.** 1993. Anhydrotetracycline, a novel effector for tetracycline controlled gene expression systems in eukaryotic cells. Nucleic acids research **21:**4411-4412.

22. **Grall, N., J. Livny, M. Waldor, M. Barel, A. Charbit, and K. L. Meibom.** 2009. Pivotal role of the *Francisella tularensis* heat-shock sigma factor RpoH. Microbiology (Reading, England) **155:**2560-2572.

23. **Guo, X. V., M. Monteleone, M. Klotzsche, A. Kamionka, W. Hillen, M. Braunstein, S. Ehrt, and D. Schnappinger.** 2007. Silencing *Mycobacterium smegmatis* by using tetracycline repressors. Journal of bacteriology **189:**4614-4623.

24. **Horzempa, J., P. E. Carlson, Jr., D. M. O'Dee, R. M. Shanks, and G. J. Nau.** 2008. Global transcriptional response to mammalian temperature provides new insight into *Francisella tularensis* pathogenesis. BMC microbiology **8:**172.

25. **Horzempa, J., R. M. Shanks, M. J. Brown, B. C. Russo, D. M. O'Dee, and G. J. Nau.** 2010. Utilization of an unstable plasmid and the I-SceI endonuclease to generate routine markerless deletion mutants in *Francisella tularensis*. Journal of microbiological methods **80:**106-108.

26. **Horzempa, J., D. M. Tarwacki, P. E. Carlson, Jr., C. M. Robinson, and G. J. Nau.** 2008. Characterization and application of a glucose-repressible promoter in *Francisella tularensis*. Applied and environmental microbiology **74:**2161-2170.

27. **Lathem, W. W., P. A. Price, V. L. Miller, and W. E. Goldman.** 2007. A plasminogen-activating protease specifically controls the development of primary pneumonic plague. Science (New York, N.Y **315:**509-513.

28. **LoVullo, E. D., C. R. Molins-Schneekloth, H. P. Schweizer, and M. S. Pavelka, Jr.** 2009. Single-copy chromosomal integration systems for *Francisella tularensis*. Microbiology (Reading, England) **155:**1152-1163.

29. **LoVullo, E. D., L. A. Sherrill, and M. S. Pavelka, Jr.** 2009. Improved shuttle vectors for *Francisella tularensis* genetics. FEMS microbiology letters **291:**95-102.

30. **LoVullo, E. D., L. A. Sherrill, L. L. Perez, and M. S. Pavelka, Jr.** 2006. Genetic tools for highly pathogenic *Francisella tularensis* subsp. *tularensis*. Microbiology (Reading, England) **152:**3425-3435.

31. **Margolis, J. J., S. El-Etr, L. M. Joubert, E. Moore, R. Robison, A. Rasley, A. M. Spormann, and D. M. Monack.** 2010. Contributions of *Francisella tularensis* subsp. *novicida* chitinases and Sec secretion system to biofilm formation on chitin. Applied and environmental microbiology **76:**596-608.

32. **Meyer, T. H., J. F. Menetret, R. Breitling, K. R. Miller, C. W. Akey, and T. A. Rapoport.** 1999. The bacterial SecY/E translocation complex forms channel-like structures similar to those of the eukaryotic Sec61p complex. Journal of molecular biology **285:**1789-1800.

33. **Rigel, N. W., H. S. Gibbons, J. R. McCann, J. A. McDonough, S. Kurtz, and M. Braunstein.** 2009. The accessory SecA2 system of *Mycobacteria* requires ATP binding and the canonical SecA1. The Journal of biological chemistry **284:**9927-9936.

34. **Scholz, O., E. M. Henssler, J. Bail, P. Schubert, J. Bogdanska-Urbaniak, S. Sopp, M. Reich, S. Wisshak, M. Kostner, R. Bertram, and W. Hillen.** 2004. Activity reversal of Tet repressor caused by single amino acid exchanges. Molecular microbiology **53:**777-789.

35. **Segers, K., and J. Anne.** 2011. Traffic jam at the bacterial sec translocase: targeting the SecA nanomotor by small-molecule inhibitors. Chemistry & biology **18:**685-698.

36. **Shaner, N. C., M. Z. Lin, M. R. McKeown, P. A. Steinbach, K. L. Hazelwood, M. W. Davidson, and R. Y. Tsien.** 2008. Improving the photostability of bright monomeric orange and red fluorescent proteins. Nature methods **5:**545-551.

37. **Starr, T., R. Child, T. D. Wehrly, B. Hansen, S. Hwang, C. Lopez-Otin, H. W. Virgin, and J. Celli.** 2012. Selective subversion of autophagy complexes facilitates completion of the *Brucella* intracellular cycle. Cell host & microbe **11:**33-45.

38. **Tarnok, A., M. Dorger, I. Berg, G. Gercken, and T. Schluter.** 2001. Rapid screening of possible cytotoxic effects of particulate air pollutants by measurement of changes in cytoplasmic free calcium, cytosolic pH, and plasma membrane potential in alveolar macrophages by flow cytometry. Cytometry **43:**204-210.

39. **Valent, Q. A., P. A. Scotti, S. High, J. W. de Gier, G. von Heijne, G. Lentzen, W. Wintermeyer, B. Oudega, and J. Luirink.** 1998. The *Escherichia coli* SRP and SecB targeting pathways converge at the translocon. The EMBO journal **17:**2504-2512.

# Chapter 4

## RipA modulates the acyl chain specificity and stability of LpxA in *Francisella tularensis*.[1]

### Overview

*Francisella tularensis* is a Gram-negative bacterium that infects hundreds of species including humans, and has evolved unique mechanisms to grow efficiently within a plethora of cell types. Using transposon mutagenesis we identified RipA, a conserved cytoplasmic membrane protein with unknown function. RipA is dispensable for growth in defined media, but is required for growth inside host cells. As a means to determine RipA function, we isolated and mapped independent extragenic suppressor mutants in Δ*ripA* that restored growth in host cells. Each suppressor mutation mapped to one of two essential genes, *lpxA* or *glmU*, which are both involved in lipid A synthesis. We repaired one of the suppressor mutations in *lpxA* (S102) and demonstrated that the mutation was responsible for the suppressor phenotype. We hypothesize that the mutation in S102 alters the stability of LpxA, which compensated for the absence of RipA function. LpxA is an essential protein, which uses the precursors UDP-N-acetylglucosamine (UDP-

[1] Attributions:
Cheryl Miller performed all the experiments in this chapter. Eric LoVullo designed the inducible gene expression system for *lpxA* (Figure 10). Artur Romanchuk and Corbin Jones aligned the sequenced genome of S102 and identified the polymorphisms (Table 1). Ronald Jenkins and Garry Dotson developed the continuous fluorescent enzyme assay for LpxA and made the hydroxypalmytic-ACP necessary for the experiments with *F. tularensis* LpxA (Figure 12).

GlcNAc), and acyl-ACP to begin lipid A synthesis. We found that the ratio of C:18 to C:16 fatty acids in lipid A was greater in the presence of RipA. Furthermore, LpxA was more abundant in the presence of RipA. Induced expression of *lpxA* in the Δ*ripA* strain stopped bacterial division. We also found that the LpxA S102 protein was less stable and therefore less abundant than wild type LpxA protein. These data suggest RipA modulates the activity and abundance of LpxA in *F. tularensis* as a way to adapt to the host cell environment.

## Introduction

*Francisella tularensis* is a highly virulent Gram-negative bacterial pathogen that causes systemic infections in hundreds of animal species, including humans. Key pathogenic properties of *F. tularensis* are its ability to invade and replicate within many different host cell types and to suppress the initial host inflammatory response by innate immune cells. We previously identified a protein termed RipA, which is conserved among all sequenced *Francisella* species (9). RipA is dispensable for growth in minimal media, but is required for *F. tularensis* virulence in mouse models of infection (9). RipA is a homooligomeric cytoplasmic membrane protein that contains two cytoplasmic domains that are essential for RipA function (25). The Δ*ripA* strain infects host cells and escapes the phagosome entering the cytoplasm similar to wild type *F. tularensis*, but fails to replicate within the cytosol (9). Both transcription and translation of *ripA* are elevated at neutral pH coinciding with *F. tularensis* leaving the acidified vacuole and entering the neutral cytoplasm (10). The *F. tularensis* Δ*ripA* strain stimulates a robust host inflammatory response activating the inflammasome and MAPK pathways, a response

which is not seen with wild type *F. tularensis* (12). In *Francisella novicida*, Δ*ripA* activates increased levels of AIM2-dependent pyroptosis, suggesting the bacterial membrane is compromised (27). Determining RipA function would provide an important insight into the specific mechanisms used by *F. tularensis* to grow within eukaryotic cells. Given the scant information obtained from bioinformatics analysis of RipA, and the eclectic group of organisms that express RipA-like proteins (25), we took genetic and biochemical approaches to determine RipA function. We isolated five independent extragenic suppressor mutations of Δ*ripA* that restored intracellular growth, and all suppressor mutations mapped to either *lpxA* or *glmU*. Both *lpxA* and *glmU* encode essential enzymes involved in lipid A synthesis (1, 24). Repairing one of the mutations in *lpxA* abrogated the suppressor phenotype supporting that the mutation in *lpxA* was responsible for the suppressor phenotype. LpxA is a UDP-N-acetylglucosamine acyltransferase that catalyzes the transfer of an acyl chain from acyl carrier protein (ACP) to UDP-N-acetylglucosamine (UDP-GlcNAc) to make lipid A, which is the hydrophobic anchor of lipopolysaccharide (LPS) (6). The active site and substrate binding pocket of LpxA is well characterized in *Escherichia coli* (39). LpxA forms a trimer composed of three identical subunits with each subunit composed of two domains (30). The N-terminal domain forms a left-handed helix of short parallel β-sheets and the C-terminal domain is composed of four α-helices. The active site in LpxA is located in a cleft between the two subunits, and the amino acids essential for LpxA function in *E. coli* are K76, H122, H125, H144, M156, A158, H160, V171, G173, and R204 (39, 40). *E.coli* LpxA has a strict preference for C:14 (hydroxymyristoyl) fatty acids, and this preference is referred to as a hydrocarbon ruler (39). LpxA from *F. tularensis* shares 44% identity

and 66% similarity with *E. coli* LpxA, but does not share the same hydrocarbon ruler (28). Instead, *F. tularensis* LpxA has evolved a relaxed acyl chain specificity and can attach longer fatty acids onto the 3' hydroxyl acyl of UDP-GlcNAc: incorporating either stearoyl (3-OH C18:0), or palmitoyl (3-OH C16:0) fatty acids.

Herein we describe the isolation and characterization of an extragenic suppressor mutation of Δ*ripA* in *F. tularensis* subspecies *holarctica* live vaccine strain (LVS) that mapped to *lpxA* and restored intracellular growth. We show that RipA and LpxA co-immunoprecipitate, and RipA is involved in modulating the ratio of C:18 to C:16 acyl chain specificity of LpxA in *F. tularensis*. Induced expression of *lpxA* in the absence of *ripA* is detrimental to bacterial growth, and the suppressor mutation T36N in LpxA renders the protein less stable. In summary, *F. tularensis* uses RipA to modulate LpxA activity.

## Materials And Methods

### *Bacterial Strains*

All bacterial strains, plasmids, and primers used in this study are listed in Table 3. *F. tularensis* subsp. *holarctica* LVS was obtained from Ft. Collins, CO. *Francisella* strains were maintained on chocolate agar supplemented with 1% IsoVitalex (BD), Chamberlains defined media (CDM) (4), or in BHI supplemented with 1% IsoVitalex at 37°C.

***Whole Genome Sequencing and PCR Verification***

Genomic DNA was purified from 10 ml cultures of *F. tularensis* grown in CDM using the MasterPure DNA purification kit (Epicentre). DNA was dissolved in 200 µl of EB buffer at 50 ng $\mu l^{-1}$ and submitted for whole genome sequencing at the High-Throughput Sequencing Facility at the University of North Carolina at Chapel Hill. Using the Genome Analyzer IIx (Illumina) we produced 36 bp single-end reads that were mapped the to the annotated genome on NCBI (NC_007880). By aligning the reads from the suppressor mutant strain to this reference we could identify the suppressor mutation. Alignments were made using SOAP with default parameters. Average sequence coverage was over 50 for the 1.89 Mb genome (19). Single nucleotide polymorphisms, deletions and insertions were located using SOAP and BLAT (16). A total of 4 mutations and 55 zero coverage regions identified. Mutations also present in our wild type laboratory strain and the Δ*ripA* strain were discarded as background mutations, leaving one unique mutation present in S102. To verify all polymorphisms detected by Illumina sequencing we PCR amplified the regions of interest and sequenced all strains including wild type *F. tularensis*, Δ*ripA*, and all suppressors (Genewiz, Inc.). Following further confirmatory sequencing all but one mutation were eliminated as background mutations.

***Gentamicin Protection Assay***

J774A.1 macrophage-like cells and TC-1 epithelial cells were inoculated with LVS at a multiplicity of infection (MOI) of 100. All LVS strains were grown overnight in CDM prior to inoculation. The cells were incubated with the bacterial inoculum for 2 hours (J774A.1) or 4 hours (TC-1) and then incubated with media containing 25 µg $ml^{-1}$ gentamicin to kill extracellular bacteria. At 4 hours (J774A.1) or 6 hours (TC-1), and at

24 hours post infection medium was removed, cells were scraped from the plate, serially diluted in PBS, and plated to determine the number of viable bacteria. To enrich for extragenic suppressor mutations in Δ*ripA* the infection was extended to 36 hours before bacteria were enumerated.

***Extragenic Suppressor Repair Using Allelic Exchange***

The *lpxA* (FTL_0539) allele plus 100bp of flanking DNA was PCR amplified from *F. tularensis* LVS genomic DNA. The amplified fragment was cut with BamHI and NotI and ligated into the SacB suicide vector, pMP812 (21). Allelic exchange was achieved by transformation, selection for plasmid co-integration, and counter selection on media containing 10% sucrose. DNA sequencing confirmed replacement of the mutant allele with the wild type (23).

***Co-immunoprecipitation of LpxA and RipA***

LpxA-HA was immunoprecipitated from mid-exponential phase *F. tularensis* LVS expressing *lpxA-HA* on a plasmid grown in CDM and pelleted by centrifugation at 13,000 xg for 5 minutes. Bacterial pellets were lysed using 150 mM NaCl, 1% Triton X-100, 50 mM Tris HCl (pH 8.0) and incubated for 30 minutes while shaking. Cell debris was removed by centrifugation for 5 minutes at 13,000 xg. Protein lysates were then incubated with 80 µl of µMACS$^{TM}$ Anti-HA MicroBeads (Miltenyi Biotec) for 30 minutes at 4°C. Following the manufacturers protocol, the proteins bound to the µMACS$^{TM}$ Anti-HA MicroBeads (Miltenyi Biotec) were loaded onto the µ column in the magnetic field of the µMACS separator. The column was washed with 5 column volumes of 150 mM NaCl, 1% Igepal CA-630, 0.5% sodium deoxycholate, 0.1% SDS,

and 50mM Tris HCl (pH 8.0) and the protein bound to LpxA-HA were eluted using hot 50mM Tris HCL (pH 6.8), 50 mM DTT, 1% SDS, 1 mM EDTA, 0.005% bromphenol blue, and 10% glycerol. All samples were analyzed by SDS-PAGE and western blot. Immunoprecipitation was performed on lysates of the strain with *ripA*-HA integrated in the chromosome and *lpxA*-V5 on a plasmid (Table S1, SKI22) as described above following the manufacturer's protocol for μMACS$^{TM}$ Epitope Tag Protein Isolation Kit (Miltenyi Biotec).

***Membrane Fractionation***

Membranes were fractionated as described previously by ultracentrifugation and Sarkosyl extraction (9). Briefly, mid-exponential phase bacteria were lysed by bead beating two times for 45 seconds using Lysing Matrix Tubes (MP Biomedicals). The lysates were clarified at max speed in a microcentrifuge for 5 minutes and crude membranes pelleted by ultracentrifugation for 2 hours at 100,000 xg. To enrich for cytoplasmic membranes from the pelleted crude membrane fraction 0.5% Sarkosyl was added overnight to selectively solubilize the inner membrane. The outer membrane was separated from the inner membrane by ultracentrifugation for 1 hour at 100,000 xg.

***Membrane Purification and Thin Layer Chromatography***

*F. tularensis* 100 ml cultures were grown to optical density of 1.0 ($OD_{600}$) or a T225 flask of J774A.1 cells were infected with *F. tularensis* at an MOI of 500. The bacteria were harvested by centrifugation and washed twice with PBS. The pellet was suspended in 8 ml of PBS. To the cell suspension 10 ml of chloroform and 20 ml of methanol were added to form a single phase (chloroform, methanol, and aqueous ratio of 1:2:0.8, v/v/v)

as previously described (42). After one hour of incubation at room temperature, the insoluble debris was removed by centrifugation at 3000 xg for 30 minutes. The supernatants were transferred to clean solvent-resistant bottles, and 10 ml of chloroform and 10 ml of PBS were added to generate a two-phase system. After mixing, the samples were centrifuged at 3000 xg for 15 minutes, and the lower phase and interface was collected. Samples were dried under a stream of nitrogen or in a speed vac. Thin layer chromatography was performed on purified membrane fractions dissolved in a total of 10 µl of chloroform and methanol (4:1) and spotted onto a silica gel 60 Å chromatography plate (Whatman). The plate was developed in the solvent chloroform, methanol, water, and acetic acid (25:15:4:2, v/v/v/v) and sprayed with 10% sulfuric acid in ethanol and charred at 100°C for 20 minutes.

***Western Blots***

Mini-Protean® TGX™ 4-20% precast gels (BioRad) were loaded with equal amounts of total protein from indicated samples and run at 250V using Tris-glycine SDS running buffer. For western blot assays, gels were transferred to nitrocellulose membranes and then blocked overnight with 1% bovine serum albumin in PBS-Tween 20. All antibodies were incubated at room temperature for 2 hours then washed with 3 volumes of PBS-Tween 20. The primary antibodies used were anti-RipAaa1-19, mouse anti-HA monoclonal antibody (Sigma), mouse anti-V5 monoclonal antibody (Sigma), mouse anti-*F.tularensis* LPS (US Biologicals F6070-C2), monoclonal anti-IglC (BEIresources NR-3196), monoclonal anti-IglB (BEIresources NR-3195). The secondary antibodies used were goat anti-rabbit IgG IRDye 680CW and 800CW or goat anti-mouse IgG IRDye

680CW and 800CW. Proteins were detected using near infrared fluorescence at 700 nm or 800 nm with the Odyssey Infrared Imaging System (LI-COR Biosciences).

***Lipid A Purification***

*F. tularensis* 100 ml cultures were grown to $OD_{600}$ of 1.0. The cells were harvested by centrifugation at 10,000 xg for 10 minutes in a RC5C centrifuge with the GSA rotor (Sorvall Instruments). Cells were resuspended in 10 ml of TE buffer with 50 μg $ml^{-1}$ proteinase K and incubated for one hour at 65°C. LPS was precipitated with 0.3 M sodium acetate and three volumes of 100% ethanol after incubation at -20°C for 2 hours, the LPS was centrifuged for 10 minutes at 10,000 xg as previously described (28). The pellet was suspended in 5 ml of water and LPS was precipitated with ethanol and sodium acetate a second time. The LPS pellet was suspended in 5 ml of water with 20 μg $ml^{-1}$ each of DNase and RNase and incubated for 2 hours at 37°C. Both 5 ml of LPS and 5 ml of phenol were warmed separately to 65°C then combined, mixed by vortexing, and incubated at 65°C for 30 minutes. LPS was then cooled on ice and centrifuged at 2000 xg for 10 minutes in an Allegra 6R centrifuge (Beckman Coulter). The aqueous layer and interface were collected. LPS was then ethanol precipitated 3X as above with 0.3 M sodium acetate and 100% ethanol. The LPS pellet was then suspended in 5 ml of 1% acetic acid and incubated at 100°C for three hours to separate the O-antigen from lipid A. Samples were then centrifuged at 14,000 xg for 30 minutes in a 5424 centrifuge (Eppendorf). The lipid A pellet was washed in water and centrifuged again for 30 minutes at 14,000 xg. The lipid A pellet was suspended in 60 μl of water. Then 50 μl of

methanol, and 100 μl of chloroform was added to the lipid A pellet and centrifuged at 8,000 xg for 10 minutes. The bottom organic layer and the interface were collected.

***Positive Ion Mode Mass Spectrometry on Lipid A***

Purified Lipid A samples were analyzed using a matrix-assisted laser desorption ionization Fourier transform mass spectrometer (MALDI-FTMS). Spectra were obtained in a positive-ion mode using 1:1 matrix of methanol to 2,-5 dihydrozybenzoic acid (DHB). Lipid A samples were dissolved into (3:1, v/v) chloroform and methanol.

***Negative Ion Mode Mass Spectrometry on Purified Membrane Samples***

Purified membrane samples were analyzed in negative ion mode using electrospray ionization ESI/MS via direct infusion (42). Samples were dissolved in (2:1, v/v) chloroform and methanol containing 1% piperidine. Mass spectra were collected on a QSTAR XL quadrupole time-of-flight tandem mass spectrometer (ABI/MDS-Sciex).

***Quantitative RT-PCR***

Total RNA was isolated from mid exponential phase cultures using RiboPure-Bacteria kit (Ambion) adding TRIzol, bead beating, then adding chloroform to separate the aqueous phase containing the RNA. DNA was removed using DNase (Promega) for 30 minutes at 37°C. Quantitative reverse transcriptase PCR (qRT-PCR) was performed in a 96-well format using the SensiFAST SYBR One-Step Kit (Bioline) following the manufacturer's protocol. Thermocycling and detection were performed using the iCycler thermal cycler (Bio-Rad). Both a positive control using a genomic DNA ladder and a negative control with no reverse transcriptase was analyzed for each run. All *lpxA* starting quantity (SQ) values were normalized to the mean SQ values for *gyrA*. Data represent three

independent experiments performed in triplicate. Significance was determined using an unpaired two-tailed *t*-test with unequal variance.

***Anhydrotetracycline Inducible Gene Expression System for lpxA and ripA***

The *E. coli-F. tularensis* shuttle vector was created with *lpxA* under the control of the *rpsLp-tetR* as previously described (20). The *E. coli-F. tularensis* shuttle vector containing *ripA* or *lpxA* was introduced into wild type LVS and the Δ*ripA* strain via electroporation as described previously (23). Transformants were selected on chocolate agar supplemented with 1% IsoVitalex and 200 μg $ml^{-1}$ Hygromycin B (Hyg; Roche Applied Sciences). In *F. tularensis,* 100 ng $ml^{-1}$ of anhydrotetracycline (ATc; Sigma-Aldrich) was used to induce expression of *lpxA* or *ripA* as previously described (20).

***Circular Dichroism***

Spectra from a Chirascan Plus: steady state Circular Dichroism/Fluorescence spectrometer with titration and automated temperature ramping capabilities were recorded at 25°C using 0.1 cm water-jacketed cell. LpxA samples were diluted to 3-10 μM in 10 mM potassium phosphate, pH 8.0. Spectra were measured from 260 to 190 nm. Molar ellipticity was calculated:

$$[\theta] = \frac{\Delta A}{C * I}$$

ΔA is the change is CD spectra obtained from 260 to 190 nm, C is the molar concentration of LpxA, and I the cell path length. Following polarimetric conversions molar ellipticity was reported in degrees $cm^2$ $dmol^{-1}$.

### *LpxA-His$_6$ Purification for Enzyme Assay*

Strains of interest were inoculated into 500 ml of Luria-Bertani (LB) medium containing 100 μg ml$^{-1}$ of Ampicillin and were incubated while shaking at 37°C until an $OD_{600}$ of 1.0 was reached. The cultures were induced with 1 mM IPTG followed by incubation at 25°C for four hours. Cells were harvested by centrifugation at 10,000 xg for 10 minutes at 4°C, and processed immediately or frozen at -80°C. Cells were resuspended in 6 ml of 20 mM Hepes, 100 mM NaCl at pH 8.0. Cell suspensions were disrupted by French press at 20,000 psi. Cellular debris was removed by centrifugation at 14,000 xg for 5 minutes at 4°C in a 5424 centrifuge (Eppendorf). Soluble crude cytosol was loaded onto 3 ml of nickel-nitriol-triacetic acid (Ni-NTA) resin (Qiagen). The resin was washed with 10 column volumes of loading buffer containing 500 mM NaCl and then eluted with 20 mM Hepes and 500 mM imidazole (pH 8.0). Purified *F. tularensis* LpxA-His$_6$ was desalted using Slide-A-Lyzer Dialysis Cassette (Thermo Scientific) and dialyzed against 20 mM Hepes pH 8.0. Protein concentrations were determined by BCA assay. The purification, and acylation of holo-ACP was carried out as described previously, except hydroxypalmitic acid (C16:0) was used in place of hydroxymyrstic acid (C14:0) (14).

### *Fluorescent Enzyme Assay for LpxA-His$_6$*

Following the procedure developed by Dotson and Jenkins, the assay was performed at 25°C in 20 mM Hepes (pH 8.0) at a final volume of 100 μl monitoring the conversion of ThioGlo 1 (methyl10(2,5-dioxo-2,5-dihydro-1H-pyrrol-1-yl)-9-methoxy-3-oxo-3H-benzo [f] chromene-2-carboxylate) to ThioGlo-ACP produced in the LpxA acyltransferase-catalyzed reaction (14). To the appropriate well 40 μM of acyl-ACP, 4 mM UDP-GlcNAc, and 10 μM ThioGlo were added. To initiate the reaction, 10 nM LpxA-His$_6$

was added directly to the well and mixed gently. The SpectraMax M2*e* plate reader (Molecular Devices) was used to continuously monitored at $\lambda_{ex}$ = 379 nm and $\lambda_{em}$ = 513 nm for 10 minutes at 15 second intervals. Control reactions lacking individual substrate or enzyme components were performed to demonstrate that an increase in fluorescence was both enzyme and substrate dependent. To calculate initial rates linear regression plots were generated for the first two minutes of the reaction.

## Results

### *Extragenic Suppressor Mutation Enrichment in the ΔripA Background*

As shown previously (9), following infection of host cells, wild type *F. tularensis* grew two logs in 24 hours, while typically there was no detectable growth of the Δ*ripA* strain (Fig. 1). However, we routinely recovered colonies of the Δ*ripA* strain from the host cell cytoplasm 24 hours post invasion. We therefore wanted to determine if any of the recovered Δ*ripA* strains had spontaneous extragenic suppressor mutations that restored intracellular growth. To enrich for extragenic suppressor mutations in the Δ*ripA* strain we performed several rounds of infections lasting 36 hours each in J774A.1 cells whereby the bacteria isolated from the first round of infections were then used to inoculate a new flask of J774A.1 cells (Fig. 1). Using the repeated rounds of infections in host cells, five independently derived extragenic suppressors of the Δ*ripA* strain were isolated. Using whole genome sequencing with the Genome Analyzer IIx (Illumina) we mapped the suppressor mutations in one of the suppressors we obtained during enrichments in Figure 1, named S102, by conducting comparative analysis aligning the

sequencing reads from the suppressor mutant strain to the annotated genome on NCBI (NC_007880) (Table 1). The sequencing results were remarkably similar to the published annotated genome, with only 4 polymorphisms detected and 55 zero coverage regions detected (Table 1). Of the 55 zero coverage regions, 54 mapped to insertion sequence (IS) elements. IS elements have small inverted repeats, where the short sequence reads cannot span the entire length of the conserved repeated sequence, allowing the reads to align to incorrect IS elements in the genome (Table 4). The LVS genome contains 59 ISFtu1 elements and 43 ISFtu2 elements that range in size from about 100bp to about 900bp. The remaining zero coverage region was the *ripA* (FTL_1914) locus, confirming that the extragenic suppressor mutation was in a Δ*ripA* background.

To determine if the mutations identified by whole genome sequencing were unique to S102 and not just variations present in our laboratory strain, the regions of interest were PCR amplified and analyzed using wild type *F. tularensis*, Δ*ripA* and Δ*ripA* suppressor genomic DNA. All the strains tested had two polymorphisms, confirming that the laboratory strain is similar but not identical in sequence to the annotated genome online (NC_007880) (Table 1). The first polymorphism was a base pair change in FTL_0146, an ABC transporter ATP-binding protein that caused an R341L missense mutation. The second polymorphism was a point mutation in FTL_1388, a L-aspartate oxidase, leading to the missense A93T mutation. The Δ*ripA* strain contained an additional missense mutation in FTL_0717, ribonuclease E, K38T likely acquired during the deletion process of *ripA*.

The only unique mutation found in the suppressor strain, S102, was located within FTL_0539, which encodes LpxA (Table 1). *lpxA* is located in an essential operon containing five genes involved in membrane synthesis. LpxA is an acyltransferase that catalyzes the first step in lipid A biosynthesis, using UDP-N-acetylglucosamine (UDP-GlcNAc) and acyl-ACP to synthesize the core component of lipopolysaccharide. The polymorphism within *lpxA* was a point mutation leading to the substitution T36N. The amino acid substitution is located within the hexapeptide transferase domain close to the N-terminus, and not within the active pocket. Thus, the location of the mutation is unlikely to alter the active pocket but could alter protein stability.

Four of the five independently derived extragenic suppressor mutations mapped to *lpxA* and the mutations resulted in amino acid substitutions located primarily along the left-handed helix of the short parallel β-sheet of LpxA (Fig. 2). The fifth extragenic suppressor mutation mapped to a gene encoding GlmU, which is also involved in the synthesis of lipid A. GlmU is an essential bifunctional acetyltransferase and an uridyltransferase that performs the last two sequential steps in the synthesis of UDP-GlcNAc. UDP-GlcNAc is an important component of both lipid A—the anchor of LPS, and peptidoglycan (Fig. 3). S103 contained a missense mutation within the uridyltransferase domain of *glmU* resulting in a substitution E57D (Table 1).

***LpxA T36N Rescued Growth of ΔripA in Eukaryotic Cells***

To determine if the unique mutation found in *lpxA* was responsible for the suppressor phenotype, we repaired S102 *lpxA* base pair mutation, changing adenine 107 back to wild type cytosine, resulting in the reversion of T36N to N36T. S102 proliferated

in 24 hours in both J774A.1 and TC-1 cells (Fig. 4A and B). The repaired *lpxA* abrogated the suppressor growth phenotype in both J774A.1 and TC-1 cells demonstrating that the single point mutation in *lpxA* was responsible for the suppressor phenotype (Fig. 4A and B). Given the exceptional difficulty manipulating the essential operon containing *lpxA* in *F. tularensis* we were unable to repair the other suppressor mutations.

***LpxA and RipA Co-immunoprecipitate***

RipA is a cytoplasmic membrane protein containing two domains that are essential for function and are accessible to the cytoplasm (25). LpxA is a soluble protein that interacts with acyl-ACP on the cytoplasmic membrane. To evaluate interactions between RipA and LpxA we performed immune precipitation reactions using *F. tularensis* lysates. The first precipitation reaction was performed with a *F. tularensis* strain containing the wild type copy of *ripA* in the chromosome and *lpxA-HA* expressed from a plasmid. LpxA-HA bound to an anti-HA agarose column immunoprecipitated with RipA (Fig. 5). The reciprocal co-immunoprecipitation was performed with *ripA-HA* integrated into the chromosome and *lpxA-V5* expressed from a plasmid. In both conditions LpxA and RipA co-precipitated, but the interaction was weak (Fig. 5). The two proteins are likely only involved in transient binding or their interaction may be facilitated by another protein. Given the possibility that RipA and LpxA likely interact, we next wanted to determine if the localization of LpxA was altered in the Δ*ripA* strain. Membrane fractions were separated using ultracentrifugation and Sarkosyl extraction for the strain containing *lpxA-HA* on a plasmid. The soluble, inner membrane, and outer membrane fractions were normalized to equivalent total protein and analyzed by Western

blot. LpxA-HA was present in the inner membrane fraction in both the wild type *F. tularensis* stain and the Δ*ripA* strain, suggesting localization of LpxA was not influenced by the presence or absence of RipA (Fig. 6). Based on these results we conclude that RipA and LpxA interact in the inner membrane, but RipA does not impact the subcellular localization of LpxA.

### *Membrane Composition and LPS are not Altered by the Extragenic Suppressor Mutation in lpxA*

There is substantial diversity among bacterial fatty acids profiles and *F. tularensis* is unique for its relative abundance of long chain saturated and monoenoic acids (13). *F. tularensis* LVS has a lipid content of 21% by dry weight, and the two major phospholipid components are phosphatidylethanolamine (PE; 76%) and phosphatidylglycerol (PG; 24%) (2). In *F. tularensis* PE contains a high proportion of 24:0 fatty acids, while PG contains mainly C18:0 and C22:0 fatty acids. Another unique property of the membrane composition of *F. tularensis* is the abundant amount of free lipid A present on the outer membrane of the bacteria that is not attached to O-antigen sugars (37). In *F. novicida* two forms of free lipid A were identified: one containing a galactosamine sugar attached to the 1' phosphate position (compound A1), and the other containing a glucose sugar attached to the 6' OH group on glucosamine (compound A2) (37). We analyzed the lipid profile of purified membrane fractions from wild type *F. tularensis*, Δ*ripA* and S102 in order to identify any differences in the membrane composition between the strains. As reported previously, the most abundant components of the purified membrane fractions were PE, PG, phosphatidylcholine (PC), and lipid A (Fig. 7A) (37). We also observed

similar quantities of free lipid A in *F. tularensis* LVS as seen in *F. novicida,* however no compound A2 was detected corresponding with a glucose sugar linked to the 6' position of lipid A, confirming previous findings (32, 37). In all broth grown strains analyzed, there was a similar composition of lipids as determined by thin layer chromatography (TLC) (Fig. 7A). Others have shown that *F. tularensis* membrane profiles changed during intracellular growth (3). To determine if RipA is involved in modifying the membrane during host infection, we purified bacterial membrane fractions from J774A.1 cells infected with either wild type *F. tularensis* LVS or Δ*ripA* and subsequently analyzed the lipid profiles by TLC. We observed changes in the membrane composition of *F.tularensis* inside J774A.1 cells as compared to broth grown organisms, but the changes were not influenced by the absence of *ripA* (Fig. 7B). In addition, there were no consistent changes among the LPS banding pattern of wild type *F. tularensis*, Δ*ripA*, and S102 observed by western blot (Fig. 7C).

***Mass Spectrometry Lipid A Profiles for Wild Type F. tularensis, ΔripA, and ΔripA Suppressor S102 are Similar***

Lipid A is an essential component of the outer membrane of most Gram-negative bacteria (33). No deletions or transposon insertions in *lpxA* have been isolated in *F. tularensis* and we were not successful at making a Δ*lpxA* strain (unpublished results). Thus, it is likely that *lpxA* is essential in *F. tularensis* (11). To determine if the suppressor mutation in S102 *lpxA* disrupted LpxA function we assessed the structure and quantity of lipid A produced in wild type *F. tularensis* LVS, Δ*ripA*, and S102. Purified lipid A was analyzed using matrix-assisted laser desorption ionization Fourier transform

mass spectrometer (MALDI-FTMS) in positive ion mode (Fig. 8A-C). Each of the three samples contained a peak at 1549 m/z corresponding with an intact lipid A molecule with a 1' phosphate and 3' stearoyl acyl chain (3-OH C18:0). Another peak was present in each sample at 1521 m/z that corresponded with lipid A containing a shorter palmitoyl acyl chain on the 3' position of glucosamine (3-OH C16:0). Confirmatory fragment ions that are naturally generated by neutral loss of acyl chains from the parent ion were observed at 683 m/z and 655 m/z corresponding with the palmitoyl and stearoyl acyl chains located on the 3-OH of glucosamine. These data are consistent with the previously published *F. tularensis* lipid A structures (28, 32, 37). Similar results were obtained using electrospray ionization mass spectrometry ESI/MS in negative ion mode (Fig. 8D-F). All samples contained lipid A with the 1' phosphate and the 3' stearoyl acyl chain (3-OH C18:0) at 1504 m/z. The 1476 m/z corresponded with lipid A with the shorter palmitoyl chain on the 3' position of glucosamine (3-OH C16:0). There were no unique structures present in the lipid A samples from the suppressor when compared to wild type and all strains contained detectable amounts of lipid A. However the ratio of the 18/16 carbon chains for the Δ*ripA* strain was consistently lower than wild type suggesting a preference for longer acyl chain lengths by LpxA in the presence of RipA (Fig. 8G).

### *LpxA Protein Levels are Significantly Lower in the ΔripA Strain Compared to Wild Type*

A potential consequence of RipA-LpxA interaction is that RipA may stabilize LpxA. To determine if RipA influences the stability of LpxA we first quantified the amount of LpxA protein present in wild type *F. tularensis* and the Δ*ripA* strain. At one

hour post chloramphenicol treatment LpxA protein levels were 2-fold higher in wild type *F. tularensis* than in Δ*ripA,* when normalized to the loading control IglB (Fig. 9A and B). The LpxA-HA T36N protein levels were low in both wild type and Δ*ripA*, suggesting that the suppressor mutation in LpxA may reduce protein stability (Fig. 9A and B). To further analyze whether the observed difference in LpxA protein levels were due to protein stability or changes in transcription, we quantified *lpxA* mRNA in wild type and Δ*ripA* strains. We performed quantitative real time PCR on *lpxA* and normalized transcript levels to the housekeeping gene *gyrA*. The relative transcript levels of *lpxA* were not significantly different between wild type *F. tularensis* and Δ*ripA* indicating that the regulation of *lpxA* is posttranscriptional (Fig. 9C).

***Inducing Expression of lpxA Negatively Affects the Δripa Strain***

Given that LpxA and RipA physically interact, and the protein concentration of LpxA in wild type *F. tularensis* was significantly higher than Δ*ripA,* we hypothesize that elevated levels of LpxA protein in the absence of RipA could be detrimental for growth and therefore responsible for the failure of Δ*ripA* to grow *in vivo*. To test if LpxA activity and the flux of UDP-GlcNAc and acyl-ACP are important for bacterial cell viability we created an anhydrotetracycline (ATc) inducible expression system for *lpxA* to control the amount of LpxA present in both wild type *F. tularensis* and Δ*ripA* (20). When *lpxA* expression was induced in the Δ*ripA* strain the bacteria stopped growing (Fig. 10A and B), whereas, growth of wild type *F. tularensis* was barely affected by the increased expression of *lpxA*. These results suggest that activity and amount of LpxA is very tightly regulated in the cell and is dependent on RipA. Conversely, when *ripA* expression was

induced in the suppressor mutant strain containing LpxA T36N, growth of *F. tularensis* was only slightly reduced (Figure 10C and D). These results suggest that the activity or amount of LpxA is modulated in a RipA dependent manner.

***LpxA T36N is Less Stable than Wild Type LpxA and has Reduced Enzyme Activity***

The coils of the β-helix of LpxA are specified by hexapeptide repeats (7). There are specific side-chain interactions in the parallel β-helices, where an asparagine ladder forms H-bonds with itself or main chain amides to stabilize the tight turn of the beta-helix (17). The asparagine residue in the suppressor mutant strain could be altering the structure of the protein and affecting the function of LpxA. However, LpxA exhibits unusually high stability due to the natural nanotube formed by the left-handed parallel β-helix and does not unfold completely until the protein reaches temperatures as high as 525 K (7). The requirement for such high temperatures precluded a melting curve assessment for LpxA. Figure 11A shows the circular dichroism (CD) spectra of LpxA wild type using three concentrations ranging from 125 μg $ml^{-1}$ to 65 μg $ml^{-1}$. At all concentrations the large maximum near 194 nm and minimum near 208 nm and 220 nm correspond with the secondary structure of LpxA representing CD spectra for α-helices, left-handed β-helices, and β-turns. The molar ellipticity values for all concentrations of wild type were the same while the values for LpxA T36N displayed much less secondary structure (Fig. 11B). LpxA T36N was loaded at 65 μg $ml^{-1}$, but spectra were present for only about 37 μg $ml^{-1}$ (Fig. 11B). The CD spectrum and molar ellipticity values for LpxA T36N suggests that 56% of the protein is not folded into the correct secondary structure and is different from wild type LpxA.

To determine if the T36N mutation in LpxA altered enzyme activity, we used the newly developed continuous fluorescent enzyme assay for LpxA, which measures the time-dependent turnover of LpxA catalyzed acyl group transfer (Fig. 11C) (14). The assay monitors the rate of holo-ACP production by detecting fluorescent ThioGlo 1(methyl 10-(2,5-dioxo-2,5-dihydro-1H-pyrrol-1-yl)-9-methoxy-3-oxo-3H-benzo[f]chromene-2-carboxylate) that conjugates to ACP once the acyl group is transferred to LpxA. Control reactions in which individual components were omitted showed little increase in fluorescence, showing that the production of holo-ACP was being measured. Initial velocities were calculated using linear regression analysis during the first two minutes of the assay (Table 2). The initial rate of LpxA T36N activity was 33.7% lower than the initial rate of wild type LpxA from *F. tularensis* suggesting the missense T36N mutation influences the enzyme activity of LpxA (Fig. 11C). In addition, we observed significant decreases in LpxA T36N enzyme activity when compared to wild type LpxA after freezing the protein at -80 °C for as short as 5 minutes, supporting the hypothesis that the LpxA T36N mutation reduces protein stability and also decreases enzyme activity (Fig. 11D). The initial rate of LpxA activity for wild type was only reduced by 7.4% when frozen at -80 °C, while the initial rate of LpxA T36N activity dropped by 88.5% (Table 2).

These data demonstrate that the suppressor LpxA T36N is less stable and less active than wild type LpxA. In addition, the induced expression of *lpxA* in the absence of *ripA* is detrimental to bacterial growth. Together, these findings support the conclusion that the amount of LpxA protein is modulated by *F. tularensis* in a RipA dependent manner, and this control is important for adaptation to the intracellular environment.

## Discussion

The main goal of this study was to ascribe biological function to RipA, a key factor for *F. tularensis* intracellular growth, by isolating, mapping and characterizing an extragenic mutant S102. S102 and 4 other independently derived extragenic mutations mapped to *lpxA* or *glmU*. Both enzymes (LpxA and GlmU) are essential components of the lipid A biosynthesis pathway. By taking a multidisciplinary approach, combining genetics and biochemistry, we determined RipA influences LpxA stability and LpxA specificity for longer acyl chain in *F. tularensis*. What remains to be determined is the role RipA plays during intracellular growth, and how LpxA and RipA prime the bacteria to survive and withstand the host defenses that usually kill invading pathogens. Understanding RipA function provides an important insight into the specific mechanisms used by *F. tularensis* to modulate LpxA—the first enzyme in the lipid A biosynthesis pathway.

The suppressor mutation in S102 made LpxA less stable, and the induced expression of wild type *lpxA* in the absence of *ripA* inhibited bacterial growth, supporting the conclusion that the interaction between RipA and LpxA is critical for controlling the first step in the lipid A synthesis pathway of *F. tularensis*. The tight regulation of the lipid A biosynthesis pathway may be important for adapting the membrane to withstand host environmental stresses. A decrease in the activity of LpxA may stimulate the phospholipid biosynthetic pathway to divert the pool of hydroxyacyl-ACP more towards the synthesis of phosphatidylethanolamine. Homoviscous adaptation is critical for bacteria to respond to environmental changes, such as in temperature, osmolality, salinity

and pH (41). Phosphatidylethanolamine and phosphatidylglycerol are the two major phospholipids present in *F. tularensis* contributing to 21% of the dry weight of the bacteria, which is high relative to other bacteria, and may allow *F. tularensis* to resist a diverse array of host defenses (2). Recycling of the phospholipids and sugars that are used as intermediates in the synthesis of outer membrane components is critical for bacterial bilayer stability during peak infection, and is a tightly regulated process. During intracellular growth, when long chain fatty acids are in short supply it may be critical to control the lipid A synthesis pathway so phospholipid synthesis can continue. For example, LpxC (the second step in lipid A biosynthesis) is proteolyticly regulated by FtsH to control the activity (8). The phospholipid acyl chains determine the viscosity of the membrane; with unsaturated chains providing more membrane fluidity and long saturated chains provide more rigidity (41). *F. tularensis* lipid A and phospholipids are composed of much longer fatty acid chains than seen in *E.coli*, which could in part help *F. tularensis* adapt to the intracellular environment. We show that RipA influences LpxA acyl chain specificity, increasing the amount of longer C18:0 fatty acids when compared to the amount of C16:0 fatty acids, which may provide more rigidity to the *F. tularensis* membrane and perhaps provide more bilayer stability. This increased rigidity of the membrane may protect *F. tularensis* from cytoplasmic stresses such as pH changes, which is critical for pathogenesis. This hypothesis would be in agreement with the elevated transcription and translation of *ripA* at neutral pH coinciding with *F. tularensis* leaving the acidified vacuole and entering the neutral cytoplasm (10).

LPS is the major glycolipid molecule present on the cell surface of most Gram-negative bacteria that constitutes the interface between the environment and the interior

of the bacterial cell. LPS is made up of a hydrophobic domain known as lipid A (endotoxin), a non-repeating core oligosaccharide, and a distal polysaccharide (O-antigen). The O-antigen sugars are not required for growth in the laboratory, but help bacteria resist antibiotics, the complement pathway, and other environmental stresses (31). Lipid A is referred to as endotoxin in Gram-negative bacteria because it induces a massive cytokine response and production of nitric oxide when recognized by host cell TLR4/MD2 receptors (29). *Escherichia coli* lipid A is a hexa-acylated disaccharide of glucosamine that is phosphorylated at both 1' and 4' positions and is easily recognized by the host cell and stimulates a robust inflammatory response (38). Several pathogens, including *F. tularensis,* have evolved ways to alter their lipid A to avoid host detection by removing phosphate groups and acyl chains (5, 15, 37). Specifically, *F. tularensis* expresses an enzyme LpxF that removes the 4' phosphate and the 3' hydroxyacyl to make a tetra-acylated disaccharide of glucosamine with a 1' phosphate (35, 36). *F. tularensis* lipid A is also unique when compared to other Gram-negative bacteria because the majority of lipid A is not attached to the O-antigen sugars of LPS and is referred to as free lipid A (37). The resulting lipid A molecule is not recognized by TLR4 and thus does not provoke a significant host inflammatory response (34). The ability to prevent host innate immune detection of lipid A is a key component in *F. tularensis* pathogenesis (26). In addition to immune evasion, LPS plays an important positive role in the assembly of many outer membrane proteins, and the molecular nature and biochemical basis of this process remains poorly understood (18). We have only just begun to appreciate the complexity of this process and the genetic analysis presented here may provide important clues in understanding the biogenesis of the outer leaflet in the outer membrane. The O-

antigen sugars help bacteria resist antibiotics, the complement pathway, and other environmental stresses such as nitric oxides (31). LPS is also important for host cell attachment. It is unusual for *F. tularensis* to have the majority of the lipid A free of O-antigen. What role free lipid A plays in the pathogenesis of *F. tularensis* is not fully understood, but may provide a means for *F. tularensis* to regulate the flux and usage of critical substrates such as UDP-GlcNAc needed for peptidoglycan synthesis and other cell envelope components. *F. tularensis* has evolved a number of strategies to modify the components of the cell envelope to adapt to intracellular environments.

In conclusion, we have identified a new protein involved in controlling LpxA acyl chain specificity and ultimately lipid A synthesis, which may be an important player in membrane remodeling during host cell infections. However, the precise changes in *F. tularensis* membrane composition during intracellular growth need to be further characterized.

## Figures

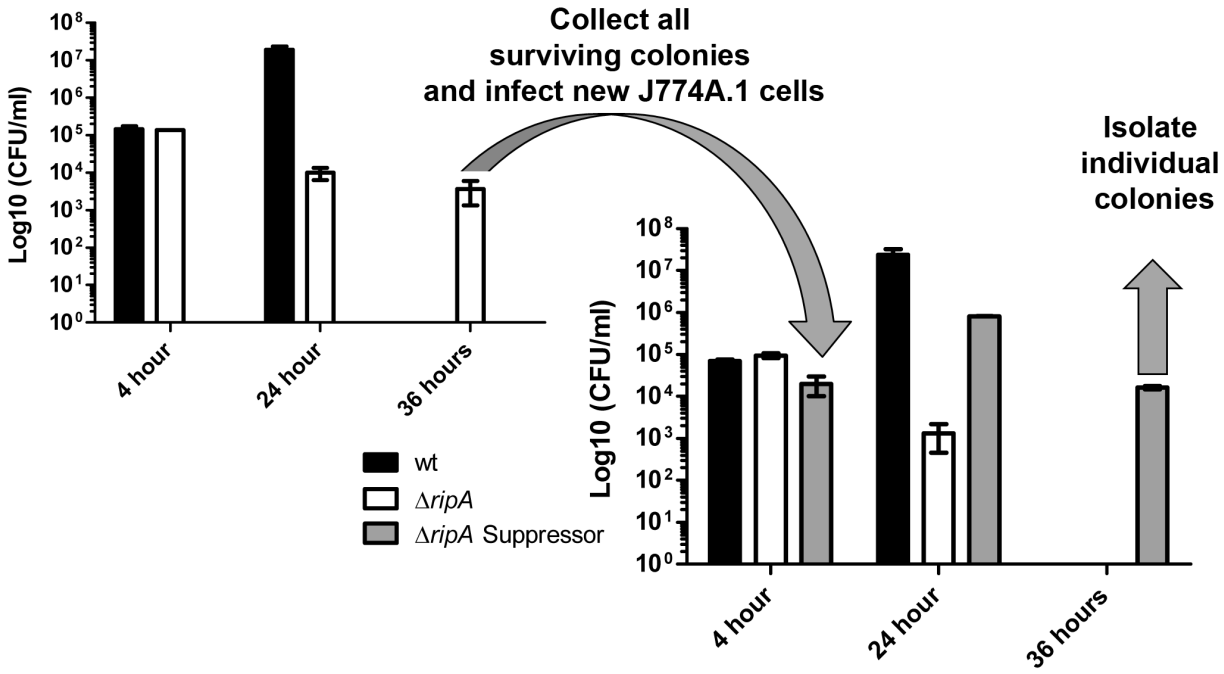


**Figure 4.1. Extragenic suppressor enrichment in J774A.1 macrophage like cells**

Gentamicin protection assays were performed with a multiplicity of infection (MOI) of 100 using wild type *F. tularensis*, and the Δ*ripA* strain. The infection was extended to 36 hours to allow time for extragenic suppressor mutations to arise in the Δ*ripA* strain under selective pressure. All surviving colonies were collected from the Δ*ripA* mutant at 36 hours and were used to infect another flask of J774A.1 macrophages at an MOI of 100. Individual colonies recovered from the second infection were saved for suppressor analysis.

| Strain | Gene | Name | aa substitution | Suppressor name |
|---|---|---|---|---|
| Δ*ripA* | FTL_0539 | UDP-N-acetylglucosamine acyltransferase (LpxA) | D144N | S101 |
| Δ*ripA* | FTL_0539 | UDP-N-acetylglucosamine acyltransferase (LpxA) | T36N | S102 |
| Δ*ripA* | FTL_0453 | UDP-N-acetylglucosamine -pyrophosphorylase/ glucosamine-1-phosphate N- acetyltransferase (GlmU) | E57D | S103 |
| RipA Y35A4 | FTL_0539 | UDP-N-acetylglucosamine acyltransferase (LpxA) | G188C | S104 |
| *ripA*::Tn5 | FTL_0539 | UDP-N-acetylglucosamine acyltransferase (LpxA) | D75Y | S105 |

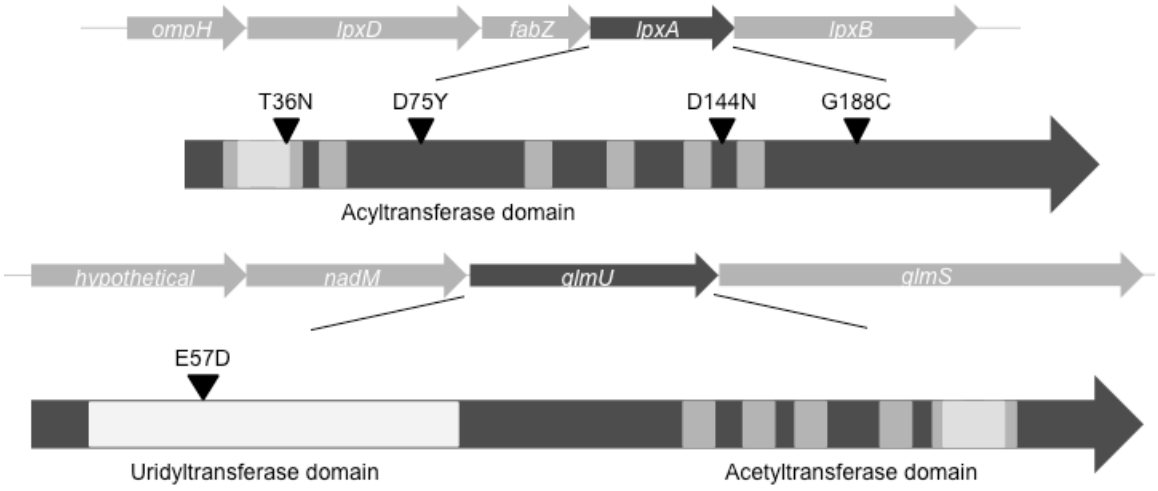


**Figure 4.2. Extragenic suppressor mutations map to *lpxA* and *glmU***

Four of the five independently derived extragenic suppressor mutations mapped to *lpxA*. *lpxA* is centrally located in an essential operon containing five genes. The amino acid substitutions in LpxA were mainly located along the left-handed helix of the short parallel β-sheet. LpxA contains hexapeptide repeats that is a signature of an acetyltransferase enzyme (shown in gray). One extragenic suppressor mutation mapped to *glmU*, which is also centrally located in an essential operon containing 4 genes. The amino acid substitution mapped within the uridyltransferase domain located close to the N-terminus. LpxA and GlmU are both involved in membrane synthesis, and both proteins contain hexapeptide transferase signature domains.

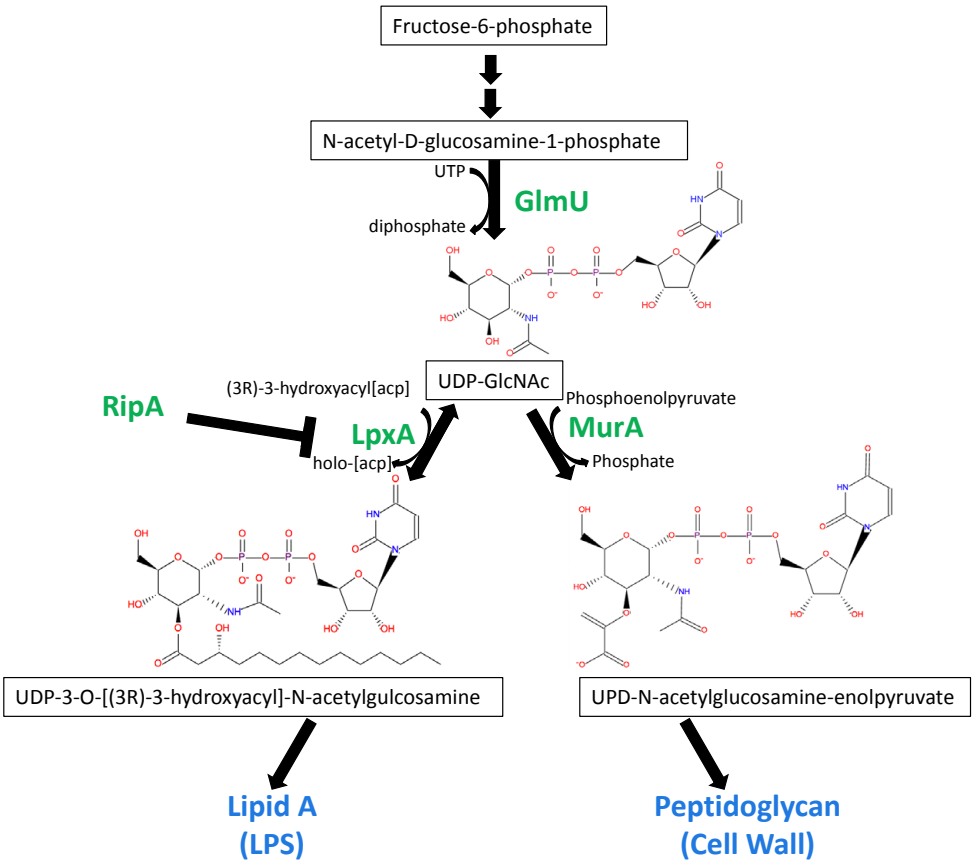


**Figure 4.3. The biosynthetic pathway of LpxA and GlmU**

UDP-N-acetylglucosamine (UDP-GlcNAc) is synthesized from fructose-6-phosphate with the last two sequential steps synthesized by the bifunctional acetyltransferase and uridyltransferase, GlmU. The substrate UDP-glucosamine is either used by LpxA in conjunction with acyl-ACP in a reversible reaction to make a precursor molecule of lipid A, or is used by MurA to make a precursor molecule of the cell wall.

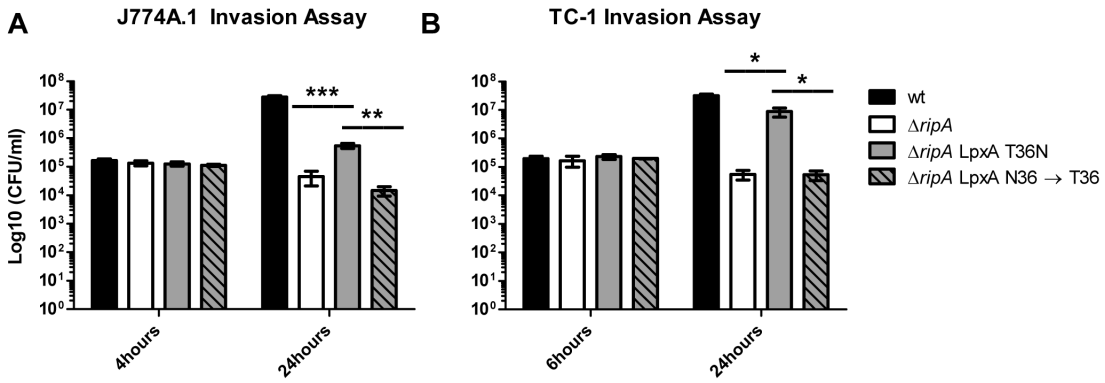


**Figure 4.4. The S102 extragenic suppressor mutant phenotype and repair in J774A.1 and TC-1 cells**

Intracellular replication of wild type *F. tularensis* LVS, Δ*ripA,* S102 (T36N), and the strain containing the repaired S102 extragenic suppressor mutation (LpxA N36 → T) was assessed within J774A.1 macrophages (A) and TC-1 epithelial cells (B) using the gentamicin protection assay. Each graph is the mean of three independent experiments done in triplicate, and the error bars represent the standard deviation. Statistical significance was determined using Student's *t* tests comparing LpxA T36N to Δ*ripA* or to LpxA N36 → T36. *, $P < 0.05$; **, $P < 0.001$; ***, $P < 0.0001$.

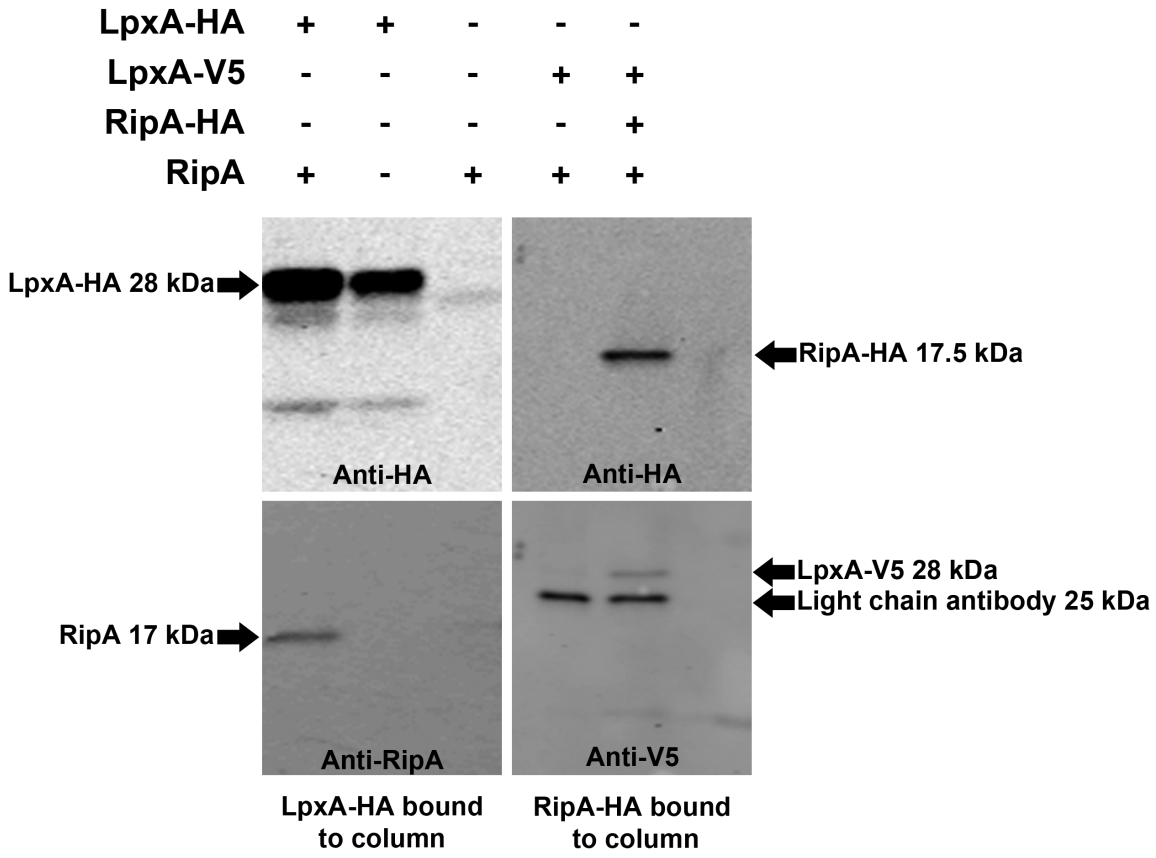


**Figure 4.5. LpxA and RipA co-immunoprecipitate**

Western blot of immune precipitated proteins from whole cell lysates of *F. tularensis.* Left two western blots demonstrate LpxA-HA C-terminal tagged protein pulls out RipA when probed with primary antibodies to anti-HA and anti-N-terminal RipAaa1-19. Right two western blots demonstrate that RipA-HA C-terminal tagged protein pulls out LpxA-V5 protein. Western blots on the right were probed with primary antibodies to anti-HA and anti-V5. This figure is a representative of at least three independent experiments.

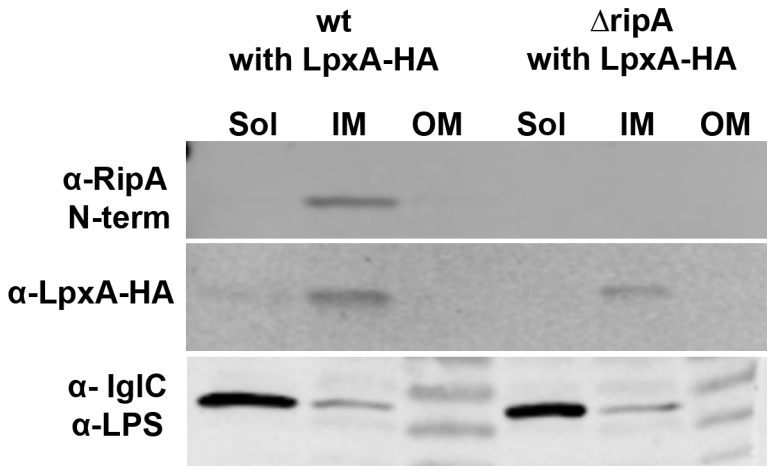


**Figure 4.6. LpxA localizes to the inner membrane**

Membrane fractionation separating the soluble (Sol), inner membrane (IN), and outer membrane (OM) fractions using ultracentrifugation and Sarkosyl extractions. Fractions from wild type LVS with *lpxA-HA* in trans, and the Δ*ripA* strain with *lpxA-HA* in trans were probed with the N-terminal RipAaa1-19 antibody for an inner membrane control, the IglC antibody for the soluble fraction control (a small fraction of IglC was also present in the inner membrane fraction), and LPS antibody for the outer membrane control. The monoclonal anti-HA antibody was used to probe for LpxA-HA. This figure is a representative of three independent experiments.

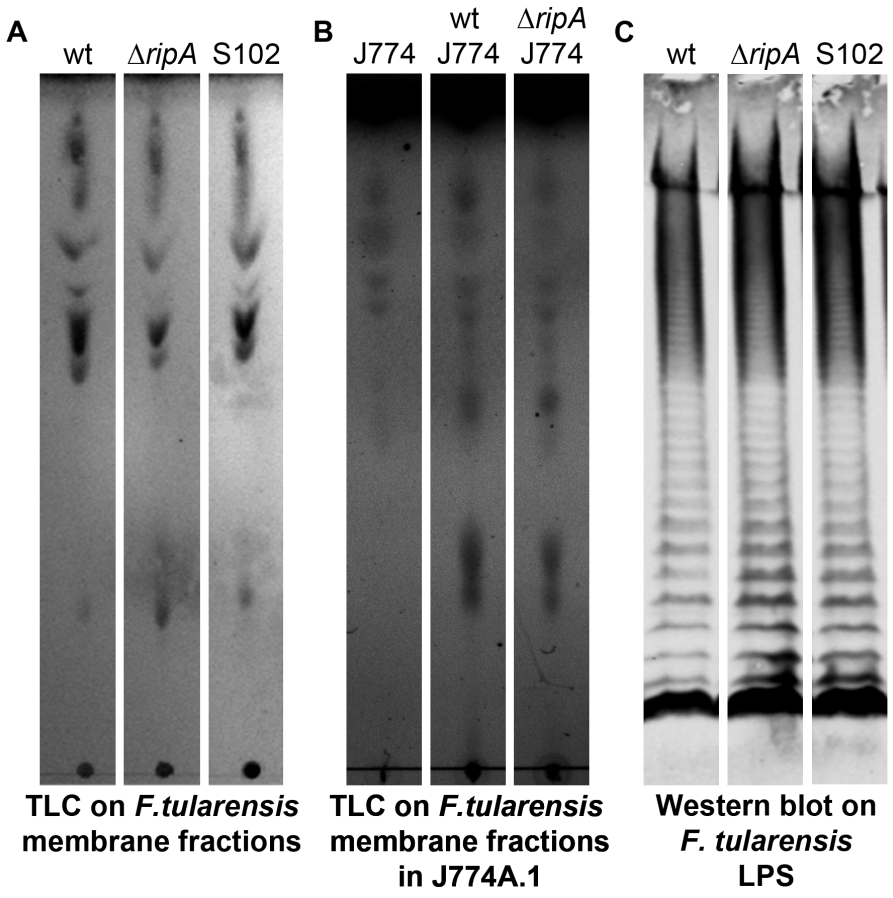


**Figure 4.7. Membrane and LPS composition of suppressor S102**

**(A)**Thin layer chromatography on purified membrane fractions from LVS, Δ*ripA*, and S102 using the Bligh and Dyer method (8). The plate was developed in the solvent chloroform, methanol, water, and acetic acid (25:15:4:2, v/v/v/v) and sprayed with 10% sulfuric acid in ethanol and charred at 100°C for 20 minutes. **(B)** Thin layer chromatography on purified membrane fractions from J774A.1 macrophages and J774A.1 infection with LVS, or Δ*ripA* using the same Bligh and Dyer method **(C)** LPS western blots on whole cell lysates from LVS, Δ*ripA*, and S102. The blot was probed with *Francisella tularensis*, LPS antibody. All experiments shown here are representatives, and were repeated at least three times.

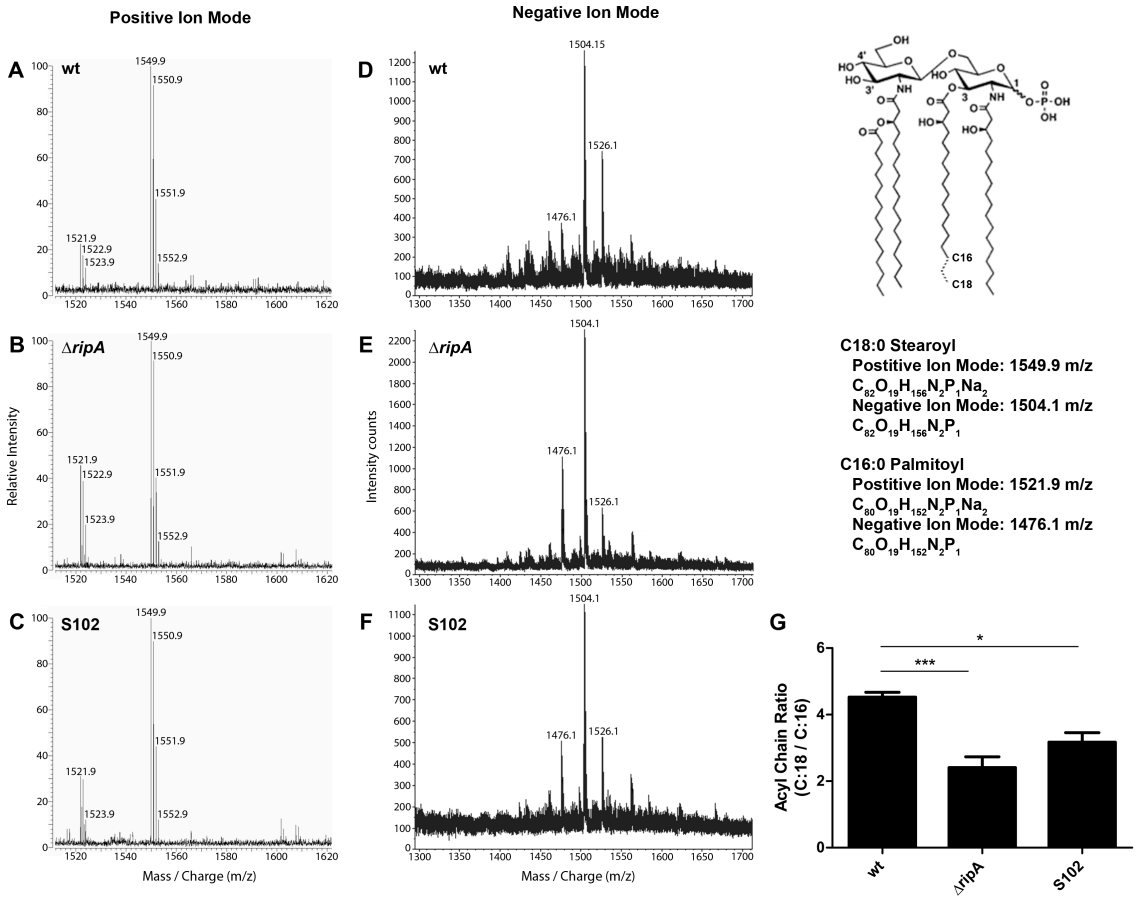


**Figure 4.8. Mass spectrometry on lipid A and membrane fractions**

Lipid A samples were analyzed using a matrix-assisted laser desorption ionization Fourier transform mass spectrometer (MALDI- FTMS). Spectra were obtained in a positive-ion mode. **(A)** Wild type LVS, **(B)** Δ*ripA*, and **(C)** S102 all have a peak at m/z 1549 and m/z 1521, which corresponds with the intact lipid A molecule with a 1' phosphate and a 3' stearoyl or palmitoyl acyl chain, respectively. Purified membrane samples were analyzed using electrospray ionization mass spectrometer ESI/MS in negative ion mode. **(D)** Wild type LVS, **(E)** Δ*ripA*, and **(F)** S102 all have a peak at m/z 1504 and m/z 1476, which also correspond with lipid A containing either a 3' stearoyl

acyl chain (3-OH C18:0) or a palmitoyl acyl chain on the 3' position of glucosamine (3-OH C16:O), respectively. **(G)** Relative abundance of stearoyl (C18:0) to palmitoyl (C16:0) acyl chain for wild type LVS, Δ*ripA,* and S102. Mass spectrometry was repeated at least three times and one representative experiment is shown. Statistical significance for acyl chain specificity was calculated using Student's *t* tests with unequal variance comparing the wild type ratio to Δ*ripA* or to S102 ratios. *, $P < 0.05$; ***, $P < 0.00001$.

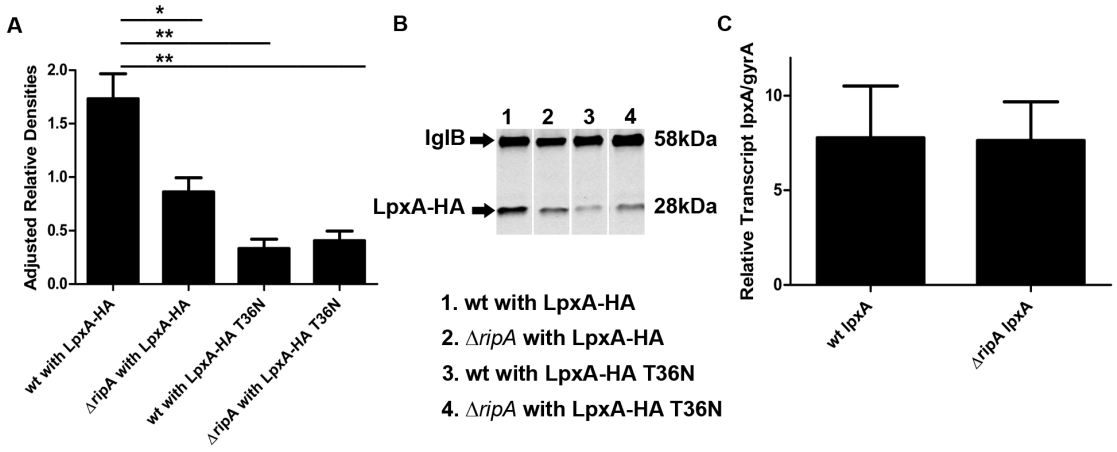


**Figure 4.9. RipA is necessary for stability of LpxA**

(A) Relative protein concentrations were determined on mid log phase cultures treated with 1.75 mg $ml^{-1}$ chloramphenicol for an hour to stop protein translation. The relative abundance of LpxA protein was quantified using Image J with IglB as a loading control for equal protein from three independent experiments. Statistical significance was determined by comparing LpxA-HA adjusted relative protein values for wild type to each of the respective mutants. *, $P < 0.05$; **, $P < 0.005$. (B) Representative western blot probed for LpxA-HA and IglB protein loaded with equal protein. (C) Transcript levels of *lpxA* in wild type *F. tularensis* and the Δ*ripA* strain measured by qRT-PCR. Data represent the relative transcript of *lpxA* normalized to *gyrA* from three independent experiments done in triplicate the relative transcripts were not statistically different.

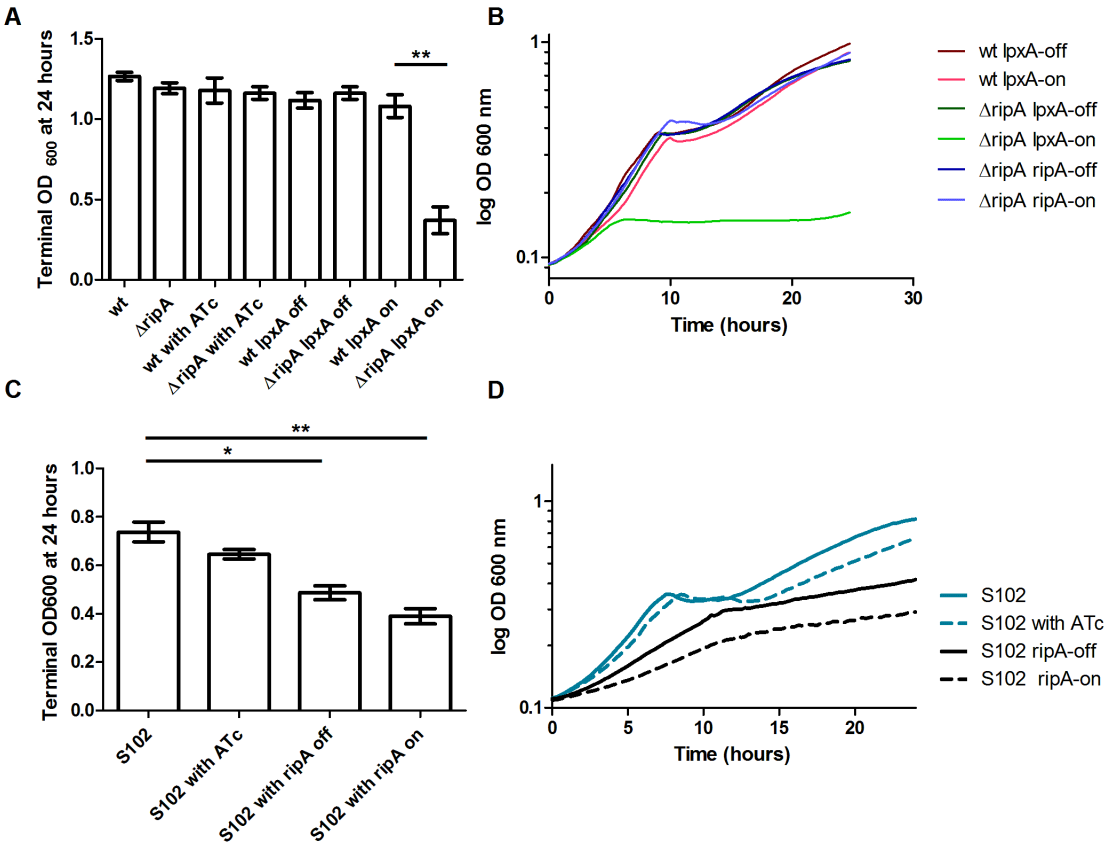


Figure 4.10. Induced expression of *lpxA* stops Δ*ripA* Growth

(A) Terminal $OD_{600}$ at 24 hours of strains grown in CDM with or without 100 ng $ml^{-1}$ of anhydrotetracycline (ATc). LVS, Δ*ripA,* LVS containing *lpxA* in trans, and Δ*ripA* containing *lpxA* in trans. ATc was used to induce expression of desired genes under the control of the *rpsLp-tetR* system (9). (B) Representative growth curve in CDM with induced expression of *lpxA* or *ripA* using 100 ng $ml^{-1}$ of ATc. (C) Terminal $OD_{600}$ at 24 hours of S102 and S102 with *ripA* in trans, under the control of the *repsLp-tetR* system. (D) Representative growth curve in CDM where *ripA* expression was induced with 100 ng $ml^{-1}$ of ATc. The growth curves were repeated at least three times and statistical significance was determined using Student's *t* tests *, $P < 0.01$; **, $P < 0.001$.

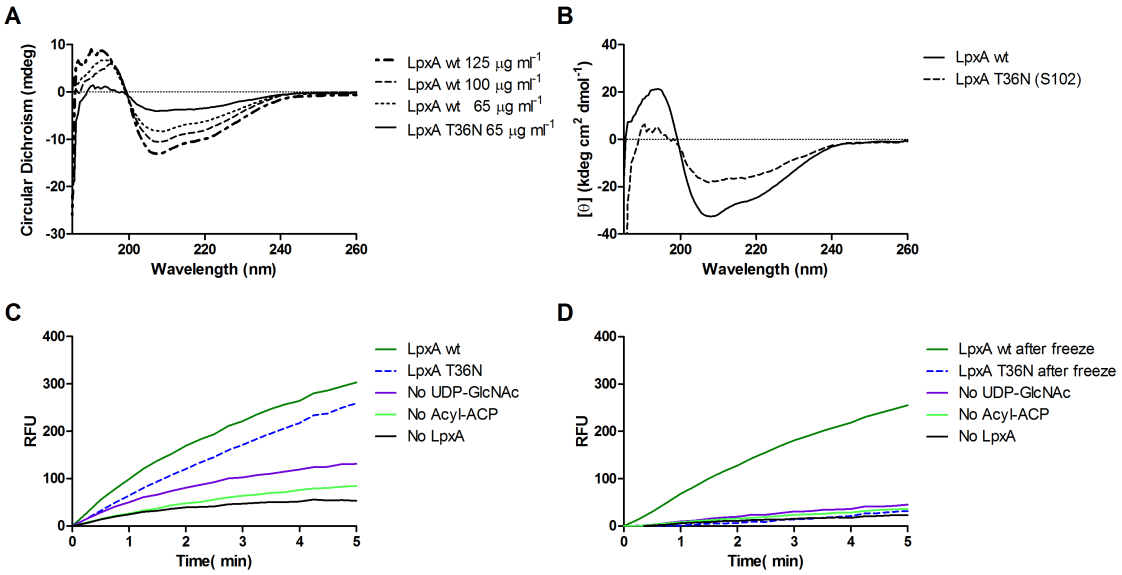


**Figure 4.11. Circular dichroism spectra and enzyme assay with LpxA and LpxA T36N**

(A) Circular dichroism spectra for wild type LpxA at 125 μg $ml^{-1}$, 100μg $ml^{-1}$, and 65 μg $ml^{-1}$ (dotted lines), and LpxA T36N at 65 μg $ml^{-1}$ (solid line). (B) Molar ellipticity calculated from the CD spectra (C) Graphs of the complete LpxA reaction with wild type *F. tularensis* LpxA-His (dark green), LpxA-His T36N (dotted blue), and control reactions without, either nucleotide (purple), acyl-ACP (light green), or acyltransferase (black). (D) Graphs of the complete LpxA reaction after LpxA samples were frozen at -80°C. Wild type *F. tularensis* LpxA-His (dark green), LpxA-His T36N (dotted blue), and control reactions without, either nucleotide (purple), acyl-ACP (light green), or acyltransferase (black). The complete LpxA mixture contained 20mM Hepes (pH 8.0), 40 μM 3-hydroxypalmitoyl-ACP, 4 mM UDP-GlcNAc, 10 nM *F. tularensis* LpxA-$His_6$ (added 5 minutes after ThioGlo) in a final volume of 100ul. The reaction was incubated at 25°C, and its progress was monitored continuously at λex = 379 nm and λem = 513 nm for 10 minutes at 15 second intervals. Control reactions were run in a similar fashion with the omission of substrate or enzyme as indicated. Each graph is a representative of three experiments.

## Tables

### Table 4.1. Whole genome sequencing results for suppressor S102

**Table 1. Polymorphisms detected by whole genome sequencing**

| Gene | Name | Amino Acid | Location | Polymorphism verified |
|---|---|---|---|---|
| **FTL_0146** | ABC transporter ATP binding protein | R341L | 152667<br>1023bp from start | wt, Δ*ripA*, and S102 |
| **FTL_0539 (*lpxA*)** | UDP-N-acetylglucosamine acyltransferase | T36N | 522331<br>107 bp from start | Unique to S102 |
| **FTL_0717 (*rne*)** | Ribonuclease E | K38T | 709489<br>114 bp from start | Δ*ripA*, and S102 |
| **FTL_1388 (*nadB*)** | L-aspartate oxidase | A93T | 1317802<br>278bp from start | wt, Δ*ripA*, and S102 |

### Table 4.2. Initial rate of LpxA-catalyzed acyl group transfer

| Name | Initial rate (μM / sec) | Statistical Significance |
|---|---|---|
| LpxA wt | 0.6648 ± 0.179 | *, $P < 0.05$ |
| LpxA T36N | 0.4408 ± 0.103 | |
| LpxA wt frozen | 0.6155 ± 0.263 | ***, $P < 0.0001$ |
| LpxA T36N frozen | 0.0509 ± 0.0196 | |

## Table 4.3. Bacterial Strains, Plasmids, and Primers

| Strain, Plasmid, or Primer | Genotype, Phenotype, or Sequence | Source |
|---|---|---|
| **Bacterial Strains** | | |
| *E. coli* DH10B | *E. coli* F-*mcr*A Δ(*mrr-hsd*RMS-*mcr*BC) φ80*lac*ZΔM15 Δ*lac*X74 *rec*A1*end*A1 *ara*D139 Δ(*ara leu*) 7697 *gal*U *gal*K *rps*L *nup*G λ- | Invitrogen |
| *E. coli* Top10 | *E. coli* F-*mcrA* Δ(*mrr-hsd*RMS-*mcr*BC) φ80*lac*ZΔM15 Δ*lac*X74 *rec*A1 *ara*D139 Δ*(ara-leu*) 7697 *gal*U *gal*K *rps*L (StrR) *end*A1 *nup*G λ- | Invitrogen |
| *E. coli* DH5 α | *E. coli* φ80*lac*ZΔM15 Δ(*lac*ZYA-*arg*F*)*U169 *rec*A1 *end*A1 *hsd*R17*(*$r_K^-$, $m_K^+$*) pho*A *sup*E44 *thi-1 gyr*A96 *rel*A1 $\lambda^-$ | Invitrogen |
| *E. coli* BL21(DE3) pLysS | *E.coli* $F^-$, *omp*T, *hsd*$S_B$ *(*$r_B$-, $m_B$-*), dcm, gal, λ(DE3), pLysS, Cm*$^r$ | Promega |
| *F. holarctica* LVS | *Francisella tularensis* subsp. *holarctica* LVS (taxid:376619) | CDC |
| Δ*ripA* | *Francisella tularensis* subsp. *holarctica* LVS | (9) |
| RipA-HA | *Francisella tularensis* subsp. *holarctica* LVS with RipA-HA chromosomally integrated | (25) |
| SKI12 | *E.coli* BL21(DE3) pLysS with LpxA-$His_6$ from *F. tularensis* LVS | This work |
| SKI13 | *E.coli* BL21(DE3) pLysS with LpxA-$His_6$ D144N from F. tularensis LVS S101 | This work |
| SKI14 | *E.coli* BL21(DE3) pLysS with LpxA-$His_6$ T36N from *F. tularensis* LVS S102 | This work |
| SKI15 | *E.coli* BL21(DE3) pLysS with RipA-$His_6$ from *F. tularensis* LVS | This work |
| SKI16 | *Francisella tularensis* subsp. *holarctica* LVS with LpxA T36N | This work |
| SKI17 | *Francisella tularensis* subsp. *holarctica* LVS with LpxA N36→T | This work |
| SKI18 | *Francisella tularensis* subsp. *holarctica* LVS containing pSKI07 | This work |
| SKI19 | *Francisella tularensis* subsp. *holarctica* LVS Δ*ripA* containing pSKI07 | This work |
| SKI20 | *Francisella tularensis* subsp. *holarctica* LVS containing pSKI08 | This work |
| SKI21 | *Francisella tularensis* subsp. *holarctica* LVS Δ*ripA* containing pSKI08 | This work |
| SKI22 | *Francisella tularensis* subsp. *holarctica* LVS containing pSKI09 | This work |
| SKI23 | *Francisella tularensis* subsp. *holarctica* LVS containing pEDL20 | (23) |
| SKI24 | *Francisella tularensis* subsp. *holarctica* LVS Δ*ripA* containing | (23) |

| | | |
|---|---|---|
| | pEDL20 | |
| SKI25 | *Francisella tularensis* subsp. *holarctica* LVS Δ*ripA* containing pSKI09 | This work |
| SKI26 | *Francisella tularensis* subsp. *holarctica* LVS with RipA-HA chromosomally integrated with pSKI10 | This work |
| SKI27 | *Francisella tularensis* subsp. *holarctica* LVS with pSKI10 | This work |
| **Plasmids** | | |
| pSKI05 | pET23a+*lpxA*-$His_6$ from *F. tularensis* LVS AmpR | This work |
| pSKI06 | pET23a+*lpxA*-$His_6$ T36N from *F. tularensis* LVS S102 AmpR | This work |
| pSKI07 | pMP822 with LpxA-HA HygR *blaB* promoter | This work |
| pSKI08 | pMP822 with LpxA-HA T36N HygR *blaB* promoter | This work |
| pSKI09 | *FTRp-lpxA, rpsLp-tetR,* HygR | This work |
| pSKI10 | *FTRp-lpxA-V5, rpsLp-tetR,* HygR | This work |
| pSKI11 | pMP812 with wt *F. tularensis lpxA* | This work |
| pEDL20 | *FTRp-ripA, rpsLp-tetR,* HygR | (20) |
| pET23a+ | N-terminal T7-Tag / C-terminal His-Tag with T7 promoter | (14) |
| pMP812 | sacB suicide vector, KanR, SucS | (21) |
| pMP590 | *sacB* suicide vector, KmR, SucS | (23) |
| pMP822 | *E.coli-F.tularensis* shuttle vector, HygR *blaB* promoter | (22) |
| pMP831 | *E.coli-F. tularensis* shuttle vector, HygR | (21) |
| pEDL50 | Conjugative *sacB* suicide vector, HygR, SucS | (20) |
| **Primers** | 5'→3' | |
| Sequencing Validation | | |
| FTL_0146F | ggatgagccttttctgcac | This work |
| FTL_0146R | gcataacgagcccagtcaat | This work |
| FTL_0717F | ggcgaagaaacaagaattgc | This work |
| FTL_0717R | atgacgatagaaccgccaga | This work |
| FTL_1388F | gcaggtgtagttgctgctattg | This work |
| FTL_1388R | atcatcgcactgccattacc | This work |
| FTL_0453F | tatcagcagcagcaacttgg | This work |
| FTL_0453R | ccaactattgcaccttcacg | This work |
| FTL1914F | atccggcgaagatttcatta | This work |

| | | |
|---|---|---|
| FTL1914R | tgaggtaaccaagcaatttcg | This work |
| FTL_0539F | tgttgagaaagctggtggtg | This work |
| FTL_0539R | ttcgcgaagtaccaatcaca | This work |
| Chromosomal Gene Disruption and Vector Cloning | | |
| LpxA F | ggcggtccgctaatcgtgatacatagtttggcagtagtacatgag | This work |
| LpxA-HA R | cccctcgag**ttatccaccaccagcataatctggaacatcataaggatagccacc**tcttagtata cctcttcgcgaagtac | This work |
| LpxA-V5 R | gggacccggg**ttatccagtagaatctagtcctagtagtgggtttggtattggttttcc**tcctctta gtatacctcttcgcgaagtac | This work |
| LpxA F pET23 | cagcatatgctaatcgtgatacatagtttggcagtagtacatgag | This work |
| LpxA R pET23 | cccctcgagtcttagtatacctcttcgcgaagtacc | This work |
| Real Time PCR | | |
| gyrA RT F | ctatacgctagtagatggacaaggtaactt | This work |
| gyrA RT R | ctatacgctagtagatggacaaggtaactt | This work |
| lpxA LVS F | gtcgtggatttacgcctgaagag | This work |
| lpxA LVS R | tcttcttttgccatcgctttg | This work |

Underlined text indicates restriction sites
Bold and underlined text indicates His-tag, HA-tag, or V5 tag

## Table 4.4 Zero Coverage Regions Detected by Whole Genome Sequencing

**Zero Coverage Regions Detected**

| **Gene** | Name | | Location | |
|---|---|---|---|---|
| | | Size | start | stop |
| **FTL_0678** | isftu1 | 315 | 665342 | 665657 |
| **FTL_0678** | isftu1 | 215 | 665722 | 665937 |
| **FTL_0678** | isftu1 | 11 | 666002 | 666013 |
| **FTL_0678** | isftu1 | 79 | 666074 | 666153 |
| **FTL_0969** | isftu1 | 2595 | 937366 | 939961 |
| **FTL_0969** | isftu1 | 151 | 938026 | 938177 |
| **FTL_1127** | isftu1 | 881 | 1072296 | 1073177 |
| **FTL_1195** | isftu1 | 150 | 1143319 | 1143469 |
| **FTL_1195** | isftu1 | 215 | 1143534 | 1143749 |
| **FTL_1446** | isftu1 | 211 | 1372642 | 1372853 |
| **FTL_1446** | isftu1 | 432 | 1372918 | 1373350 |
| **FTL_1462** | isftu1 | 390 | 1386695 | 1387085 |

| | | | | |
|---|---|---|---|---|
| **FTL_1462** | isftu1 | 429 | 1387150 | 1387579 |
| **FTL_1463** | isftu2 | 159 | 1387646 | 1387805 |
| **FTL_1463** | isftu2 | 499 | 1387862 | 1388361 |
| **FTL_1471** | isftu1 | 794 | 1395471 | 1396265 |
| **FTL_1505** | isftu1 | 389 | 1437352 | 1437741 |
| **FTL_1505** | isftu1 | 434 | 1437806 | 1438240 |
| **FTL_1516** | isftu2 | 162 | 1446331 | 1446493 |
| **FTL_1516** | isftu2 | 535 | 1446562 | 1447097 |
| **FTL_1572** | isftu2 | 600 | 1500255 | 1500855 |
| **FTL_1572** | isftu2 | 130 | 1500922 | 1501052 |
| **FTL_1610** | isftu1 | 323 | 1538210 | 1538533 |
| **FTL_1610** | isftu1 | 506 | 1538519 | 1539025 |
| **FTL_1627** | isftu1 | 150 | 1556619 | 1556769 |
| **FTL_1627** | isftu1 | 216 | 1556834 | 1557050 |
| **FTL_1627** | isftu1 | 390 | 1557115 | 1557505 |
| **FTL_1630** | isftu1 | 888 | 1560158 | 1561046 |
| **FTL_1643** | isftu1 | 151 | 1573322 | 1573473 |
| **FTL_1643** | isftu1 | 219 | 1573538 | 1573757 |
| **FTL_1643** | isftu1 | 391 | 1573818 | 1574209 |
| **FTL_1680** | isftu2 | 345 | 1614000 | 1614345 |
| **FTL_1687** | isftu1 | 434 | 1620255 | 1620689 |
| **FTL_1687** | isftu1 | 311 | 1620754 | 1621065 |
| **FTL_1718** | isftu1 | 395 | 1649522 | 1649917 |
| **FTL_1718** | isftu1 | 434 | 1649974 | 1650408 |
| **FTL_1757** | isftu1 | 435 | 1691942 | 1692377 |
| **FTL_1757** | isftu1 | 389 | 1692442 | 1692831 |
| **FTL_1815** | isftu1 | 392 | 1748889 | 1749281 |
| **FTL_1815** | isftu1 | 435 | 1749342 | 1749777 |
| **FTL_1851** | isftu2 | 716 | 1782910 | 1783626 |
| **FTL_1885** | isftu1 | 313 | 1818680 | 1818993 |
| **FTL_1885** | isftu1 | 434 | 1819054 | 1819488 |
| **FTL_1891** | isftu1 | 434 | 1822911 | 1823345 |
| **FTL_1891** | isftu1 | 389 | 1823410 | 1823799 |
| **FTL_1894** | transposase (IS4) | 429 | 1825412 | 1825841 |
| **FTL_1914** | ripA | 535 | 1847061 | 1847596 |
| **FTL_1925** | isftu1 | 390 | 1857283 | 1857673 |
| **FTL_1925** | isftu1 | 289 | 1857738 | 1858027 |
| **FTL_1925** | isftu1 | 76 | 1858094 | 1858170 |
| **FTL_1926** | isftu2 | 158 | 1858699 | 1858857 |
| **FTL_1944** | isftu1 | 75 | 1873330 | 1873405 |
| **FTL_1944** | isftu1 | 9 | 1873472 | 1873481 |
| **FTL_1944** | isftu1 | 219 | 1873542 | 1873761 |
| **FTL_1944** | isftu1 | 390 | 1873826 | 1874216 |

## References


1. **Anderson, M. S., C. E. Bulawa, and C. R. Raetz.** 1985. The biosynthesis of gram-negative endotoxin. Formation of lipid A precursors from UDP-GlcNAc in extracts of *Escherichia coli*. J Biol Chem **260:**15536-15541.

2. **Anderson, R., and A. R. Bhatti.** 1986. Fatty acid distribution in the phospholipids of *Francisella tularensis*. Lipids **21:**669-671.

3. **Barker, J. H., J. W. Kaufman, D. S. Zhang, and J. P. Weiss.** 2013. Metabolic labeling to characterize the overall composition of *Francisella* Lipid A and LPS grown in broth and in human phagocytes. Innate Immun.

4. **Chamberlain, R. E.** 1965. Evaluation of live Tularemia vaccine prepared in a chemically defined medium. Appl Microbiol **13:**232-235.

5. **Coats, S. R., T. T. Pham, B. W. Bainbridge, R. A. Reife, and R. P. Darveau.** 2005. MD-2 mediates the ability of tetra-acylated and penta-acylated lipopolysaccharides to antagonize *Escherichia coli* lipopolysaccharide at the TLR4 signaling complex. J Immunol **175:**4490-4498.

6. **Crowell, D. N., M. S. Anderson, and C. R. Raetz.** 1986. Molecular cloning of the genes for lipid A disaccharide synthase and UDP-N-acetylglucosamine acyltransferase in *Escherichia coli.* J Bacteriol **168:**152-159.

7. **Das, A., and C. Mukhopadhyay.** 2010. LpxA: a natural nanotube. Biopolymers **93:**845-853.

8. **Emiola, A., P. Falcarin, J. Tocher, and J. George.** 2013. A model for the proteolytic regulation of LpxC in the lipopolysaccharide pathway of *Escherichia coli*. Comput Biol Chem **47C:**1-7.

9. **Fuller, J. R., R. R. Craven, J. D. Hall, T. M. Kijek, S. Taft-Benz, and T. H. Kawula.** 2008. RipA, a cytoplasmic membrane protein conserved among *Francisella* species, is required for intracellular survival. Infect Immun **76:**4934-4943.

10. **Fuller, J. R., T. M. Kijek, S. Taft-Benz, and T. H. Kawula.** 2009. Environmental and intracellular regulation of *Francisella tularensis ripA*. BMC microbiology **9:**216.

11. **Gallagher, L. A., E. Ramage, M. A. Jacobs, R. Kaul, M. Brittnacher, and C. Manoil.** 2007. A comprehensive transposon mutant library of *Francisella novicida*, a bioweapon surrogate. Proc Natl Acad Sci U S A **104:**1009-1014.

12. **Huang, M. T., B. L. Mortensen, D. J. Taxman, R. R. Craven, S. Taft-Benz, T. M. Kijek, J. R. Fuller, B. K. Davis, I. C. Allen, W. J. Brickey, D. Gris, H. Wen, T. H. Kawula, and J. P. Ting.** 2010. Deletion of *ripA* alleviates suppression of the inflammasome and MAPK by *Francisella tularensis*. J Immunol **185:**5476-5485.

13. **Jantzen, E., B. P. Berdal, and T. Omland.** 1979. Cellular fatty acid composition of *Francisella tularensis*. J Clin Microbiol **10:**928-930.

14. **Jenkins, R. J., and G. D. Dotson.** 2012. A continuous fluorescent enzyme assay for early steps of lipid A biosynthesis. Analytical biochemistry **425:**21-27.

15. **Kawahara, K., H. Tsukano, H. Watanabe, B. Lindner, and M. Matsuura.** 2002. Modification of the structure and activity of lipid A in *Yersinia pestis* lipopolysaccharide by growth temperature. Infect Immun **70:**4092-4098.

16. **Kent, W. J.** 2002. BLAT--the BLAST-like alignment tool. Genome Res **12:**656-664.

17. **Khurana, R., and A. L. Fink.** 2000. Do parallel beta-helix proteins have a unique fourier transform infrared spectrum? Biophysical journal **78:**994-1000.

18. **Kloser, A. W., M. W. Laird, and R. Misra.** 1996. *asmB*, a suppressor locus for assembly-defective OmpF mutants of *Escherichia coli*, is allelic to *envA* (*lpxC*). J Bacteriol **178:**5138-5143.

19. **Li, R., Y. Li, K. Kristiansen, and J. Wang.** 2008. SOAP: short oligonucleotide alignment program. Bioinformatics **24:**713-714.

20. **Lovullo, E. D., C. N. Miller, M. S. Pavelka, Jr., and T. H. Kawula.** 2012. TetR-based Gene Regulation Systems for *Francisella tularensis*. Applied and environmental microbiology.

21. **LoVullo, E. D., C. R. Molins-Schneekloth, H. P. Schweizer, and M. S. Pavelka, Jr.** 2009. Single-copy chromosomal integration systems for *Francisella tularensis*. Microbiology (Reading, England) **155:**1152-1163.

22. **LoVullo, E. D., L. A. Sherrill, and M. S. Pavelka, Jr.** 2009. Improved shuttle vectors for *Francisella tularensis* genetics. FEMS microbiology letters **291:**95-102.

23. **LoVullo, E. D., L. A. Sherrill, L. L. Perez, and M. S. Pavelka, Jr.** 2006. Genetic tools for highly pathogenic *Francisella tularensis* subsp. *tularensis*. Microbiology (Reading, England) **152:**3425-3435.

24. **Mengin-Lecreulx, D., and J. van Heijenoort.** 1993. Identification of the *glmU* gene encoding N-acetylglucosamine-1-phosphate uridyltransferase in *Escherichia coli*. J Bacteriol **175:**6150-6157.

25. **Mortensen, B. L., J. R. Fuller, S. Taft-Benz, E. J. Collins, and T. H. Kawula.** 2012. *Francisella tularensis* RipA protein topology and identification of functional domains. J Bacteriol.

26. **Okan, N. A., S. Chalabaev, T. H. Kim, A. Fink, R. A. Ross, and D. L. Kasper.** 2013. Kdo hydrolase is required for *Francisella tularensis* virulence and evasion of TLR2-mediated innate immunity. mBio **4:**e00638-00612.

27. **Peng, K., P. Broz, J. Jones, L. M. Joubert, and D. Monack.** 2011. Elevated AIM2-mediated pyroptosis triggered by hypercytotoxic *Francisella* mutant strains is attributed to increased intracellular bacteriolysis. Cell Microbiol **13:**1586-1600.

28. **Phillips, N. J., B. Schilling, M. K. McLendon, M. A. Apicella, and B. W. Gibson.** 2004. Novel modification of lipid A of *Francisella tularensis*. Infection and immunity **72:**5340-5348.

29. **Raetz, C. R., Z. Guan, B. O. Ingram, D. A. Six, F. Song, X. Wang, and J. Zhao.** 2009. Discovery of new biosynthetic pathways: the lipid A story. J Lipid Res **50 Suppl:**S103-108.

30. **Raetz, C. R., and S. L. Roderick.** 1995. A left-handed parallel beta helix in the structure of UDP-N-acetylglucosamine acyltransferase. Science **270:**997-1000.

31. **Raetz, C. R., and C. Whitfield.** 2002. Lipopolysaccharide endotoxins. Annu Rev Biochem **71:**635-700.

32. **Schilling, B., M. K. McLendon, N. J. Phillips, M. A. Apicella, and B. W. Gibson.** 2007. Characterization of lipid A acylation patterns in *Francisella tularensis*, *Francisella novicida*, and *Francisella philomiragia* using multiple-stage mass spectrometry and matrix-assisted laser desorption/ionization on an intermediate vacuum source linear ion trap. Anal Chem **79:**1034-1042.

33. **Steeghs, L., R. den Hartog, A. den Boer, B. Zomer, P. Roholl, and P. van der Ley.** 1998. Meningitis bacterium is viable without endotoxin. Nature **392:**449-450.

34. **Telepnev, M., I. Golovliov, T. Grundstrom, A. Tarnvik, and A. Sjostedt.** 2003. *Francisella tularensis* inhibits Toll-like receptor-mediated activation of intracellular signalling and secretion of TNF-alpha and IL-1 from murine macrophages. Cell Microbiol **5:**41-51.

35. **Wang, X., M. J. Karbarz, S. C. McGrath, R. J. Cotter, and C. R. Raetz.** 2004. MsbA transporter-dependent lipid A 1-dephosphorylation on the periplasmic surface of the inner membrane: topography of *Francisella novicida* LpxE expressed in *Escherichia coli*. J Biol Chem **279:**49470-49478.

36. **Wang, X., A. A. Ribeiro, Z. Guan, S. N. Abraham, and C. R. Raetz.** 2007. Attenuated virulence of a *Francisella* mutant lacking the lipid A 4'-phosphatase. Proc Natl Acad Sci U S A **104:**4136-4141.

37. **Wang, X., A. A. Ribeiro, Z. Guan, S. C. McGrath, R. J. Cotter, and C. R. Raetz.** 2006. Structure and biosynthesis of free lipid A molecules that replace lipopolysaccharide in *Francisella tularensis* subsp. *novicida*. Biochemistry **45:**14427-14440.

38. **Williams, A. H., and C. R. Raetz.** 2007. Structural basis for the acyl chain selectivity and mechanism of UDP-N-acetylglucosamine acyltransferase. Proc Natl Acad Sci U S A **104:**13543-13550.

39. **Wyckoff, T. J., S. Lin, R. J. Cotter, G. D. Dotson, and C. R. Raetz.** 1998. Hydrocarbon rulers in UDP-N-acetylglucosamine acyltransferases. The Journal of biological chemistry **273:**32369-32372.

40. **Wyckoff, T. J., and C. R. Raetz.** 1999. The active site of *Escherichia coli* UDP-N-acetylglucosamine acyltransferase. Chemical modification and site-directed mutagenesis. J Biol Chem **274:**27047-27055.

41. **Zhang, Y. M., and C. O. Rock.** 2008. Membrane lipid homeostasis in bacteria. Nature reviews. Microbiology **6:**222-233.

42. **Zhao, J., and C. R. Raetz.** 2010. A two-component Kdo hydrolase in the inner membrane of *Francisella novicida*. Molecular microbiology **78:**820-836.

# Chapter 5

## PanG, A New Ketopantoate Reductase Involved in Pantothenate Synthesis[1][2]

### Overview

Pantothenate, commonly referred to as vitamin $B_{5,}$ is an essential molecule in the metabolism of living organisms and forms the core of coenzyme A. Unlike humans, some bacteria and plants are capable of *de novo* biosynthesis of pantothenate making this pathway a potential target for drug development. *Francisella tularensis* subspecies *tularensis* Schu S4 is a zoonotic bacterial pathogen that is able to synthesize pantothenate, but is lacking the known ketopantoate reductase (KPR) genes, *panE* and *ilvC,* found in the canonical *Escherichia coli* pathway. Described herein is a gene encoding a novel KPR, for which we propose the name *panG* (FTT1388) that is conserved in all sequenced *Francisella* species and is the sole KPR in Schu S4.

---

[1] Reprinted with permission from: Cheryl N. Miller, Eric D. LoVullo, Todd M. Kijek, James R. Fuller, Jason C. Brunton, Shaun P. Steele, Sharon A. Taft-Benz, Anthony R. Richardson, and Thomas H. Kawula. PanG, a new ketopantoate reductase involved in pantothenate synthesis. *J. Bacteriol.* 2013, 195(5):965 DOI: 10,1128/JB.01740-12.

[2] Attributions: Cheryl Miller performed all the experiments in this chapter with the following exceptions. Eric LoVullo helped developing the project and helped create the KPR double deletions in *F. novicida* and *E. coli* (Figure 2). Eric LoVullo also created the plasmids pEDL70 and pEDL71 for the complementation experiments. Todd Kijek and James Fuller initially started the project on pantothenate by repairing the LVS *panD* mutation (Figure 7).

Homologs of this KPR are present in other pathogenic bacteria such as *Enterococcus faecalis*, *Coxiella burnetii*, and *Clostridium difficile*. Both the homologous gene from *E. faecalis* V583 (EF1861) and the *E. coli panE* functionally complemented *Francisella novicida* lacking any KPR. Furthermore, *panG* from *F. novicida* can complement an *E.coli* KPR double mutant. A Schu S4 Δ*panG* strain is a pantothenate auxotroph and was genetically and chemically complemented with *panG in trans* or with the addition of pantolactone. There was no virulence defect in the Schu S4 Δ*panG* strain as compared to wild type in a mouse model of pneumonic tularemia. In summary, we characterized the pantothenate pathway in *Francisella novicida* and *tularensis* and identified an unknown and previously uncharacterized KPR that can convert 2-dehydropantoate to pantoate, PanG.

## Introduction

Coenzyme A (CoA) is a ubiquitous cofactor found in all domains of life and plays a central role in carbon and energy metabolism. Pantothenate forms the core of CoA; however animals and some microorganisms lack the ability to synthesize pantothenate. The pantothenate biosynthetic pathway is present in some plants, fungi, bacteria and archaea making the pathway a strong candidate for the discovery of novel antibiotics (22). The pantothenate biosynthesis pathway was first genetically and chemically defined in *Escherichia coli* and *Salmonella enterica* serovar Typhimurium and is composed of four enzymes that use the precursors 2-oxoisovalerate and L-aspartic acid to make pantothenate (9, 27) (Fig. 1A). In one branch of the pathway aspartate-1-decarboxylase, PanD, converts L-aspartate to β-alanine and in a separate branch two enzymes PanB, a ketopantoate hydroxymethyltransferase, and PanE, a ketopantoate

reductase (KPR), convert 2-oxoisovalerate to pantoate (8). The acetohydroxy acid isomerase, IlvC, has also been shown to function as a KPR in *E. coli* and *S.* Typhimurium converting 2-dehydropantoate to pantoate, similar to PanE (11, 36). In some species, e.g. *Corynebacterium glutamicum*, IlvC is the sole KPR (29). In the final step of the pantothenate synthesis pathway, pantoate and β-alanine are ligated by the pantothenate synthase, PanC, to form pantothenate (6). The published genomes of *Francisella* species contain *panB, panC,* and *panD*. No homolog of *E. coli* PanE exists in the sequenced *Francisella* genomes and the most virulent strain of *F. tularensis* Schu S4 contains a frameshift mutation in *ilvC* suggesting a gap in the pantothenate biosynthetic pathway. Combining the known nutritional requirements of *Francisella* species with the sequenced genomes revealed that several strains require exogenous pantothenate for growth (30). Interestingly, the most virulent strain Schu S4 lacks a recognizable KPR and is a pantothenate prototroph, while LVS has a KPR but is clearly auxotrophic (4, 21). The genetic basis for differences in the requirement for pantothenate among *Francisella* strains is not known.

*Francisella* belongs to the γ-proteobacteria and includes a number of species that share greater than 95% genomic similarity but differ in their ability to cause the disease tularemia in humans (5, 37). Of all the species, *Francisella tularensis* subsp. *tularensis* is the most virulent exhibiting the highest morbidity and mortality, while also having a very low infectious dose of less than 10 bacteria (21, 39). *F. tularensis* subsp. *holarctica* is also highly infectious for humans but clinical disease associated with this bacterium is typically mild (42). The live vaccine strain (LVS) was derived from a *F. tularensis* subsp. *holarctica* strain and is attenuated in humans. *Francisella novicid*a is rarely associated

with human disease. As a facultative intracellular pathogen, *Francisella* must acquire the nutrients needed to support growth while within host cells. Several genetic screens for replication defective mutants have implicated biosynthetic pathways as contributing factors to the pathogenesis of *Francisella* species (34). Interruption in genes involved in purine, aromatic amino acids, and biotin biosynthesis results in attenuation of *F. tularensis* within a mouse model of tularemia (31-33, 44). Collectively, these studies highlight the contribution of *de novo* biosynthetic pathways to the ability of *F. tularensis* to survive within the host environment. Using *F. novicida,* a genome wide mutant screen identified two genes contained in the putative pantothenate operon that are required for pulmonary and systemic infections in mice. Inactivation of FTN_1351 (*panG*) or FTN-1355 (*coaX*) resulted in mutant strains impaired in their ability to proliferate in the organs of infected mice (20). Furthermore, transcriptional profiling of *F. tularensis* revealed a dramatic increase in expression of the *F. tularensis* homologs of *panB*, *panC* and *panD*, as well as the homologs of FTN_1351 (*panG*) and FTN_1355 (*coaX*) in strains grown within bone marrow derived macrophages. This suggests that pantothenate biosynthesis may play a role in adaptation of *Francisella* to its intracellular niche (46). The requirement for *de novo* synthesis of pantothenate in virulence was demonstrated in a different intracellular pathogen, *Mycobacterium tuberculosis* where a double mutant in *panC* and *panD* was attenuated in both BALB/c and SCID mouse models of infection (38). Collectively the published data suggests that pantothenate biosynthesis may contribute to virulence of *Francisella* and the disparity in the requirement for pantothenate among *Francisella* strains led us to investigate the genetic basis for pantothenate biosynthesis in several species of *Francisella*.

## Materials And Methods

### *Bacterial strains and cell culture*

*Escherichia coli* strains (Table 1) were grown at 37°C in Luria-Bertani (LB) broth, on LB agar, or in M9 minimal media supplemented with 1 μg/ml thiamine, 3.4 mM valine, 3 mM isoleucine, and 3 mM leucine. Unless otherwise noted all *F. tularensis* strains (Table 1) were grown at 37°C on chocolate agar (25 g BHI $l^{-1}$, 10μg hemoglobin $l^{-1}$, 15g agar l-1) supplemented with 1% IsoVitalex (Becton-Dickson) or in Chamberlain's Defined Medium (CDM) (4). When necessary Hygromicin B (Hyg; Roche Applied Science) was used at 200 μg $ml^{-1}$, sucrose was used at 5% for *E.coli* or 10% for *F. tularensis* (w/v), Ampicillin (Amp; Roche Applied Science) was used at 100 μg $ml^{-1}$, L-arabinose (Sigma-Aldrich) was used at 10 mM, and Kanamycin (Km; Sigma-Aldrich) was used at 50 μg $ml^{-1}$ for *E. coli* and 10 μg $ml^{-1}$ for *F. tularensis*.

### *Growth Assays*

Growth assays for *F. tularensis* and *F. novicida* were performed at 37°C while shaking in an Infinite M200 or M200 pro (Tecan) in 96 well microtiter plates with absorbance ($OD_{600}$) monitored every fifteen minutes. Bacterial strains grown overnight on chocolate agar were resuspended in PBS to a Klett reading of 100 (approximately 1 $X10^9$ CFU/ml). Resuspended cultures were diluted 1:20 into test media. The test media consisted of CDM, or CDM without calcium pantothenate (Sigma-Aldrich). Genetic complementation *in trans* was evaluated in CDM lacking pantothenate. Chemical complementation was evaluated in CDM lacking pantothenate and supplemented with

100 μM pantolactone (Sigma-Aldrich), which can act in place of pantoate (43) or 100 μM β-alanine (Sigma-Aldrich).

***Construction of a double mutant using Flp/Frt recombination in F. novicida***

To create the *ilvC*::Tnflp/*panG*::Tn mutant ("flp" signifies a cured Km cassette) we performed Flp-mediated recombination of *ilvC*::Tn bearing the T20 insertion by introducing pFFlp-hyg, a temperature-sensitive plasmid, by electroporation and isolated Km sensitive colonies grown at 30°C (14). Removal of the Km cassette left an 80 base pair insertion with the expected single FRT site remaining. Once the Km resistance marker was excised pFFlp-hyg was cured by growing the culture overnight at 37°C. The *panG* mutation was introduced by transformation of genomic DNA from the *panG*::Tn strain into the *ilvC*::Tnflp mutant and selecting for Km resistant colonies, creating the double mutant (14). For genetic complementation mutant strains were transformed with their respective plasmids (25). Plasmids were first transformed with the addition of 1 μl of TypeOne Restriction Inhibitor (Epicentre) into a restriction mutant FTN_1698::Tnflp strain (14).

***Construction of the E.coli double mutant ilvC::flp/panE::kan using FLP/FRT recombination and λ-Red recombineering***

Using λ-Red recombineering the double mutant *ilvC*::flp/*panE*::kan mutant ("flp" signifies a cured Km cassette) was created in *E. coli* by first introducing pFlp2 into *ilvC*::kan (JW3747-2) by electroporation and isolated Km sensitive colonies (2, 10). Removal of the kanamycin cassette left the signature single FRT site of FLP/FRT recombination creating *ilvC*::flp. Once the Km resistance marker was excised pFlp2 was cured by growing the culture overnight and plating on LB with 5% sucrose minus NaCl

and the resulting colonies were screened for Amp sensitivity. Next the λ-Red recombineering plasmid, pKD46, was introduced into the *ilvC*::flp strain by electroporation (17). When the absorbance of *ilvC*::flp with pKD46 reached 0.1 $OD_{600}$, 10mM of L-arabinose was added to induce expression of the λ-Red recombineering proteins: Gam, Bet and Exo. The *panE*::kan mutation was introduced by transformation into the *ilvC*::flp mutant using PCR fragments generated from genomic DNA of *panE*::kan (JV0415-1) and colonies were selected for Km resistance.

***F. novicida Coenzyme A levels***

*F. novicida* was grown overnight on chocolate agar plates at 37°C then resuspended to an absorbance of 0.2 $OD_{600}$ in 50ml of CDM lacking pantothenate and incubated for 5 hours. The cells were pelleted at 10,000 x g for 5 minutes at 4°C and then resuspended in 0.5ml of cold PBS and snap frozen in liquid nitrogen. The cells were thawed and bead beaten 2 times for 30 seconds at 4°C using lysing matrix B tubes (MP Biomedicals). Cell debris was removed by centrifuging at 14,000 x g for 2 minutes. Protein concentration was determined by BCA assay for each sample. To deproteinize the lysates 100µl of cold 1N perchloric acid was added to each sample and centrifuged at 14,000 x g at 4°C for 2 minutes to pellet precipitated protein. To neutralize the supernatant 30µl of cold 3M potassium bicarbonate was added to the samples. The concentrations of CoA were determined for each sample using PicoProbe™ Acetyl CoA Assay Kit (BioVision). The manufacturer's protocol was followed except the CoA quenching solution was not used, thereby allowing us to determine total concentration of CoA in each sample.

***Replacing LVS panD ($panD_{LVS}$) with F. novicida panD ($panD_{U112}$)***

The putative *panD* (FTN_1354) allele was PCR amplified from *F. novicida* genomic DNA. The amplified DNA was subcloned into the TOPO pCRII vector (Invitrogen) for propagation and maintenance. The BamHI-NotI fragment containing the *F. novicida panD* allele was ligated into the *sacB* suicide vector pMP590 and electroporated into LVS. Allelic exchange was performed as previously described (26).

***Deletion of FTT1388 (panG) in Schu S4***

The putative *panG* (FTT1388) allele plus 300bp of DNA flanking each end was PCR amplified from *F. tularensis* Schu S4 genomic DNA. The amplified fragment was cut with BamHI and NotI then ligated into the *sacB* suicide vector, pEDL50 (24). Using splice junction PCR FTT1388 (*panG*) was eliminated from the plasmid creating a product with *Aat*II restriction sites on either end. The PCR product was digested with AatII and ligated, forming pSKI01. Conjugation and allelic exchange were then performed to introduce the clean in frame deletion of *panG* into *F. tularensis* Schu S4 as previously described (18, 24).

***Mouse infection***

Groups of six-week-old C57BL/6 mice were anesthetized and inoculated intranasally with 50 CFU of Schu S4 or Schu S4 Δ*panG* (FTT1388). Mice were euthanized on days 1 and 3 post-infection and lungs, livers, and spleens were aseptically removed and homogenized into 2ml of sterile PBS using a Biojector (BIOSPEC Products, Inc.). Bacterial CFU for each organ were enumerated by plating serial dilutions of tissue

homogenates onto chocolate agar. The infection experiments were approved and performed according to the animal care and use guidelines established by IACUC.

## Results

### *Organization of the Francisella pantothenate biosynthesis pathway*

The advances in whole genome sequencing have made identification of metabolic pathways through the use of sequence homology common. However, little experimental evidence is associated with these annotations and gaps exist in many annotated metabolic pathways including *F. tularensis* and *F. novicida*. Bioinformatics analysis suggests the pantothenate biosynthesis pathway in *F. novicida* is much like *E. coli,* putatively using PanB, PanD, PanC, and IlvC to convert L-aspartate and 2-oxoisovalerate into pantothenate (Fig. 1A). Using *F. novicida* blastp (NCBI) generated Expect values of $7e10^{-69}$ for PanB, $6e10^{-58}$ for PanC, $3e10^{-20}$ for PanD, and $8e10^{-22}$ for IlvC relative to the characterized *E. coli* K12 enzymes (1). Interestingly, no homolog of *E. coli* PanE was identified in any of the 36 sequenced *Francisella* genomes. In addition the *ilvC* gene in *F. tularensis* Schu S4 contains a frameshift mutation, which creates a premature stop codon after amino acid 74 suggesting a gap in the pantothenate biosynthetic pathway. LVS also has a truncation in the *panD* gene shortening the encoded protein from 111 amino acids to 91 amino acids.

Unlike *E. coli,* the *panB*, *panC*, and *panD* genes of *Francisella* species are organized into a predicted operon (Fig. 1B and C), which is conserved in all the sequenced *Francisella* strains (13). In addition to *panBCD*, this putative operon contains additional predicted Open Reading Frames (ORF) both 5' and 3' of *panBCD* (Fig. 1C). There is an annotated

ORF immediately 5' of *panBCD* that encodes an uncharacterized conserved protein (*panG*) containing a domain of unknown function, DUF2520 (28). The ORF 3' of *panBCD* encodes a putative type III pantothenate kinase (CoaX), which catalyzes the first dedicated step in CoA synthesis from pantothenate (3, 47). *Francisella tularensis* also contains another *coaX* homolog, FTT0112, which is not part of the putative operon.

***The Francisella panBCD genes are required for growth in the absence of pantothenate***

We used the *F. novicida* comprehensive two-allele transposon mutant library to assess the functionality of individual components of the pantothenate biosynthesis pathway (15). The pantothenate biosynthetic pathway in *F. novicida* was characterized by complementing auxotrophic mutants with metabolic intermediates of pantothenate biosynthesis.

FTN_1352 (PanB) is a ketopantoate hydroxymethyl transferase that catalyzes the conversion of 2-oxoisovalerate to 2-dehydropantoate (Fig. 1A). Functional inactivation of *panB* results in mutant strains deficient in 2-dehydropantoate and loss of pantothenate synthesis. The *panB*::Tn exhibited limited growth in CDM lacking pantothenate and growth of this mutant was restored by supplementation with pantolactone (an alternative substrate to pantoate) (Fig. 2A) thereby bypassing the PanB/IlvC branch (43). Supplementation with β-alanine alone was not sufficient to support growth of this mutant (Fig. 2A) demonstrating that FTN_1352 functions in the PanB/IlvC branch of the pathway and is consistent with the annotation of FTN_1352 as *panB*.

FTN_1353 (PanC) encodes pantothenate synthase, which catalyzes the formation of pantothenate from L-pantoate and β-alanine (Fig. 1A). Inactivation of *panC* results in a

strain that requires the addition of pantothenate for growth and neither supplementation with pantolactone nor β-alanine rescued growth. This indicates that the FTN_1353 transposon mutation interrupts the pantothenate biosynthesis pathway downstream of both the PanD and PanB/IlvC branches, consistent with the phenotype of a pantothenate synthase mutant (Fig. 2B).

FTN_1354 (PanD) is a L-aspartate α-decarboxylase that forms β-alanine from L-aspartate (Fig. 1A) and inactivation of *panD* results in a strain that is auxotrophic for β-alanine. Consistent with this phenotype *panD*::Tn exhibited growth defects in CDM lacking pantothenate and was rescued by the addition of β-alanine. Supplementation with pantolactone failed to restore growth of *panD*::Tn (Fig. 2C). These results demonstrate that inactivation of FTN_1354 results in a loss of β-alanine synthesis and are consistent with the prediction that FTN_1354 is a functional PanD (8).

FTN_1040 (IlvC) is known to function as an acetohydroxy acid isomerase essential for branch chain amino acid synthesis and can also function as a KPR in *E. coli* and *S.* Typhimurium (35). As the only recognized enzyme with KPR activity within *F. novicida* genome, we were surprised to find that the *ilvC*::Tn transposon mutant in *F. novicida* did not require pantothenate for growth (Fig. 2D). This result suggested that there was another unrecognized enzyme with sufficient KPR activity to support pantothenate biosynthesis within *F. novicida ilvC*::Tn.

FTN_1351 (*panG*) is annotated as an uncharacterized conserved gene and is part of the putative pantothenate operon, so we tested the *panG::*Tn pantothenate growth requirement. Under each condition *panG*::Tn grew suggesting that either PanG may not

be involved in pantothenate synthesis or it is functionally redundant with IlvC in KPR activity (Fig. 2E).

To determine if IlvC in *F. novicida* is a functional acetohydroxy acid isomerase we grew wild type *F. novicida* U112 and *ilvC*::Tn in CDM with and without branch chain amino acids (Fig. 2F). Only wild type U112 could grow in CDM without branch chain amino acids supporting our hypothesis that IlvC is functioning as an acetohydroxy acid isomerase in *F. novicida*.

***A new class of ketopantoate reductase found in a number or pathogenic organisms***

Ketopantoate reductases (KPR) have a dinucleotide-binding domain called a Rossmann-fold that consists of a βαβ pocket to accommodate the coenzyme NADPH (23). Within the Rossmann-fold is a consensus sequence GXGXXG, which appears at the border between the first beta sheet and the alpha helix (16). In *E. coli* the PanE N-terminal Rossmann-fold domain and the C-terminal alpha-helical domain form a cleft, and at that cleft is a conserved-essential residue Lys176 that forms the hydrogen bond with C2 hydroxyl of pantoate (6). Pantoate also forms additional interactions with conserved residues Ser244, Asn98, and Asn180 (6). PanE and IlvC each have an N-terminal NADB_Rossmann superfamily domain (28). IlvC is an acetohydroxy acid isomerase, which can also function as a KPR and requires two cofactors NADPH and $Mg^{2+}$ for the reduction of 2-dehydropantoate (40).

Bioinformatic analysis of PanG (FTN_1351) gave little insight into its function. The comparison of the sequence to PanE and other known KPR revealed no significant matches (11, 41). Phylogenetic analysis indicated that PanG is in a distinct group separate from annotated KPRs using the Jukes-Cantor genetic distance model (Fig. 3).

There is no Rossmann domain identified in the C-terminal region of FTN_1351 and the GXGXXG motif is not present (16). The C-terminal region of FTN_1351 has a domain of unknown function, DUF2520 (E-value of $1.5e10^{-6}$), that often accompanies an N-terminal Rossmann domain suggesting the protein could function as an uncharacterized KPR (28). We made a double mutant, *ilvC*::Tnflp/*panG*::Tn, in *F. novicida* to determine if FTN_1351 protein could function as a KPR. The double mutant did not grow in media lacking pantothenate (Fig. 4A). Growth of the double mutant was restored when complemented *in trans* with *panG* expressed under its native promoter, with *ilvC* driven by the *Francisella blaB* promoter or when the media was supplemented with pantolactone (Fig. 4A and B). This result confirms that IlvC is active in the *F. novicida* pantothenate metabolic pathway and that FTN_1351 is a novel KPR, which we named *panG*. Homologs of PanG are also found in other pathogenic bacteria including *Enterococcus faecalis*, *Coxiella burnetii*, and *Clostridium difficile*. Blastp analysis of *F. tularensis* Schu S4 PanG (FTT1388) revealed that this protein has significant homology with *Enterococcus faecalis* V583 (EF1861) ( Expect value = $2e10^{-11}$ ), *Coxiella burnetii* (CBU1660)( Expect value = $2e10^{-7}$), and *Clostridium difficile* (CD630-15140) ( Expect value = $8e10^{-6}$ ) (1). In *E. faecalis* and *C. difficile* the *panG* genes are organized similarly in putative pantothenate operons (Fig. 1B). Expression of the *E. faecalis* V583 gene in *F. novicida ilvC*::Tnflp/*panG::*Tn restored growth of this mutant strain to near wild type levels in CDM lacking pantothenate, confirming genetically that EF1861 is a functional KPR (Fig. 4C). PanE an analog KPR from *E. coli* (EC 1.1.1.169) is not present in any sequenced genome of *Francisella,* and expression of this gene restored growth of *F. novicida ilvC*::Tnflp/*panG::*Tn in media lacking pantothenate (Fig. 4D). Expression of

the *F. novicida panG* gene in the *E.coli* KPR double mutant, *ilvC*::flp/*panE*::kan, restored growth in M9 minimal media lacking pantothenate, confirming genetically that PanG is a functional KPR in *E.coli* (Fig. 4E).

***Francisella novicida Coenzyme A Levels***

Coenzyme A is made from pantothenate, cysteine, and adenosine and is an essential cofactor in the first step of the TCA cycle. To determine the contribution of PanG and IlvC in the production of pantothenate synthesis and subsequent CoA synthesis we measured the concentration of CoA after five hours of pantothenate depletion in wild type *F. novicida*, *ilvC*::Tn, *panG*::Tn, and *ilvC*::Tnflp/*panG*::Tn. CoA levels were not significantly different between wild type and *ilvC*::Tn suggesting that PanG can fulfill the requirement for KPR activity in *F. novicida* (Fig. 5). The CoA levels of the *panG*::Tn mutant strain were less than half of wild type levels and similar to the *ilvC*::Tnflp/*panG*::Tn double mutant suggesting that PanG is responsible for the majority of KPR activity in *F. novicida* (Fig. 5).

***Francisella tularensis LVS is a β-alanine auxotroph***

Early studies revealed varying nutritional requirements of *Francisella* strains for pantothenate that appeared to correlate with virulence in mice (4, 30). We assessed the requirement for pantothenate with three different strains of *Francisella*: *F. tularensis* Schu S4, *F. tularensis* LVS, and *F. novicida* U112. Each strain grew logarithmically in complete CDM (Fig. 6A-D). *F. tularensis* Schu S4 and *F. novicida* U112 grow logarithmically under each dropout condition suggesting both strains have complete pantothenate biosynthesis pathways (Fig. 6). However, *F. tularensis* LVS failed to grow

in media without pantothenate indicating that LVS is a pantothenate auxotroph. This result is in agreement with the observations of Chamberlain (4). Additionally, we observed that growth of LVS could be restored by the addition of β-alanine indicating that LVS lacks PanD activity (Fig. 6D). Comparison of the nucleotide sequences of the putative *panGBCD* genes among *Francisella* species revealed that *F. tularensis* LVS contains a base substitution in the annotated *panD* gene. This substitution creates a Q92 Ochre stop, resulting in a truncation of PanD by 20 amino acids. To determine if LVS β-alanine auxotrophy is due to a non-functional *panD*, we replaced $panD_{LVS}$ with the functional $panD_{U112}$ via allelic exchange. As predicted, *F. tularensis* LVS harboring the $panD_{U112}$ allele grew similarly in CDM with or without added pantothenate (Fig. 7). This demonstrates that the observed pantothenate auxotrophy of LVS results from a lack of PanD activity. This truncation in PanD is unique to LVS, we questioned whether the lack of PanD activity contributed to the attenuated phenotype of this strain. However, repair of *panD* activity in *F. tularensis* LVS $panD_{U112}$ did not confer a competitive advantage relative to *F. tularensis* LVS $panD_{LVS}$ in a mouse model of pneumonic tularemia (data not shown). Thus, the LVS *panD* mutant allele does not contribute to the attenuated phenotype of this strain.

***Francisella tularensis Schu S4 ΔpanG is a pantothenate auxotroph***

The Δ*panG* (FTT1388) strain in Schu S4 requires pantothenate for growth, and can be rescued with the addition of pantolactone in CDM lacking pantothenate or with *panG* expressed *in trans*. Schu S4 does not have a functional IlvC protein, at least in regards to its KPR activity, due to a frameshift mutation, making PanG the sole KPR. The Δ*panG*

strain can be complemented *in trans* with the *panG* gene from *F. novicida* driven by the *F. novicida* native promoter (Fig. 8B). Given that *F. novicida panG* (FTN_1351) was identified in a screen to be required for virulence in a mouse model of infection (20) and *F. tularensis panG*, *panB*, *panC, panD and coaX* genes were highly upregulated within bone marrow derived macrophages, suggested that pantothenate production and ultimately CoA synthesis may play a role in adaptation of *Francisella* to its intracellular niche (46). We wanted to determine if Δ*panG* was important for infection in mice. With an intranasal inoculum of 50 CFU we saw no difference in lung, liver or spleen burdens when comparing Δ*panG* to wild type Schu S4 at one or three days post inoculation (Fig. 8C-E).

## Discussion

Pantothenate forms the core of Coenzyme A and is a precursor to acyl carrier protein (ACP) making it essential in both energy and lipid metabolism. We characterized the genes that function in pantothenate biosynthesis in *Francisella* using genetic and chemical complementation approaches. These genes are organized into a putative operon, which also included a hypothetical protein, PanG (FTN_1351), that we discovered is a novel KPR responsible for converting 2-dehydropantoate to pantoate. PanG (FTN_1351) does not have the known conserved Rossmann-domain that is typically associated with KPRs. However, PanG does contain a C-terminal DUF2520, which usually accompanies an N-terminal Rossmann-like domain. PanG rescued growth of an *E. coli* KPR double mutant in the absence of pantothenate and the *panG* homolog from *E. faecalis* V583 (EF1861) complemented KPR function in the *F. novicida* double mutant. EF1861 also contains a predicted C-terminal DUF2520 domain in addition to a predicted N-terminal

Rossmann-like domain. The *panG* genetic data (FTN_1351 and EF1861) suggest the DUF2520 domain is involved in KPR activity. Further biochemical characterization of PanG needs to be done to determine structural binding motifs and enzymatic activity. Normally KPR proteins bind cofactors such as NAD or NADP; more work needs to be done to characterize what cofactor, is required for PanG KPR activity. There is no GXGXXG motif in PanG, which is responsible for NADP-binding in *E. coli*, however amino acids 11-16 are GXGXXA, which is found in mitochondrial flavoenzymes that bind NADP (16). Using secondary structure predictions of PanG, the GXGXXA consensus sequence starts right at the junction of a β-sheet and an α-helix that would be compatible with a KPR βαβ fold-forming sequence (7).

Functional complementation assays demonstrated that expression of *panB, panC* and *panD* were each required for growth of *F. novicida* in media devoid of pantothenate. In regard to KPR activity, only an *ilvC*::Tnflp/*panG::*Tn double mutant of *F. novicida* created a pantothenate auxotroph, demonstrating that PanG is functionally redundant with the acetohydroxy acid isomerase, IlvC. Both the *panG* homolog from *E. faecalis* V583 and the known *panE* gene encoding a KPR from *E. coli* DH10B could functionally complement the *F. novicida* KPR double mutant *ilvC*::Tnflp/*panG::*Tn. CoA levels were not significantly different between wild type and *ilvC*::Tn after five hours of pantothenate depletion demonstrating that PanG can fulfill the requirement for KPR activity in *F. novicida*. CoA levels in both the *panG*::Tn mutant strain and the *ilvC*::Tnflp/*panG*::Tn double mutant were less than half the concentration of wild type suggesting PanG is responsible for the majority of KPR activity in *F. novicida*. We also found that the LVS strain is a β-alanine auxotroph resulting from a base substitution in *panD* causing an

amino acid substitution shortening the aspartate-1-decarboxylase. While the lack of PanD activity appears unique to the LVS strain, it does not contribute to the attenuation of this strain in mice. In addition, the Schu S4 frameshift in *ilvC* produced a nonfunctional protein, in regards to KPR activity. We demonstrated that PanG is the sole KPR in Schu S4 since creating an in frame *panG* deletion resulted in a pantothenate auxotroph. However, the Schu S4 Δ*panG* strain did not have a demonstrable virulence defect in a mouse model of pneumonic tularemia. It is not clear where or what molecule this mutant acquired from the host to satisfy its pantothenate requirement. Given that mice have a blood plasma pantothenate level of 20μM, while humans only have 2-4μM, it is possible that a *F. tularensis* pantothenate synthesis mutant could be attenuated in humans but not mice (45). It is possible that mice have excess pantothenate in their blood stream considering their diet is supplemented with pantothenate in addition to that naturally acquired from their gut flora. *E. coli* can produce and secrete 15 times more pantothenate than required for CoA biosynthesis, and ruminants obtain sufficient quantities of pantothenate from their gut microorganisms (12, 19). Virtually all bacteria, including *F. tularensis*, can take up pantothenate, but *F. tularensis* does not have an annotated *panF* homolog responsible for sodium-cotransport of pantothenate (22). It appears *F. tularensis* is able to obtain pantothenate, a CoA precursor (such as phosphopantheine), or CoA from the host and is likely storing sufficient quantities of pantothenate to support logarithmic growth for several rounds of replication while inside cells where pantothenate may be limited. Pantothenate is immediately phosphorylated once taken up by host cells and could affect *F. tularensis* ability to acquire pantothenate. Further work will be needed to determine how *F. tularensis* acquires pantothenate or

other substituents of CoA from the host. It may be a valuable endeavor to look further down in the CoA pathway for potential drug targets for *Francisella tularensis*, starting with the putative type III pantothenate kinases (FTT1392 and FTT0112), which is the first committed step in CoA biosynthesis.

## Figures

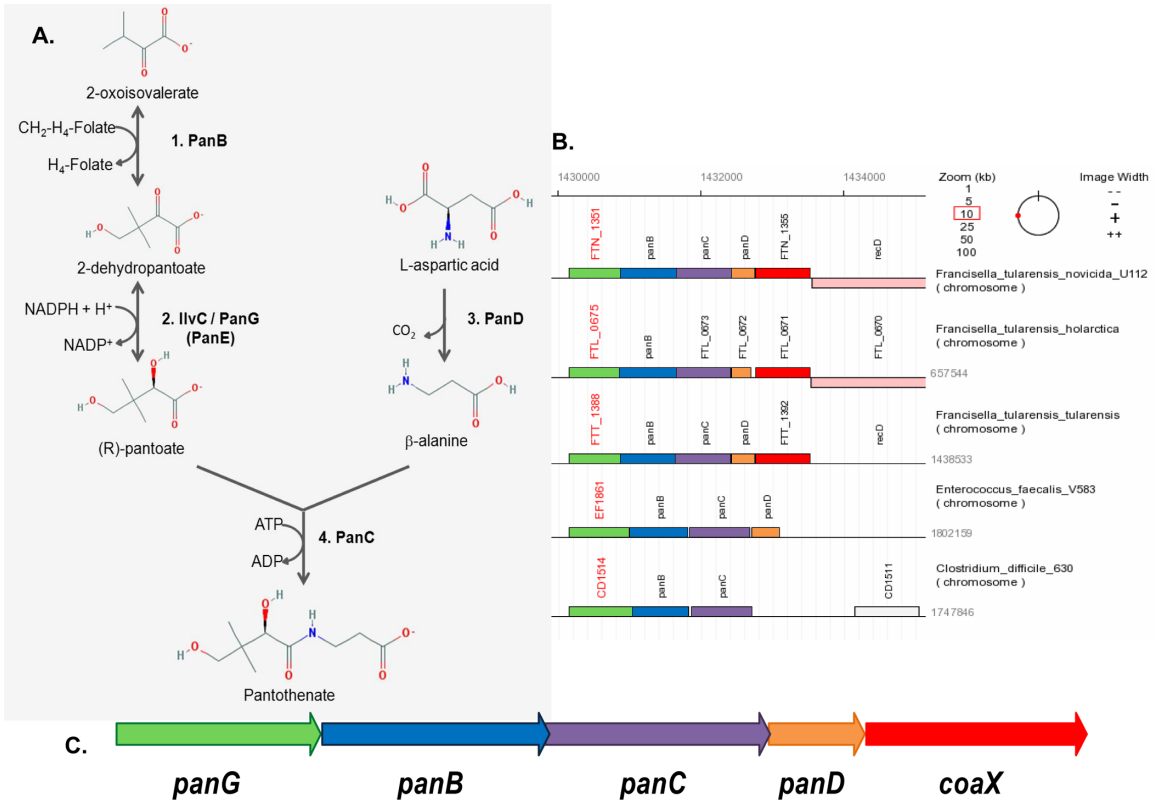


**Figure 5.1. The biosynthetic pathway in *Francisella* species and the putative pantothenate operon.**

(A.) The pantothenate biosynthetic pathway consists of two converging arms. PanB the ketopantoate hydroxymethyltransferase converts 2-oxoisovalerate with tetrahydrofolate to form 2-dehydropantoate. The substrate 2-dehydropantoate is then converted to (R)-pantoate by a number of enzymes including IlvC and PanG that are both capable of ketopantoate reductase (KPR) activity. On the other branch of the pathway PanD, an aspartate-1-decarboxylase, converts L-aspartic acid to β-alanine. The pathway converges with PanC, the pantothenate synthase that ligates (R)-pantoate with β-alanine to form pantothenate. Molecules were made in PubChem Compound on NCBI and the pathway was constructed using KEGG metabolic pathway 00770 as a reference

http://www.genome.jp/kegg-bin/show_pathway?FTN_00770. (B.) The genomic organization of the putative pantothenate operon is conserved among sequenced *Francisella* strains containing the genes *panGBCD* and the pantothenate kinase *coaX*. (C.) Synteny diagram of the putative operon in *F. novicida*, *F. tularensis* LVS, *F. tularensis* Schu S4, *E. faecalis* V583, and *C. difficile* 630 (13).

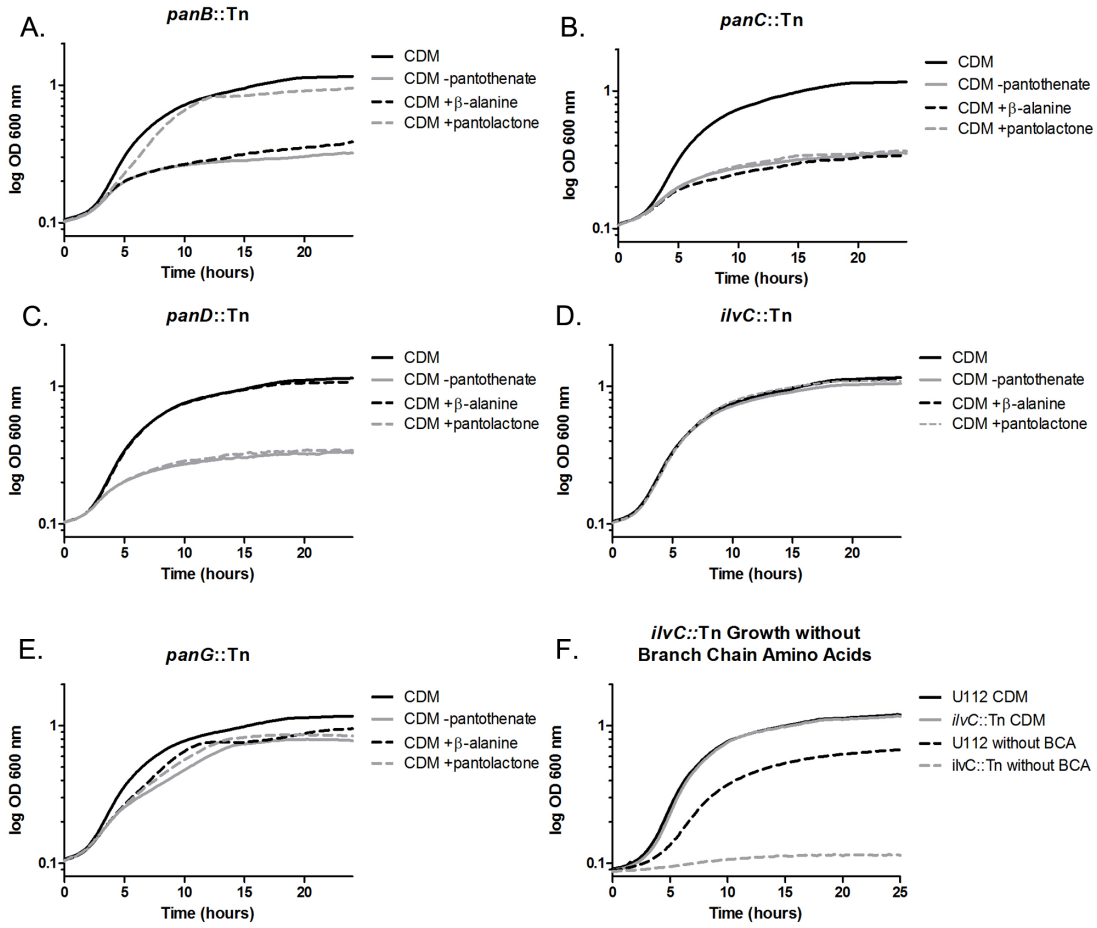


**Figure 5.2. Functional complementation of *panB*::Tn, *panC*:Tn, *panD*::Tn, *ilvC*::Tn, and *panG*::Tn.**

Functional complementation of the pantothenate biosynthetic genes in *F. novicida* transposon mutant strains grown in 96 well microtiter plates with absorbance ($OD_{600}$) monitored every fifteen minutes in CDM lacking pantothenate (grey) either supplemented with β-alanine (black dotted line), pantolactone (grey dotted line), or calcium pantothenate (black). (A.) *panB*::Tn (B.) *panC*::Tn (C.) *panD*::Tn, (D.) *ilvC*::Tn, and (E.) *panG*::Tn. (F.) *F. novicida* U112 and *ilvC*::Tn growth in CDM with and without branch chain amino acids. U112 in CDM (black), *ilvC*::Tn in CDM (grey), U112 in CDM without branch chain amino acids (black dotted line), and *ilvC*::Tn in CDM without branch chain amino acids (grey dotted line). Each growth curve was repeated a minimum of three times and the graph represents the mean of three replicate experiments.

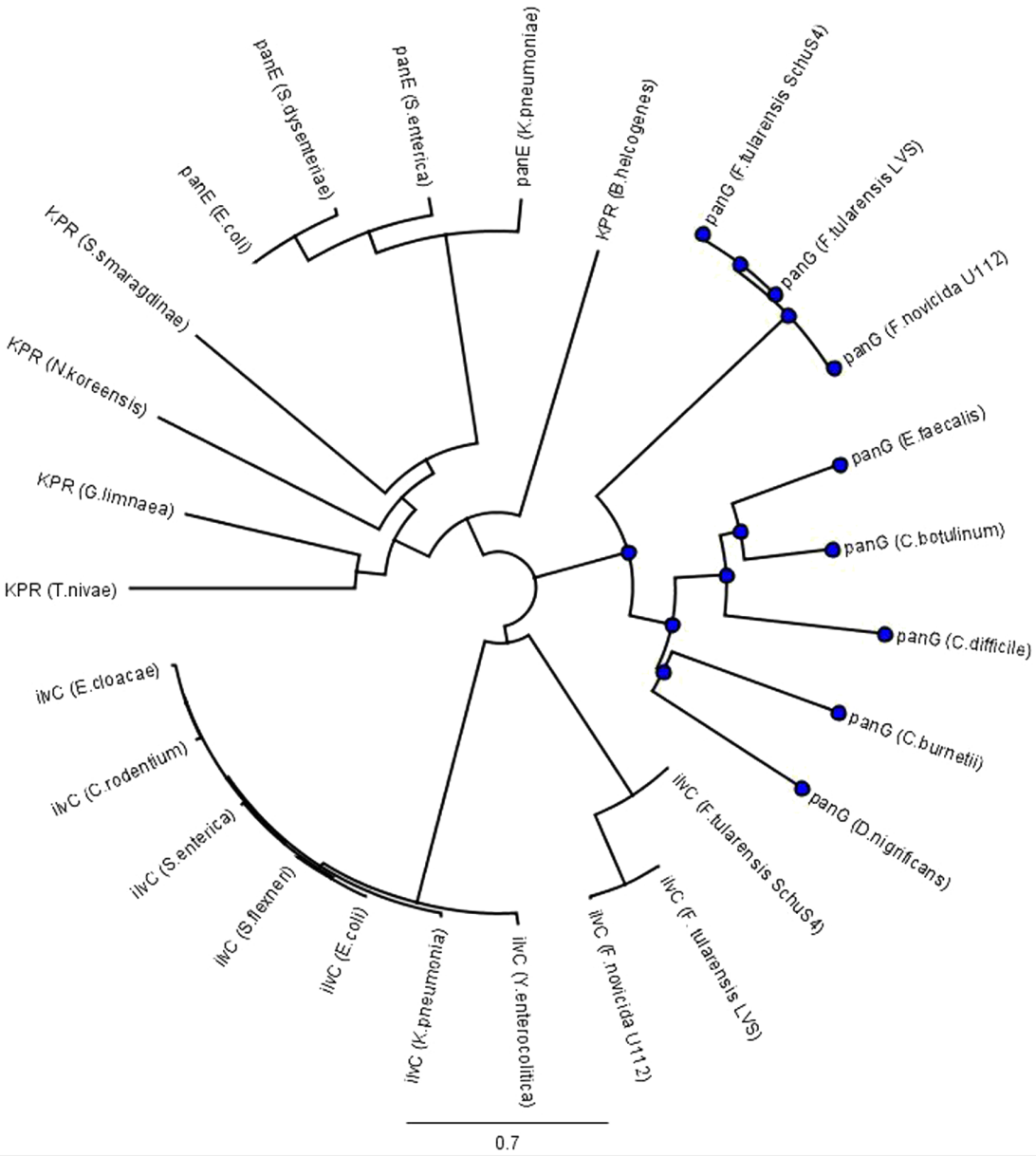


**Figure 5.3. Phylogenetic tree of known ketopantoate reductase proteins and PanG.**

The phylogenetic tree of known KPR proteins and PanG was generated using Geneious Pro 5.5.6 Tree Builder with the cost matrix set to identity and Jukes-Cantor as the genetic distance model with no outgroups. All IlvC, and PanE proteins are annotated on PubMed to be involved in pantothenate synthesis, while all PanG proteins are annotated as hypothetical proteins. *Enterococcus faecalis* V583 PanG is annotated as a hypothetical

protein EF1861, *Clostridium difficile* 630 PanG is annotated as a hypothetical protein CD630-15140, *Coxiella burnetii* RSA 493 PanG is annotated as a hypothetical protein CBU_1660, *Clostridium botulinum* BKT015925 PanG is annotated as a hypothetical protein CbC4_0183, and *Desulfotomaculum nigrificans* DSM 574 PanG is annotated as a hypothetical protein DUF2520 protein.

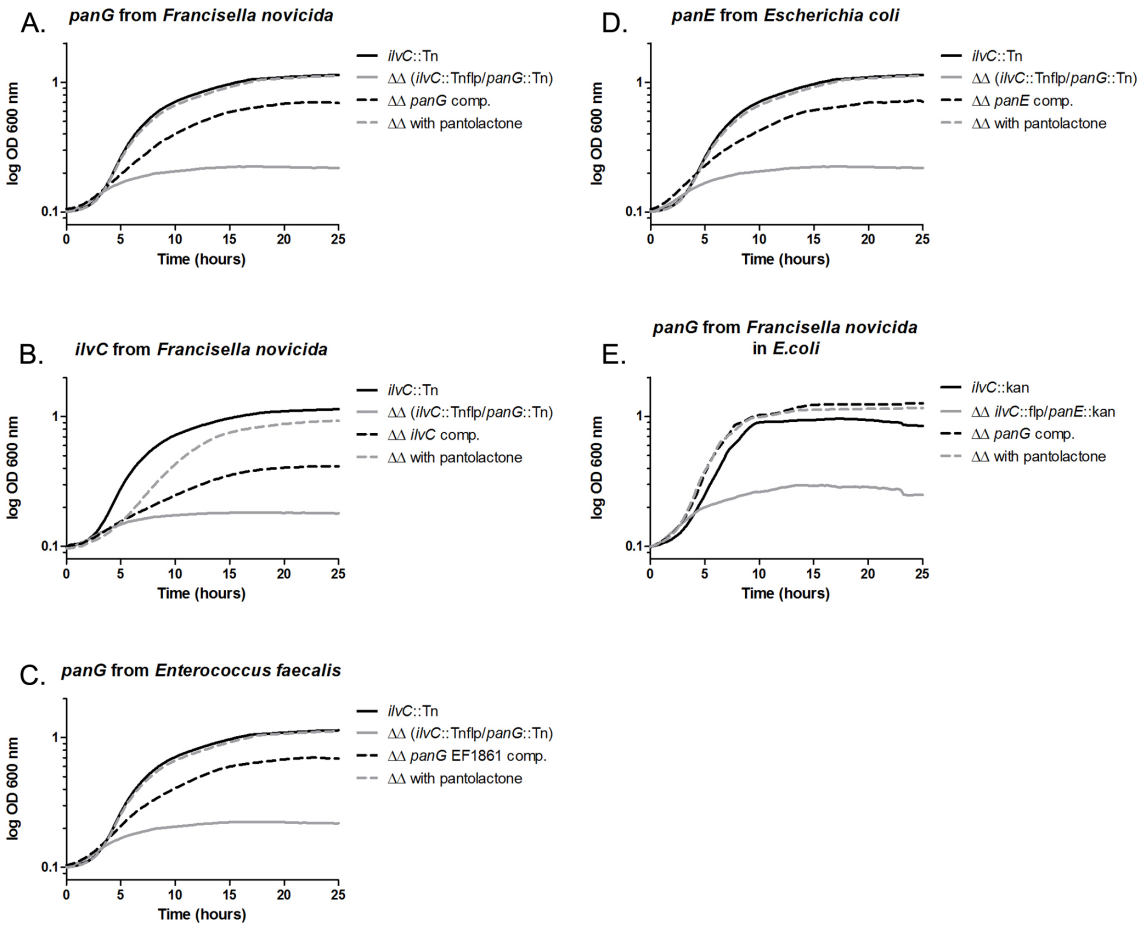


**Figure 5.4. Genetic complementation of the *F. novicida,* and *E. coli* KPR double mutant with *panG*.**

Genetic complementation of the *F. novicida ilvC*::Tnflp/*panG*::Tn double mutant with *F. novicida* FTN_1351 *panG* gene, *F. novicida ilvC* gene, *E. faecalis* V583 (EF1861) *panG* gene, *E. coli panE* and genetic complementation of *E.coli ilvC*::flp/*panE*::kan double mutant with *F. novicida panG.* Functional complementation experiments were carried out by growing *Francisella* in CDM lacking pantothenate in 96 well microtiter plates and measuring the absorbance ($OD_{600}$) every fifteen minutes for 30 hours. Competent *F. novicida* were transformed with DNA (A.) pSKI01 encoding *F. novicida panG* (FTN_1351) driven by its native promoter, (B.) pSKI04 encoding *ilvC* from *F. novicida*

driven by *F. tularensis blaB* promoter, (C.) pEDL71 encoding *panG* from *E. faecalis* driven by *F. tularensis blaB* promoter, or (D.) pEDL70 encoding *panE* from *E. coli* driven by *F. tularensis blaB* promoter. *ilvC*::Tn grown in CDM lacking pantothenate containing an empty control vector pMP822/pMP831 (black), the double mutant *ilvC*::Tnflp/*panG*::Tn containing an empty control vector (grey), *ilvC*::Tnflp/*panG*::Tn containing the respective complementing plasmid (black dotted line),and *ilvC*::Tnflp/*panG*::Tn grown in CDM supplemented with pantolactone (grey dotted line). (E.) *E.coli* double mutant *ilvC*::flp/*panE*::kan complemented with pSKI01 encoding *F. novicida panG* driven by its native promoter. *ilvC*::kan grown in M9 media lacking pantothenate containing an empty control vector (black), the double mutant *ilvC*::flp/*panE*::kan containing an empty control vector (grey), *ilvC*::flp/*panE*::kan containing the respective complementing plasmid (black dotted line),and *ilvC*::flp/*panE*::kan grown in M9 supplemented with pantolactone (grey dotted line). Each growth curve was repeated three times and the graph represents the mean of three replicate experiments.

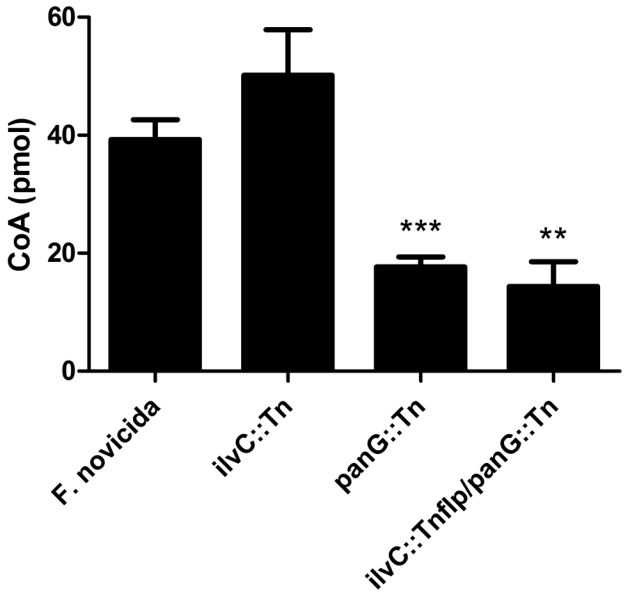


**Figure 5.5. *F. novicida* Coenzyme A levels.**

CoA concentrations were measured from 50ml cultures of wild type *F. novicida*, *ilvC*::Tn, *panG*::Tn, and *ilvC*::Tnflp/*panG*::Tn after 5 hours of pantothenate depletion. All strains were grown to the same $OD_{600}$ and were normalized to total protein. The CoA levels represented are the mean ± SD for three independent experiments. Statistical significance was determined by comparing the mutant values to wild type *F. novicida*. ***, $P < 0.0001$; ** $P < 0.001$.

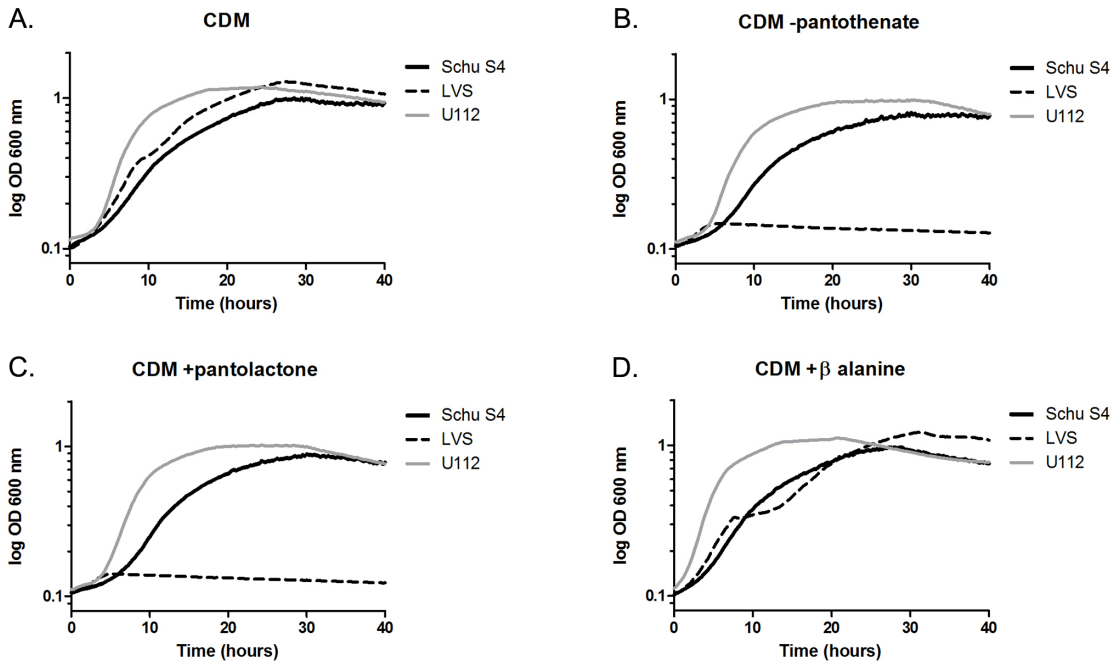


**Figure 5.6. *F. tularensis* Schu S4, *F. tularensis* LVS, *F. novicida* growth in pantothenate drop out media.**

Growth curves of *F. tularensis* subspecies *tularensis* Schu S4 (black), *F. tularensis* subspecies *holarctica* LVS (black dotted line) and *F. novicida* U112 (grey) were monitored in (A.) CDM, (B.) CDM lacking pantothenate, (C.) CDM lacking pantothenate supplemented with pantolactone, or (D.) CDM lacking pantothenate supplemented with β-alanine. Each strain was grown in triplicate in 96 well microtiter plates with absorbance ($OD_{600}$) monitored every fifteen minutes over 40 hours. Each graph represents the mean of three replicate experiments.

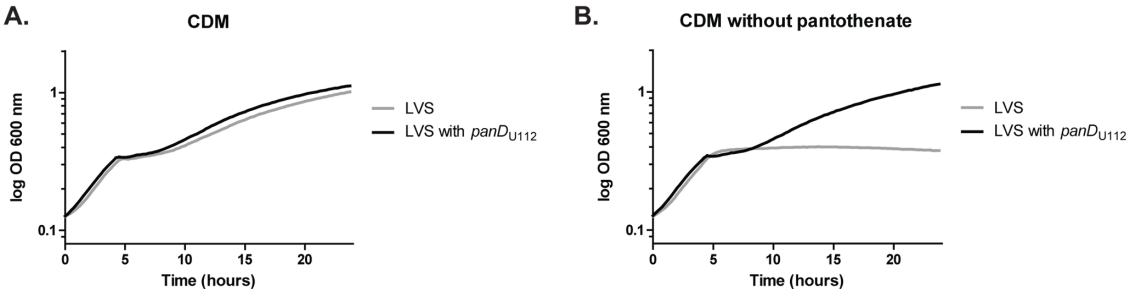


**Figure 5.7. Repair of *F. tularensis* LVS β-alanine auxotrophy.**

Growth curves of LVS (grey) and LVS with the native $panD_{LVS}$ replaced with $panD_{U112}$ from *F. novicida* U112 (black). Each strain was monitored in (A.) CDM, (B.) CDM lacking pantothenate. Both strains were grown in 96 well microtiter plates and ($OD_{600}$) determined every fifteen minutes for 24 hours. Each graph represents the mean ($OD_{600}$) of three replicate experiments.

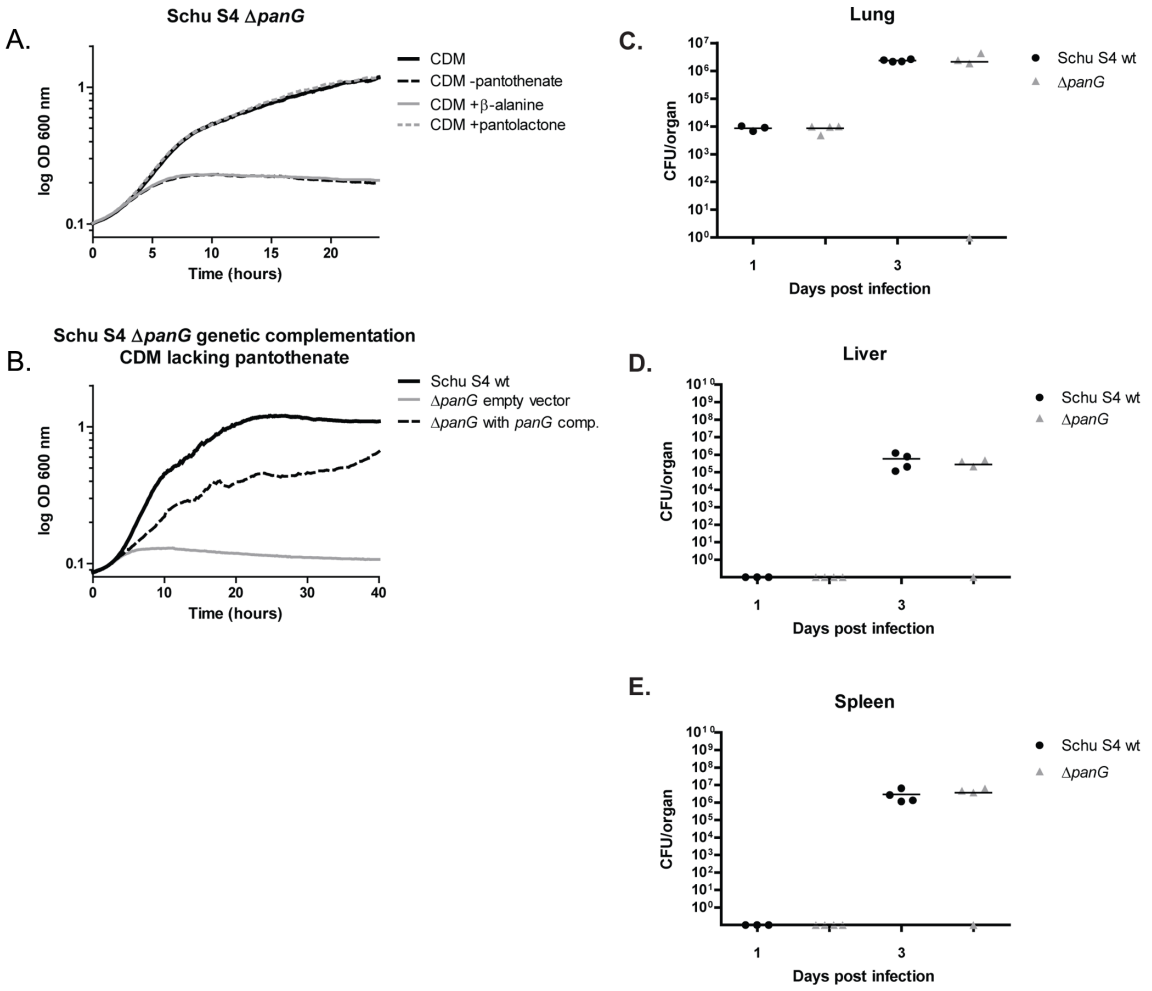


**Figure 5.8. *F. tularensis* subspecies *tularensis* Schu S4 Δ*panG* growth and virulence phenotype.**

(A.) Chemical complementation of Schu S4 Δ*panG* grown in CDM (black), CDM lacking pantothenate (black dotted line), CDM lacking pantothenate supplemented with β-alanine (grey), and CDM lacking pantothenate supplemented with pantolactone (grey dotted line). (B.) Genetic complementation of *F. tularensis* subspecies *tularensis* Schu S4 Δ*panG* with *F. novicida panG* gene expressed by the native promoter in the shuttle vector pMP831. Growth curve of *F. tularensis* subspecies *tularensis* Schu S4 (black), *F. tularensis* subspecies *tularensis* Schu S4 Δ*panG* with pMP831 (empty control vector) (grey), and *F. tularensis* subspecies *tularensis* Schu S4 Δ*panG* complemented with

pSKI01 (black dotted line). All growth curves were done in triplicate monitoring absorbance ($OD_{600}$) in a 96 well microtiter dish. Graphs represent the mean absorbance at $OD_{600}$. (C-E.) Recovery of Schu S4 or Schu S4 Δ*panG* mutant in mice following i.n. inoculation. C57BL/6 mice were infected intranasally with either wild type Schu S4 (black circles) or Schu S4 Δ*panG* (grey triangles) at a lethal dose of 50 CFU. Mice were euthanized on days 1 and 3 post infection and (C.) lung burdens, (D.) liver burdens and (E.) spleens burdens were determined and graphed. Each symbol represents data from a single mouse. There were no significant differences in recovery of mutant versus wild type organisms from any organ at any time point as determined by the nonparametric Mann-Whitney test.

# Tables

## Table 5.1. Bacterial strains and plasmids

| Strain or Plasmid | Genotype or Phenotype | Source |
|---|---|---|
| **Bacterial Strains** | | |
| *E. coli* DH10B | *E. coli* F-*mcr*A Δ(*mrr-hsd*RMS-*mcr*BC) φ80*lac*ZΔM15 Δ*lac*X74 *rec*A1*end*A1 *ara*D139 Δ(*ara leu*) 7697 *gal*U *gal*K *rps*L *nup*G λ- | Invitrogen |
| *E. coli* Top10 | *E. coli* F-*mcrA* Δ(*mrr-hsd*RMS-*mcr*BC) φ80*lac*ZΔM15 Δ*lac*X74 *rec*A1 *ara*D139 Δ*(ara-leu*) 7697 *gal*U *gal*K *rps*L (StrR) *end*A1 *nup*G λ- | Invitrogen |
| *E. coli panE::kan* JW0415-1 | *E. coli Δ(araD-araB)567, ΔlacZ4787(::rrnB-3), ΔpanE782::kan,λ-, rph-1,Δ(rhaD-rhaB)568, hsdR514* | Keio Collection |
| *E. coli ilvC::kan* JW3747-2 | *E. coli Δ(araD-araB)567, ΔlacZ4787(::rrnB-3), λ-, rph-1, ΔilvC725::kan, Δ(rhaD-rhaB)568, hsdR514* | Keio Collection |
| *F. novicida* U112 | *Francisella tularensis* subsp. *novicida* U112 (taxid:401614) | ATCC |
| *F. holarctica* LVS | *Francisella tularensis* subsp. *holarctica* LVS (taxid:376619) | CDC |
| *F. tularensis* Schu S4 | *Francisella tularensis* subsp. *tularensis* SCHU S4 (taxid:177416) | BEI Resources |
| *E. faecalis* | V583 | Lance Thurlow |
| *panB*::Tn | tnfn1_pw060328p05q156 T20 (IS*Fn*2/FRT) (FTN_1352) | Gallagher, et al. 2007 |
| *panC*::Tn | tnfn1_pw060328p03q178 T20 (IS*Fn*2/FRT) (FTN_1353) | Gallagher, et al. 2007 |
| *panD*::Tn | tnfn1_pw060323p04q175 <Kan-2> (FTN_1354) | Gallagher, et al. 2007 |
| *panG*::Tn | tnfn1_pw060420p03q142 T20 (IS*Fn*2/FRT) (FTN_1351) | Gallagher, et al. 2007 |
| *ilvC*::Tn | tnfn1_pw060420p04q122 T20 (IS*Fn*2/FRT) (FTN_1040) | Gallagher, et al. 2007 |
| FTN_1698::Tnflp | tnfn1_pw06032p08q164 ("flp" signifies a cured kanamycin cassette) | This work |
| *ilvC*::Tnflp/*panG*::Tn | tnfn1_pw060420p04q122flp/tnfn1_pw060420p03q142 ("flp" signifies a cured kanamycin cassette) | This work |
| SKI01 | *F. tularensis* Schu S4 Δ*panG* | This work |
| SKI02 | *F. novicida* U112 *ilvC*::Tnflp/*panG*::Tn with pEDL70 | This work |
| SKI03 | *F. novicida* U112 *ilvC*::Tnflp/*panG*::Tn with pEDL71 | This work |

| | | |
|---|---|---|
| SKI04 | *F. novicida* U112 *ilvC*::Tnflp/*panG*::Tn with pSKI01 | This work |
| SKI05 | *F. tularensis* Schu S4 Δ*panG* with pSKI01 | This work |
| SKI06 | *F. tularensis* Schu S4 Δ*panG* with pMP831 empty vector control | This work |
| SKI07 | *F. novicida* U112 *ilvC*::Tnflp/*panG*::Tn with pMP831 empty vector control | This work |
| SKI08 | *F. holarctica* LVS with panD from *F. novicida* U112 | This work |
| SKI09 | *E. coli ilvC*::flp/*panE*::kan (JW0415-1 and JW3747-2) | This work |
| SKI10 | *E. coli ilvC*::flp/*panE*::kan (JW0415-1 and JW3747-2) with pSKI01 | This work |
| SKI11 | *E. coli ilvC*::flp/*panE*::kan (JW0415-1 and JW3747-2) with pSKI04 | This work |
| **Plasmids** | | |
| pFFLP-hyg | Encodes *flp* under *Francisella groEL* promoter for recombination of FRT sites, TempSens, HygR | Gallagher, et al. 2008 |
| pKD46 | λ-Red recombineering plasmid GenBank: J02459.1 TempSens, AmpR | Datsenko, et al. 2000 |
| pFlp2 | Encodes flp recombinase for recombination of FRT sites, AmpR, SucS | Hoang, et al. 1998 |
| pEDL70 | pMP822.*panE,* HygR | This work |
| pEDL71 | pMP822.EF1861, HygR | This work |
| pSKI01 | pMP831.*panG* FTN_1351, HygR | This work |
| pSKI02 | pEDL50 with Δ*panG* Schu S4 construct, KmR, SucS | This work |
| pSKI03 | pMP590 with $panD_{U112}$ (FTN_1354), KmR, SucS | This work |
| pSKI04 | pMP822.*ilvC,* HygR | This work |
| pMP590 | *sacB* suicide vector, KmR, SucS | LoVullo, et al. 2006 |
| pMP822 | *E.coli-F.tularensis* shuttle vector, HygR *blaB* promoter | LoVullo, et al. 2009 |
| pMP831 | *E.coli-F. tularensis* shuttle vector, HygR | LoVullo, et al. 2009 |
| pEDL50 | Conjugative *sacB* suicide vector, HygR, SucS | LoVullo, et al. 2012 |

## References


1. **Altschul, S. F., W. Gish, W. Miller, E. W. Myers, and D. J. Lipman.** 1990. Basic local alignment search tool. Journal of molecular biology **215:**403-410.

2. **Baba, T., T. Ara, M. Hasegawa, Y. Takai, Y. Okumura, M. Baba, K. A. Datsenko, M. Tomita, B. L. Wanner, and H. Mori.** 2006. Construction of *Escherichia coli* K-12 in-frame, single-gene knockout mutants: the Keio collection. Mol Syst Biol **2:**2006 0008.

3. **Brand, L. A., and E. Strauss.** 2005. Characterization of a new pantothenate kinase isoform from *Helicobacter pylori*. The Journal of biological chemistry **280:**20185-20188.

4. **Chamberlain, R. E.** 1965. Evaluation of live Tularemia vaccine prepared in a chemically defined medium. Appl Microbiol **13:**232-235.

5. **Champion, M. D., Q. Zeng, E. B. Nix, F. E. Nano, P. Keim, C. D. Kodira, M. Borowsky, S. Young, M. Koehrsen, R. Engels, M. Pearson, C. Howarth, L. Larson, J. White, L. Alvarado, M. Forsman, S. W. Bearden, A. Sjostedt, R. Titball, S. L. Michell, B. Birren, and J. Galagan.** 2009. Comparative genomic characterization of *Francisella tularensis* strains belonging to low and high virulence subspecies. PLoS Pathog **5:**e1000459.

6. **Ciulli, A., D. Y. Chirgadze, A. G. Smith, T. L. Blundell, and C. Abell.** 2007. Crystal structure of *Escherichia coli* ketopantoate reductase in a ternary complex with NADP+ and pantoate bound: substrate recognition, conformational change, and cooperativity. The Journal of biological chemistry **282:**8487-8497.

7. **Cole, C., J. D. Barber, and G. J. Barton.** 2008. The Jpred 3 secondary structure prediction server. Nucleic acids research **36:**W197-201.

8. **Cronan, J. E., Jr.** 1980. Beta-alanine synthesis in *Escherichia coli*. Journal of bacteriology **141:**1291-1297.

9. **Cronan, J. E., Jr., K. J. Littel, and S. Jackowski.** 1982. Genetic and biochemical analyses of pantothenate biosynthesis in *Escherichia coli* and *Salmonella typhimurium*. Journal of bacteriology **149:**916-922.

10. **Datsenko, K. A., and B. L. Wanner.** 2000. One-step inactivation of chromosomal genes in *Escherichia coli* K-12 using PCR products. Proceedings of the National Academy of Sciences of the United States of America **97:**6640-6645.

11. **Elischewski, F., A. Puhler, and J. Kalinowski.** 1999. Pantothenate production in *Escherichia coli* K12 by enhanced expression of the *panE* gene encoding ketopantoate reductase. J Biotechnol **75:**135-146.

12. **Finlayson, H. J., and R. C. Seeley.** 1983. The synthesis and absorption of pantothenic acid in the gastrointestinal tract of the adult sheep. J Sci Food Agric **34:**427-432.

13. **Fong, C., L. Rohmer, M. Radey, M. Wasnick, and M. J. Brittnacher.** 2008. PSAT: a web tool to compare genomic neighborhoods of multiple prokaryotic genomes. BMC Bioinformatics **9:**170.

14. **Gallagher, L. A., M. McKevitt, E. R. Ramage, and C. Manoil.** 2008. Genetic dissection of the *Francisella novicida* restriction barrier. Journal of bacteriology **190:**7830-7837.

15. **Gallagher, L. A., E. Ramage, M. A. Jacobs, R. Kaul, M. Brittnacher, and C. Manoil.** 2007. A comprehensive transposon mutant library of *Francisella novicida*, a bioweapon surrogate. Proc Natl Acad Sci U S A **104:**1009-1014.

16. **Hanukoglu, I., and T. Gutfinger.** 1989. cDNA sequence of adrenodoxin reductase. Identification of NADP-binding sites in oxidoreductases. Eur J Biochem **180:**479-484.

17. **Hoang, T. T., R. R. Karkhoff-Schweizer, A. J. Kutchma, and H. P. Schweizer.** 1998. A broad-host-range Flp-FRT recombination system for site-specific excision of chromosomally-located DNA sequences: application for isolation of unmarked *Pseudomonas aeruginosa* mutants. Gene **212:**77-86.

18. **Horzempa, J., P. E. Carlson, Jr., D. M. O'Dee, R. M. Shanks, and G. J. Nau.** 2008. Global transcriptional response to mammalian temperature provides new insight into *Francisella tularensis* pathogenesis. BMC Microbiol **8:**172.

19. **Jackowski, S., and C. O. Rock.** 1981. Regulation of coenzyme A biosynthesis. Journal of bacteriology **148:**926-932.

20. **Kraemer, P. S., A. Mitchell, M. R. Pelletier, L. A. Gallagher, M. Wasnick, L. Rohmer, M. J. Brittnacher, C. Manoil, S. J. Skerett, and N. R. Salama.** 2009. Genome-wide screen in *Francisella novicida* for genes required for pulmonary and systemic infection in mice. Infect Immun **77:**232-244.

21. **Larsson, P., P. C. Oyston, P. Chain, M. C. Chu, M. Duffield, H. H. Fuxelius, E. Garcia, G. Halltorp, D. Johansson, K. E. Isherwood, P. D. Karp, E. Larsson, Y. Liu, S. Michell, J. Prior, R. Prior, S. Malfatti, A. Sjostedt, K. Svensson, N. Thompson, L. Vergez, J. K. Wagg, B. W. Wren, L. E. Lindler,**

**S. G. Andersson, M. Forsman, and R. W. Titball.** 2005. The complete genome sequence of *Francisella tularensis*, the causative agent of tularemia. Nat Genet **37:**153-159.

22. **Leonardi, R., Y. M. Zhang, C. O. Rock, and S. Jackowski.** 2005. Coenzyme A: back in action. Prog Lipid Res **44:**125-153.

23. **Lobley, C. M., A. Ciulli, H. M. Whitney, G. Williams, A. G. Smith, C. Abell, and T. L. Blundell.** 2005. The crystal structure of *Escherichia coli* ketopantoate reductase with NADP+ bound. Biochemistry **44:**8930-8939.

24. **Lovullo, E. D., C. N. Miller, M. S. Pavelka, Jr., and T. H. Kawula.** 2012. TetR-based Gene Regulation Systems for *Francisella tularensis*. Applied and environmental microbiology.

25. **LoVullo, E. D., L. A. Sherrill, and M. S. Pavelka, Jr.** 2009. Improved shuttle vectors for *Francisella tularensis* genetics. FEMS microbiology letters **291:**95-102.

26. **LoVullo, E. D., L. A. Sherrill, L. L. Perez, and M. S. Pavelka, Jr.** 2006. Genetic tools for highly pathogenic *Francisella tularensis* subsp. *tularensis*. Microbiology (Reading, England) **152:**3425-3435.

27. **Manch, J. N.** 1981. Mapping of a new pan mutation in *Escherichia coli* K-12. Can J Microbiol **27:**1231-1233.

28. **Marchler-Bauer, A., S. Lu, J. B. Anderson, F. Chitsaz, M. K. Derbyshire, C. DeWeese-Scott, J. H. Fong, L. Y. Geer, R. C. Geer, N. R. Gonzales, M. Gwadz, D. I. Hurwitz, J. D. Jackson, Z. Ke, C. J. Lanczycki, F. Lu, G. H. Marchler, M. Mullokandov, M. V. Omelchenko, C. L. Robertson, J. S. Song, N. Thanki, R. A. Yamashita, D. Zhang, N. Zhang, C. Zheng, and S. H. Bryant.** 2011. CDD: a Conserved Domain Database for the functional annotation of proteins. Nucleic acids research **39:**D225-229.

29. **Merkamm, M., C. Chassagnole, N. D. Lindley, and A. Guyonvarch.** 2003. Ketopantoate reductase activity is only encoded by *ilvC* in *Corynebacterium glutamicum*. J Biotechnol **104:**253-260.

30. **Nagle, S. C., Jr., R. E. Anderson, and N. D. Gary.** 1960. Chemically defined medium for the growth of *Pasteurella tularensis*. Journal of bacteriology **79:**566-571.

31. **Napier, B. A., L. Meyer, J. E. Bina, M. A. Miller, A. Sjostedt, and D. S. Weiss.** 2012. Link between intraphagosomal biotin and rapid phagosomal escape

in *Francisella*. Proceedings of the National Academy of Sciences of the United States of America **109:**18084-18089.

32. **Pechous, R., J. Celli, R. Penoske, S. F. Hayes, D. W. Frank, and T. C. Zahrt.** 2006. Construction and characterization of an attenuated purine auxotroph in a *Francisella tularensis* live vaccine strain. Infect Immun **74:**4452-4461.

33. **Pechous, R. D., T. R. McCarthy, N. P. Mohapatra, S. Soni, R. M. Penoske, N. H. Salzman, D. W. Frank, J. S. Gunn, and T. C. Zahrt.** 2008. A *Francisella tularensis* Schu S4 purine auxotroph is highly attenuated in mice but offers limited protection against homologous intranasal challenge. PLoS One **3:**e2487.

34. **Pechous, R. D., T. R. McCarthy, and T. C. Zahrt.** 2009. Working toward the future: insights into *Francisella tularensis* pathogenesis and vaccine development. Microbiol Mol Biol Rev **73:**684-711.

35. **Pledger, W. J., and H. E. Umbarger.** 1973. Isoleucine and valine metabolism in *Escherichia coli*. XXII. A pleiotropic mutation affecting induction of isomeroreductase activity. Journal of bacteriology **114:**195-207.

36. **Primerano, D. A., and R. O. Burns.** 1983. Role of acetohydroxy acid isomeroreductase in biosynthesis of pantothenic acid in *Salmonella typhimurium*. Journal of bacteriology **153:**259-269.

37. **Rohmer, L., C. Fong, S. Abmayr, M. Wasnick, T. J. Larson Freeman, M. Radey, T. Guina, K. Svensson, H. S. Hayden, M. Jacobs, L. A. Gallagher, C. Manoil, R. K. Ernst, B. Drees, D. Buckley, E. Haugen, D. Bovee, Y. Zhou, J. Chang, R. Levy, R. Lim, W. Gillett, D. Guenthener, A. Kang, S. A. Shaffer, G. Taylor, J. Chen, B. Gallis, D. A. D'Argenio, M. Forsman, M. V. Olson, D. R. Goodlett, R. Kaul, S. I. Miller, and M. J. Brittnacher.** 2007. Comparison of *Francisella tularensis* genomes reveals evolutionary events associated with the emergence of human pathogenic strains. Genome Biol **8:**R102.

38. **Sambandamurthy, V. K., X. Wang, B. Chen, R. G. Russell, S. Derrick, F. M. Collins, S. L. Morris, and W. R. Jacobs, Jr.** 2002. A pantothenate auxotroph of *Mycobacterium tuberculosis* is highly attenuated and protects mice against tuberculosis. Nat Med **8:**1171-1174.

39. **Saslaw, S., H. T. Eigelsbach, H. E. Wilson, J. A. Prior, and S. Carhart.** 1961. Tularemia vaccine study. I. Intracutaneous challenge. Arch Intern Med **107:**689-701.

40. **Shimizu, S., M. Kataoka, M. C. Chung, and H. Yamada.** 1988. Ketopantoic acid reductase of *Pseudomonas maltophilia* 845. Purification, characterization, and role in pantothenate biosynthesis. The Journal of biological chemistry **263:**12077-12084.

41. **Si, D., N. Urano, S. Shimizu, and M. Kataoka.** 2012. Cloning and overexpression of ketopantoic acid reductase gene from *Stenotrophomonas maltophilia* and its application to stereospecific production of D-pantoic acid. Appl Microbiol Biotechnol **93:**1619-1625.

42. **Sjostedt, A.** 2007. Tularemia: history, epidemiology, pathogen physiology, and clinical manifestations. Ann N Y Acad Sci **1105:**1-29.

43. **Stansly, P. G., and M. E. Schlosser.** 1945. The biological activity of pantolactone and pantoic acid. The Journal of biological chemistry **161:**513-515.

44. **Su, J., J. Yang, D. Zhao, T. H. Kawula, J. A. Banas, and J. R. Zhang.** 2007. Genome-wide identification of *Francisella tularensis* virulence determinants. Infect Immun **75:**3089-3101.

45. **Webb, M. E., A. G. Smith, and C. Abell.** 2004. Biosynthesis of pantothenate. Nat Prod Rep **21:**695-721.

46. **Wehrly, T. D., A. Chong, K. Virtaneva, D. E. Sturdevant, R. Child, J. A. Edwards, D. Brouwer, V. Nair, E. R. Fischer, L. Wicke, A. J. Curda, J. J. Kupko, 3rd, C. Martens, D. D. Crane, C. M. Bosio, S. F. Porcella, and J. Celli.** 2009. Intracellular biology and virulence determinants of *Francisella tularensis* revealed by transcriptional profiling inside macrophages. Cell Microbiol **11:**1128-1150.

47. **Yang, K., Y. Eyobo, L. A. Brand, D. Martynowski, D. Tomchick, E. Strauss, and H. Zhang.** 2006. Crystal structure of a type III pantothenate kinase: insight into the mechanism of an essential coenzyme A biosynthetic enzyme universally distributed in bacteria. Journal of bacteriology **188:**5532-5540.

# Chapter 6

## Discussion, Conclusions, And Future Directions

Substantial progress has been made identifying virulence factors in *F. tularensis* while I conducted my graduate research. During the last five years a total of 765 journal articles have been published on the species *F. tularensis* alone. Highlighted below are some of the key findings that were instrumental to understanding *F. tularensis* and the disease tularemia.

Progress has been made in characterizing the *Francisella* pathogenicity island (FPI) in the most virulent strain *F. tularensis* subsp. *tularensis* with the creation of several double deletion mutants. Interestingly, the phenotype of the double deletion of *pdpC* was different when compared to the same mutant in *F. novicida* (12, 13). Further characterization of the secreted components of the FPI in *F. tularensis* LVS showed fundamental differences when compared to *F. novicida*, where IglE, IglC, VgrG, IglI, PdpE, PdpA, IglJ and IglF were all detected to be secreted in *F. tularensis*, while only IglE, IglC, PdpA and PdpE were detected to be secreted in *F. novicida* (6). A basic understanding of the biochemical interactions that form the secretion system is needed. One example of a thorough characterization of two interacting components within the pathogenicity island was done with IglA and IglB (5).

Colin Manoil's group was able to assign function to many proteins that were previously unknown and uncharacterized using the comprehensive transposon mutant library in *F. novicida* under a variety of stress and nutritional conditions (10). Their

screen identified a new phosphofructokinase, an unusual proline biosynthetic pathway, and a novel antibiotic resistance mechanism, all of which differ from those present in model species (10).

With current advancements in technology we are now able to see dissemination in real time of *Francisella* species in mice using a microPET scanner monitoring radiolabeled $^{64}$Cu *F. novicida* (15). Ojeda's work has shown that the pulmonary route is associated with rapid septicemia, and that the cecum is a novel site of colonization of *Francisella novicida* in mice.

*Francisella noatunesis* is a recently identified species that is a serious pathogen of Atlantic cod (*Gadus morhua*), causing significant losses to the Norwegian aquaculture industry (18). The genome sequence for *Francisella noatunesis* was just published in 2012, which will allow scientists the opportunity to identify new potential drug targets and characterize the unique properties of this species of *Francisella* (18). A reservoir outside the fish host has yet to be identified for *F. noatunesis*.

LPS modification has been known to be a common strategy employed by bacterial pathogens to avoid innate immunity. Recently a two-component Kdo (3-deoxy-D-manno-octulosonic acid) hydrolase was identified that catalysis the removal of a side chain Kdo sugar from LPS precursors in *F. tularensis,* which is essential for preventing host proinflammatory cytokine production in a TLR2 dependent manner (16).

Earlier in 2009, researchers identified a heat stable bacterial component responsible for suppressing dendritic cell response to different Toll-like receptor agonists (7). This component is one example of a mechanism used by *F. tularensis* to control the host environment for optimal bacterial growth. Recently, Weiss *et al*, and we showed that the lipid composition of *F. tularensis* changes in response to the host cell environment

when compared to culture grown bacteria (Chapter 5) (2). The exact compositional changes have not been identified and further work needs to be done to characterize the new lipids that help *F. tularensis* adapt to the hostile host environment. The FabI enoyl-acyl carrier protein reductase gene was identified to be essential to bacterial viability during infection and could be responsible for some of the lipid composition differences seen during intracellular growth (11).

The host immune response is suppressed between 2 and 6 hours after F. tularensis infection indicating there may be unknown mechanism used by *F. tularensis* to suppress the immune response (4). Identifying these potential effectors will be key to understanding the control mechanisms used by *F. tularensis* to manipulate the host environment for optimal bacterial growth. DnaK is a recently identified protein that interacts with the host plasma alkaline phosphatase and inhibits its activity, which may be one mechanism used by *F. tularensis* to control the inflammatory response and create an advantageous environment in the host for bacterial growth (1).

A recent study examined immune responses in BALB/c mice vaccinated with mutant strains of *F. tularensis* that elicited varying degrees of protection against systemic and aerosol challenges with the wild type strain (17). They established correlates of protection in animal models that can relate to human vaccines, and identified that the Δ*clpB* mutant elicits superior protection compared to the live vaccine strain (17). Our laboratory demonstrated that the *F. tularensis clpB* mutant altered host immunity and induced the expression of two proinflammatory cytokines, IFN-gamma and IL-17 (3).

We have only recently appreciated the role autophagy plays in *F. tularensis* growth and virulence inside host cells. Autophagy was thought to be a mechanism involved in breakdown of cellular components and clearance of invading pathogens.

Cells clear the replication deficient mutant, Δ*dipA*, in *F. tularensis* in an autophagy dependent manner (8). Only recently has autophagy been shown to have a positive role for a few pathogens, including *Brucella abortus* (19). Earlier transcriptional analysis of host cells infected with *F. tularensis* provided evidence that *F. tularensis* affects expression of many genes involved in autophagy (9). Our lab recently published work demonstrating that ATG5 independent autophagy provides amino acids for *F. tularensis* to support intracellular growth (in press). The mechanisms and potential effectors used by *F. tularensis* to manipulate the host and acquire nutrients form autophagosomes remains a tantalizing avenue to explore.

In this dissertation we identify a *F. novicida* specific virulence factor, IclR, which is a transcriptional regulator responsible for controlling the expression of genes that are lost or disrupted in the more virulent *F. tularensis* strains (Chapter 2). Future studies with IclR include characterization of the specific IclR regulated genes responsible for the virulence differences in *F. novicida* and *F. tularensis*, and determining how these evolutionary changes impact pathogenesis of the *F. tularensis*.

We developed the first anhydrotetracycline inducible and repressible system for *F. tularensis* to control gene expression (Chapter 3) (14). Regulated expression systems are instrumental tools for identifying the unique mechanism used by *F. tularensis* to control gene expression and biosynthetic pathways. Using this tool we determined the induced expression of *lpxA* was detrimental for growth of *F. tularensis* lacking the *ripA* locus, while the wild type strain containing *ripA* was unaffected by the production of *lpxA* (Chapter 4). With this genetic tool we can continue to assign function to more genes in *Francisella*.

We identified the function of a key virulence factor, RipA by isolating, mapping and characterizing an extragenic mutant, S102 (Chapter 4). S102 and 4 other independently derived extragenic mutations mapped to *lpxA* or *glmU*. Both enzymes (LpxA and GlmU) are essential components of the lipid A biosynthesis pathway. We determined RipA influences LpxA stability and LpxA specificity for C18:0 compared to C16:0 acyl chain in *F. tularensis*. What remains to be determined is the role RipA plays during intracellular growth, and how LpxA and RipA may modify the bacterial membrane to adapt to the host environment. Understanding RipA function provides an important insight into the specific mechanisms used by *F. tularensis* to modulate LpxA—the first enzyme in the lipid A biosynthesis pathway.

RipA homologs are also found in several randomly distributed prokaryotic species, and include mainly non-pathogenic organisms. To date there are only four pathogenic bacteria known to have RipA homologs, and the role these homologs play in virulence is unknown. It is likely that RipA is a conserved virulence factor unique to *Francisella*. RipA homologs are present in Gram-positive bacteria that do not make lipid A. If RipA is important for modulating LpxA, the enzyme responsible for the first step in lipid A biosynthesis, why is RipA present in organisms that do not make lipid A? Future complementation studies performed with the RipA homologs from other prokaryotes expressed in *F. tularensis* Δ*ripA* would help determine if *Francisella* has evolved a unique virulence mechanism distinct from other prokaryotes. The complementation studies may also identify another function for RipA that has broader application to include more Gram-positive organisms.

The original immunoprecipitation experiments performed by James Fuller with RipA identified multiple putative RipA-interactors, including LpxA. Interestingly, IclR

was also identified to be a RipA interacting protein, however we were unable to identify a role RipA played in IclR transcription regulation in *F. tularensis* (unpublished results Brittany Mortensen). It may be interesting to determine if RipA helps regulates gene expression in other prokaryotic organisms containing IclR transcriptional regulators.

In chapter 4 we characterized one extragenic suppressor mutant of Δ*ripA* that restored growth inside host cells, S102, but there remain 4 other independently derived extragenic suppressor mutants that need to be characterized. One extragenic suppressor mutation mapped to *glmU*. We repaired the mutation within *glmU* and demonstrated that the mutation was responsible for the suppressor phenotype (unpublished results). We performed immunoprecipitation reactions with GlmU and RipA, however no interaction was identified (unpublished results). We measured protein concentrations of GlmU in the absence and presence of RipA and found no differences in concentrations (unpublished results). We induced expression of *glmU* in the wild type strain and the Δ*ripA* strain to determine if RipA is important for modulating GlmU activity, however we did not see any growth defects as seen with *lpxA* induced in the Δ*ripA* strain (unpublished results). The connection between GlmU and RipA remains an enigma. It seems likely that RipA binds and modulates LpxA activity, while GlmU is only indirectly involved with RipA considering GlmU performs the two sequential steps prior to LpxA in the lipid A synthesis pathway.

In addition to identifying RipA function, we also identified a novel ketopantoate reductase (KPR), PanG, involved in vitamin $B_5$ synthesis that converts 2-dehydropantoate to pantoate (Chapter 5). As a facultative intracellular pathogen, *F. tularensis* must acquire or synthesize the nutrients needed to support growth while within host cells. The genes involved in vitamin $B_5$ biosynthesis are very highly expressed in *F. tularensis* during

infection, supporting that they may contribute to the pathogenesis of *F. tularensis* (20). We experimentally validated the annotation of the vitamin $B_5$ synthesis pathway in *F. tularensis* and identified a gap in the pathway of the most virulent strain *F. tularensis* Schu S4. Homologs of this novel KPR are also found in other pathogenic bacteria such as *Clostridium difficile*, *Coxiella burnetii*, and *Enterococcus faecalis,* demonstrating broad implication for our understanding of bacterial vitamin $B_5$ synthesis.

The culmination of this work has provided new genetic tools that aided in the characterization of two novel proteins, one involved in lipid A synthesis and the other involved in vitamin $B_5$ synthesis.

This research identifying function of novel proteins in *Francisella tularensis* has led to the following finding:

1) *Francisella tularensis* and *F. novicida* have a distinctly different set of virulence factors owing to the fact that the IclR transcriptional regulator is important for the pathogenesis in *F. novicida*, while dispensable for *F. tularensis* pathogenesis due to reductive evolution of the more virulent strain.
2) Developing the anhydrotetracycline inducible expression system for *F. tularensis* has been a powerful tool used to characterizing RipA function.
3) By mapping extragenic suppressor mutations of Δ*ripA* we determined the function of RipA in *F. tularensis*. The location of the suppressor mutations mapped to two genes, *lpxA* and *glmU*, both involved in lipid A biosynthesis. RipA modulates the activity and amount of LpxA in *F. tularensis* and could be a unique virulence mechanism specific to *Francisella* species to adapting to the host environment.

4) We identified a novel ketopantoate reductase (KPR), PanG, involved in vitamin $B_5$ synthesis. Homologs of PanG are also found in three other pathogenic bacteria such as *Clostridium difficile*, *Coxiella burnetii*, and *Enterococcus faecalis,* demonstrating broad implication for our understanding of bacterial vitamin $B_5$ synthesis.

In this study we identified the function of novel proteins in *Francisella tularensis*, one of the six classified Category A Select Agents, which is a pathogen that has evolved unique strategies to survive in a broad range of hosts. We believe that the most important goal of research in the *F. tularensis* field should focus on characterizing the genes with unknown function important for infection and pathogenesis, and we have used this motivation for the research and findings we reported in this dissertation.

Within the last decade, numerous screens have been developed to identify virulence factors of *F. tularensis*, and now is the time to assign novel function to the many virulence factors that remain unknown.

## References


1. **Arulanandam, B. P., S. L. Chetty, J. J. Yu, S. Leonard, K. Klose, J. Seshu, A. Cap, J. J. Valdes, and J. P. Chambers.** 2012. *Francisella* DnaK inhibits tissue-nonspecific alkaline phosphatase. The Journal of biological chemistry **287:**37185-37194.

2. **Barker, J. H., J. W. Kaufman, D. S. Zhang, and J. P. Weiss.** 2013. Metabolic labeling to characterize the overall composition of *Francisella* Lipid A and LPS grown in broth and in human phagocytes. Innate Immun.

3. **Barrigan, L. M., S. Tuladhar, J. C. Brunton, M. D. Woolard, C. J. Chen, D. Saini, R. Frothingham, G. D. Sempowski, T. H. Kawula, and J. A. Frelinger.** 2013. Infection with *Francisella tularensis* LVS *clpB* leads to an altered yet protective immune response. Infect Immun **81:**2028-2042.

4. **Bradburne, C. E., A. B. Verhoeven, G. C. Manyam, S. A. Chaudhry, E. L. Chang, D. C. Thach, C. L. Bailey, and M. L. van Hoek.** 2013. Temporal transcriptional response during infection of type II alveolar epithelial cells with *Francisella tularensis* live vaccine strain (LVS) supports a general host suppression and bacterial uptake by macropinocytosis. The Journal of biological chemistry **288:**10780-10791.

5. **Broms, J. E., M. Lavander, and A. Sjostedt.** 2009. A conserved alpha-helix essential for a type VI secretion-like system of *Francisella tularensis*. Journal of bacteriology **191:**2431-2446.

6. **Broms, J. E., L. Meyer, K. Sun, M. Lavander, and A. Sjostedt.** 2012. Unique substrates secreted by the type VI secretion system of *Francisella tularensis* during intramacrophage infection. PLoS One **7:**e50473.

7. **Chase, J. C., J. Celli, and C. M. Bosio.** 2009. Direct and indirect impairment of human dendritic cell function by virulent *Francisella tularensis* Schu S4. Infect Immun **77:**180-195.

8. **Chong, A., T. D. Wehrly, R. Child, B. Hansen, S. Hwang, H. W. Virgin, and J. Celli.** 2012. Cytosolic clearance of replication-deficient mutants reveals *Francisella tularensis* interactions with the autophagic pathway. Autophagy **8:**1342-1356.

9. **Cremer, T. J., A. Amer, S. Tridandapani, and J. P. Butchar.** 2009. *Francisella tularensis* regulates autophagy-related host cell signaling pathways. Autophagy **5:**125-128.

10. **Enstrom, M., K. Held, B. Ramage, M. Brittnacher, L. Gallagher, and C. Manoil.** 2012. Genotype-phenotype associations in a nonmodel prokaryote. mBio **3**.

11. **Kingry, L. C., J. E. Cummings, K. W. Brookman, G. R. Bommineni, P. J. Tonge, and R. A. Slayden.** 2013. The *Francisella tularensis* FabI enoyl-acyl carrier protein reductase gene is essential to bacterial viability and is expressed during infection. Journal of bacteriology **195:**351-358.

12. **Lindgren, M., K. Eneslatt, J. E. Broms, and A. Sjostedt.** 2013. Importance of PdpC, IglC, IglI, and IglG for modulation of a host cell death pathway induced by *Francisella tularensis*. Infect Immun **81:**2076-2084.

13. **Long, M. E., S. R. Lindemann, J. A. Rasmussen, B. D. Jones, and L. A. Allen.** 2013. Disruption of *Francisella tularensis* Schu S4 *iglI*, *iglJ*, and *pdpC* genes results in attenuation for growth in human macrophages and in vivo virulence in mice and reveals a unique phenotype for *pdpC*. Infect Immun **81:**850-861.

14. **Lovullo, E. D., C. N. Miller, M. S. Pavelka, Jr., and T. H. Kawula.** 2012. TetR-based Gene Regulation Systems for *Francisella tularensis*. Applied and environmental microbiology.

15. **Ojeda, S. S., Z. J. Wang, C. A. Mares, T. A. Chang, Q. Li, E. G. Morris, P. A. Jerabek, and J. M. Teale.** 2008. Rapid dissemination of *Francisella tularensis* and the effect of route of infection. BMC microbiology **8:**215.

16. **Okan, N. A., S. Chalabaev, T. H. Kim, A. Fink, R. A. Ross, and D. L. Kasper.** 2013. Kdo hydrolase is required for *Francisella tularensis* virulence and evasion of TLR2-mediated innate immunity. mBio **4:**e00638-00612.

17. **Ryden, P., S. Twine, H. Shen, G. Harris, W. Chen, A. Sjostedt, and W. Conlan.** 2013. Correlates of protection following vaccination of mice with gene deletion mutants of *Francisella tularensis* subspecies *tularensis* strain, SCHU S4 that elicit varying degrees of immunity to systemic and respiratory challenge with wild type bacteria. Mol Immunol **54:**58-67.

18. **Sridhar, S., A. Sharma, H. Kongshaug, F. Nilsen, and I. Jonassen.** 2012. Whole genome sequencing of the fish pathogen *Francisella noatunensis* subsp. *orientalis* Toba04 gives novel insights into *Francisella* evolution and pathogenecity. BMC Genomics **13:**598.

19. **Starr, T., R. Child, T. D. Wehrly, B. Hansen, S. Hwang, C. Lopez-Otin, H. W. Virgin, and J. Celli.** 2012. Selective subversion of autophagy complexes facilitates completion of the *Brucella* intracellular cycle. Cell host & microbe **11:**33-45.

20. **Wehrly, T. D., A. Chong, K. Virtaneva, D. E. Sturdevant, R. Child, J. A. Edwards, D. Brouwer, V. Nair, E. R. Fischer, L. Wicke, A. J. Curda, J. J. Kupko, 3rd, C. Martens, D. D. Crane, C. M. Bosio, S. F. Porcella, and J. Celli.** 2009. Intracellular biology and virulence determinants of *Francisella*

*tularensis* revealed by transcriptional profiling inside macrophages. Cell Microbiol **11:**1128-1150.